ProQuest LLC.
789 East Eisenhower Parkway
P.O. Box 1346
Ann Arbor, MI 48106 – 1346

CYCLIC POLYMER LIQUID CRYSTAL STRUCTURES

DAVID R R EVERITT, BSc

A thesis submitted in partial fulfilment of the requirements of the Council for National Academic Awards for the degree of Doctor of Philosophy

October 1990

Department of Applied Physics, Sheffield City Polytechnic in collaboration with the Royal Signals and Radar Establishment, Malvern.

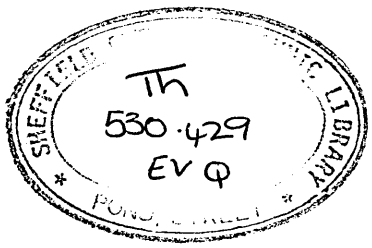
SHEFFIELD
LI BRARY
TH
530.429
EVQ

ABSTRACT

Recent advances in liquid crystal research have included the synthesis of polymeric materials which contain liquid crystalline moieties. The work presented here concerns the study of the structure-property relationships of a particular group of liquid crystalline polymers in which the polymer backbone is cyclic, with the mesogenic moieties attached as side-chains.

We have observed mesogenic phases above room temperature for materials comprising cyclic poly(dimethylsiloxane) backbones with mesogenic moieties attached by alkyl spacer units. Dielectric relaxations have been observed in the mesophases of these materials and the activation energies and extent of broadening of the relaxations have been related to the physical structure of the molecules

Theoretical studies have been undertaken by the use of the Metropolis Monte Carlo technique and a mean field calculation. Two models have been studied by the Monte Carlo technique in the NVT ensemble. In the first, each complete molecule was represented by a disc-like interactions potential and a tendency for the molecules to align in columns was revealed at low temperature and high density. In the second model, each mesogenic unit was represented separately, with the cyclic polymer represented as a constraint on the relative motions of the attached mesogens. A variety of liquid crystalline phases, from discotic nematic to calamitic nematic, were observed at low temperature as the coupling between the side-chains and the backbones was adjusted. In the mean field model energy terms were included for ring-ring interactions, mesogen-mesogen interactions and the coupling between the mesogenic moieties and the backbones. The uniaxial solution of this model also showed a shift from calamitic nematic to discotic nematic phases as the strength of the coupling was increased.

Comparisons of the results of the models and the physical measurements are presented and suggestions for future work are proposed.

ACKNOWLEDGEMENTS

I would like to thank my supervisors at the polytechnic, Dr. R.M. Wood and Dr. C.M. Care, and my contact at the Royal Signals and Radar Establishment, Dr. D. Mc Donnell, for helpful discussions throughout the period of study. I should also like to thank Dr. D.A. Dunmur of the Department of Chemistry at the University of Sheffield for the helpful liquid crystal research seminars which he organised.

I should like also to thank the Royal Signals and Radar Establishment for the use of their laboratories for the physical measurements and Dr. D.Mc Donnell and staff for their assistance. I should also like to thank the Chemistry Department of the polytechnic and the Consortium fur Elekrochemische Industrie GMBH for the provision of the physical samples.

Finally, I should like to thank the Science and Engineering Research council for the award of computing time on the CRAY X-MP/48 at the Atlas Centre of the Rutherford Appleton Laboratory.

ADVANCED STUDIES

As part of the course of study I attended the undergraduate course on Polymer Industry in the Chemistry Department of the polytechnic. In addition a course on vector programming for the CRAY computer was attended. A review of the literature relevant to the studies is included in the first chapter of this thesis.

The following conferences were attended:

CCP5 Annual Meeting, UMIST, Manchester
January 1987.

International Conference on Liquid Crystal Polymers, Bordeaux, France
July 1987.

CCP5 Annual Meeting, Birkbeck College, London
January 1988.

CONTENTS

CHAPTER 1 INTRODUCTION

The scientific study of liquid crystalline behaviour started in the middle of the last century [1]. As early as 1837, the author Edgar Allen Poe remarked on a liquid with anisotropic properties [2], while in 1888 Reinitzer [3] and Lehmann [4] were the first to observe liquid crystalline behaviour in a pure substance. The study and classification of liquid crystalline materials continued through the twentieth century, often with just a handful of devoted workers in the field. However, in the 1960s and 1970s, there was a large expansion in interest in these materials resulting in the development of liquid crystal display devices, such as those which are commonly used in digital watches and electronic calculators. More recently, there has been much interest in the synthesis of polymers which contain liquid crystalline moieties, with particular interest in the development of high tensile strength polymers and optical data storage materials. The move towards polymerisation has resulted in a wide variety of molecular structures being synthesised and studied [5].

This thesis concerns the study of novel liquid crystal systems based on cyclic poly(dimethylsiloxane) backbones with mesogenic units attached as side chains via alkyl spacers. The relationships between molecular structure and physical properties have been investigated by means of various experimental and theoretical techniques.

LIQUID CRYSTAL PHASES

Liquid crystalline phases may be observed for certain substances between the crystalline solid and isotropic liquid phases on a phase diagram [6,7]. These phases are characterised by a strong anisotropy in some of the properties of the liquid, which remains fluid. It is because the liquid crystalline phase occupies a position intermediate between solid and liquid phases that it has acquired the name 'mesophase', and a material which can exhibit such a phase is known as a 'mesogen'. A typical mesogen would have elongate rod-like molecules or flattened disc-like molecules [8], and it is the strongly anisotropic nature of the interaction between these molecules which gives rise to the macroscopic anisotropy of the fluid. A mesophase may be obtained by the melting of a pure solid mesogen, which produces a thermotropic mesophase, or by solution in a suitable solvent which produces a lyotropic mesophase. The materials studied in this project form thermotropic mesophases.

There are several distinct thermotropic mesophases, characterised by different types of anisotropic property, and it is possible for a single substance to exhibit more than one of these phases [9]. The commonly accepted classification of thermotropic liquid crystals was first proposed by Friedel [10] in 1922. Three classes of mesophase were defined according to their symmetry properties. These have been named the 'nematic', 'cholesteric' and 'smectic' phases. However, recent studies of liquid crystal structures have led to the observation of other types of mesophase not included in this classification [11].

The nematic mesophase is characterised by a high degree of long range orientational order of the molecules combined with the absence of long range translational order, as shown schematically in figure 1.1. The molecules of a nematic mesogen are often approximately rod-shaped and contain a rigid core section, and although the molecules may be polar the resulting macroscopic phase does not exhibit any polarity, unlike a ferro-magnetic structure, for example [7]. In the nematic phase there is spontaneous ordering of the molecules into approximate parallelism and the mean orientational direction is described by a unit vector, the director ($\hat{\underset{\sim}{n}}$). This director often varies within the material, but a uniformly aligned sample may be produced by the application of an electric or magnetic field, or by surface treatment of the container walls. For a material with low viscosity, uniform alignment may occur without the application of an external influence if the material is left for a time at a suitable temperature above the melting point and below the clearing point, T_c, above which the material is isotropic. It is conventional to reserve the use of the word 'homogeneous' to refer to a uniformly aligned sample, the director of which is parallel to the plane of the microscope slide or cell in which it is held for observation. The word 'homeotropic' is used when the alignment is such that the director is normal to the plane of the slide or cell.

A homogeneously aligned sample would be optically uniaxial and strongly birefringent. The birefringence gives rise to a colourful image when the sample is viewed under crossed polarisers with a crystallographic microscope. In the case where the sample is not uniformly aligned, defects in the surface of the slide or cover slip cause localised ordering which results in an overall pattern, or texture, related to the manner in

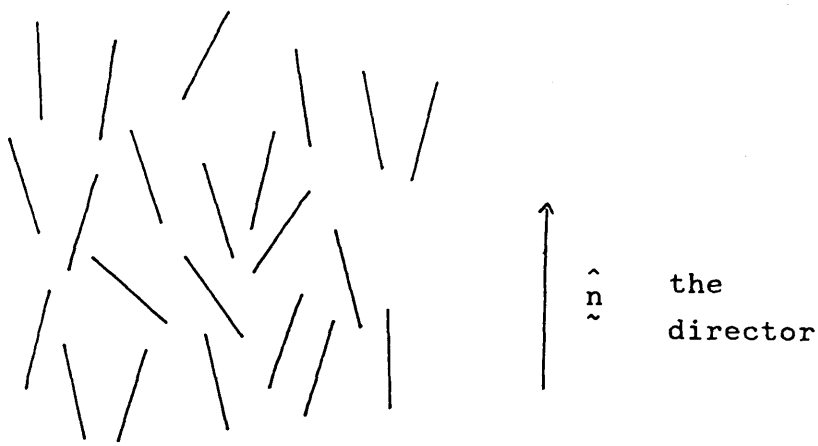

Figure 1.1 A schematic representation of a nematic phase of rod-like molecules.

p-azoxyanisole, P.A.A.

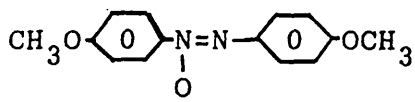

K 118 N 135.5 I

N-(p-methoxybenzylidene)-p-butylaniline, M.B.B.A.

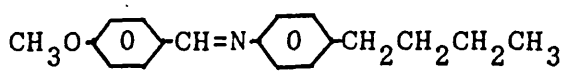

K 22 N 47 I

p-heptyl-p'-cyanobiphenyl

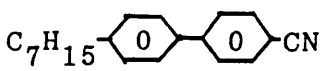

K 28.5 N 42 I

Figure 1.2 Some nematic mesogens. Transition temperatures in Celsius. 'K' - crystalline, 'N' - nematic, 'I' - isotropic. From de Jeu [7].

which the director varies within the material. Some textures are characteristic of a specific mesophase and so optical observations may be used as a first stage in the classification of a mesogenic material [9,12].

The rigid core of a nematic molecule is often provided by a closely coupled pair of benzene rings, as can be seen in the structures of the molecules of typical nematogens as shown in figure 1.2.

To enable a comparison between the extent of alignment in different mesogenic systems, a quantitative measure is needed to describe the degree of ordering. In the nematic phase, it is usual to take the average of the second order Legendre Polynomial function as such an order parameter [13,14]:

$$S = \langle P_2(\cos\theta_i) \rangle = \langle \frac{1}{2} (3\cos^2\theta_i - 1) \rangle \qquad 1.1$$

where, θ_i is the angle between the axis of the i-th molecule and the system director, and the angled brackets, '<..>', represent the thermal average over all molecules. In the nematic phase, the molecules are as likely to align anti-parallel as parallel to the director, and so the order parameter needs to reflect this by the choice of a function which has the following symmetry:

$$f(\theta_i) = f(\pi - \theta_i) \qquad 1.2$$

Hence, $\cos^2\theta_i$ is used in preference to $\cos\theta_i$ or θ_i. Rather than simply using $\langle \cos^2\theta_i \rangle$, the order parameter is constructed to take the value unity for full parallel alignment and zero for complete disorder. It also takes the value -0.5 in the event that all the molecules lie in the plane perpendicular to the director.

The order parameter may often be estimated from the measured anisotropy of some physical property of the liquid crystalline material [15-17]. The calculations often require further measurements of the same physical property in the isotropic liquid or single crystal states, and some assumption about the symmetry of the molecules is usual.

A schematic representation of the cholesteric phase is given in figure 1.3. The phase is similar to the nematic, but with a twist axis perpendicular to the director. The molecules are optically active and the pitch of the twist is temperature dependent, which has led to the use of cholesteric mesogens in digital thermometers. The name of the phase comes from the fact that many derivatives of cholesterol exhibit this phase. The chemical structures of two cholesteric mesogens are given in figure 1.4.

It is found that a nematic phase may result from a mixture of two cholesteric mesogens with opposite twist, and it is also found that a nematic material may exhibit a cholesteric phase on the addition of a little optically active material. Hence, some workers prefer to think of the cholesteric phase as simply a twisted form of the nematic phase, referring to it as 'chiral nematic'. In this case, the true nematic phase is considered to be a chiral nematic phase with infinite pitch.

The name 'smectic' is used to identify a range of mesophases which are characterised by some positional ordering of the molecules into layers, as well as orientational ordering of the elongated molecules. A variety of smectic phases have been identified and classified according to the relationships between layers

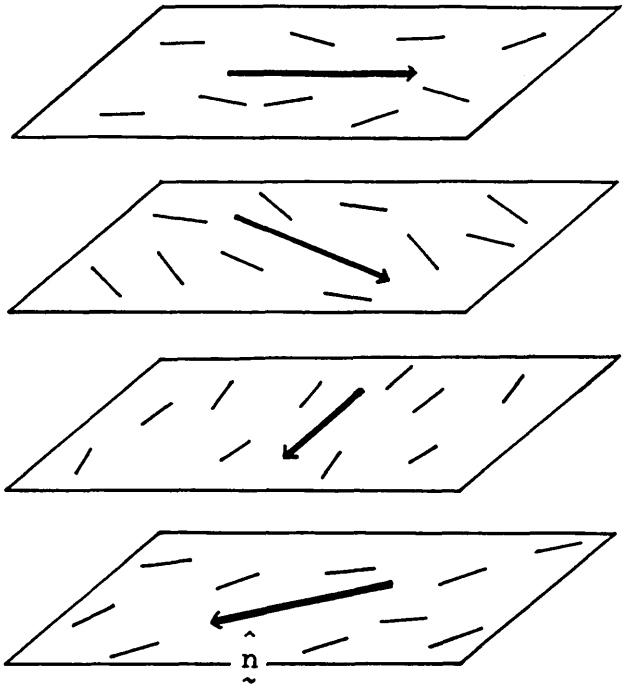

Figure 1.3 Schematic diagram of a cholesteric phase. The mesogens in a real cholesteric are not confined to specific planes.

N-(p-ethoxybenzylidene)-p'-(β-methylbutyl)aniline

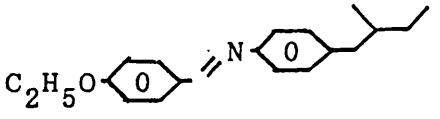

cholesteryl chloride

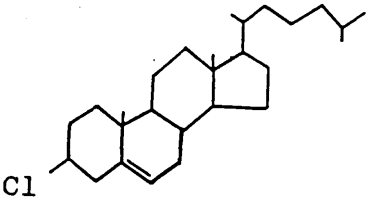

Figure 1.4 The chemical structure of two cholesteric compounds. From de Jeu [7].

and the orientational ordering. Two examples are the smectic A phase, in which the molecules align with the director normal to the planes, and the smectic C phase, in which there is a tilt angle between the director and the normal to the planes. These are shown schematically in figure 1.5.

Using geometrical arguments, Herrmann [18] concluded that there should be 18 distinct mesomorphic groups. However, until the recent discovery of discotic and other exotic phases, the limited classification according to Friedel had been considered satisfactory.

The hexagonal stacking of disc-like mesogens was first observed by Chandrasekhar et al. [19]. Disc-shaped mesogens have since been observed to pack in a variety of hexagonal columnar phases, known as discotic phases, as well as adopting nematic ordering [8,20,21]. Examples of these phases are given in figure 1.6. In the hexagonal discotic phase there is positional ordering in the plane perpendicular to the columns, but within the columns the discs are irregularly spaced.

Other liquid crystal phases have been suggested, including the possibility of cubic symmetry [11].

More recently, mesogenic units have been incorporated in polymers to give a range of liquid crystal polymer structures [5,22-25]. Liquid crystal polymers are generally divided into two structural types, the main-chain and side-chain structures, as shown in figure 1.7. However, many alternative structures are possible and some workers have even gone to the extreme of synthesising molecules which resemble the heraldic figure of their home town [26].

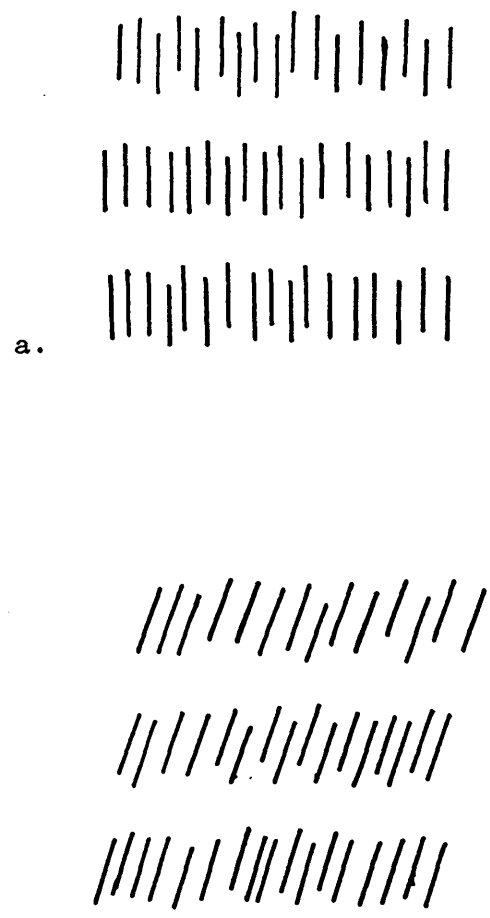

Figure 1.5 A schematic diagram of two smectic phases. a) Smectic A phase; b) Smectic C phase

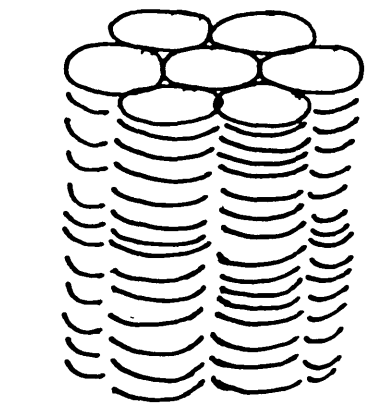

a.

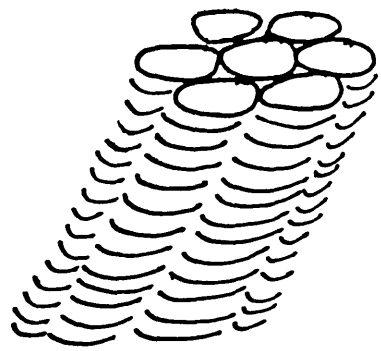

b.

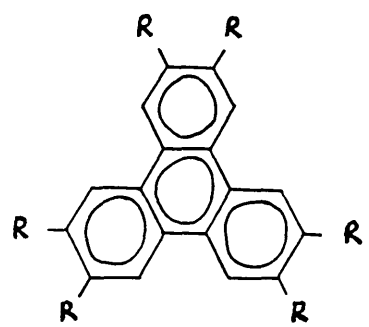

c.

Figure 1.6 Two columnar discotic phases: a) upright; b) tilted. c) Chemical structure of a typical discotic mesogen, 'R' represents an alkyl chain radical. From Chandrasekhar [8].

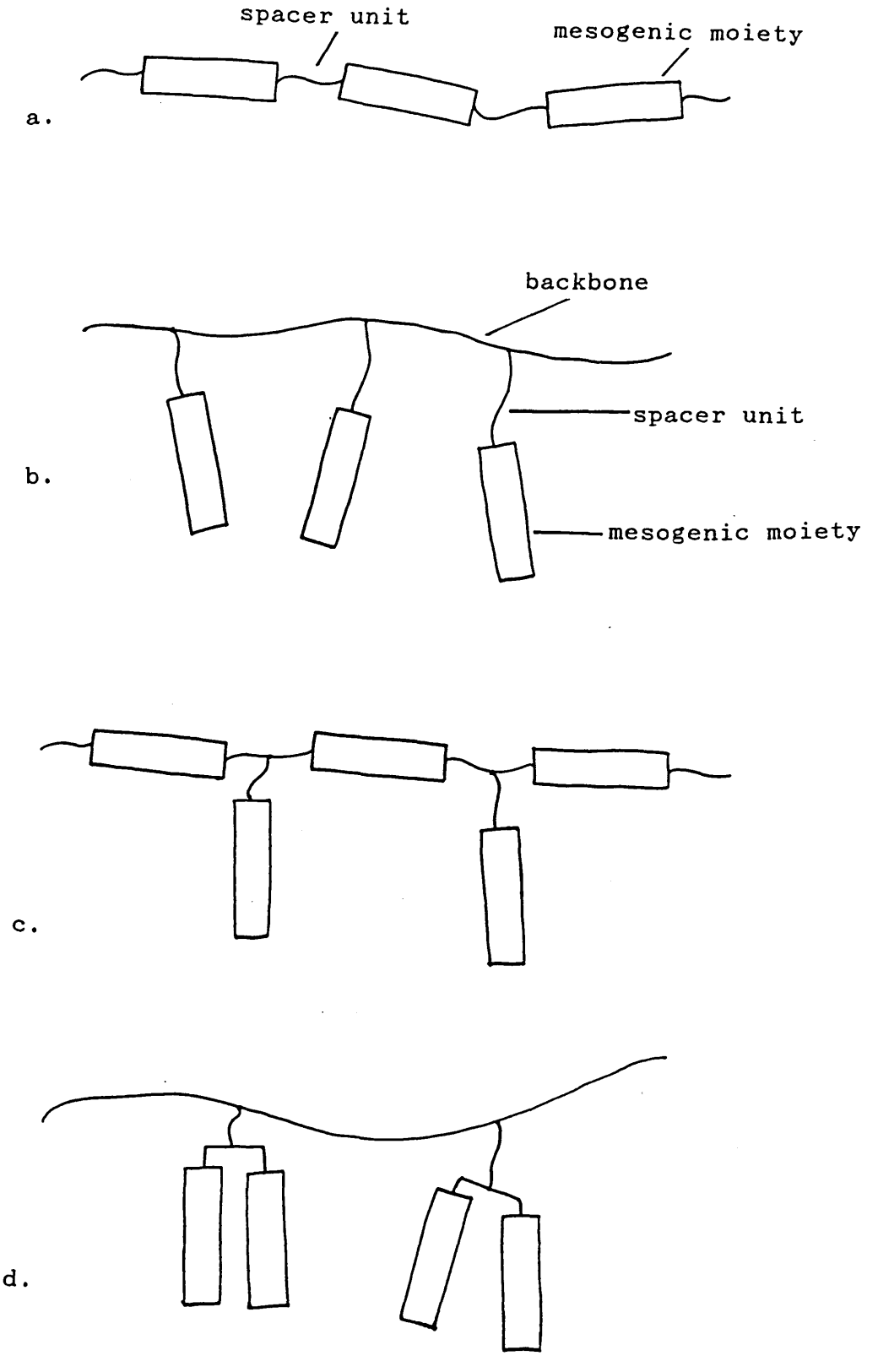

Figure 1.7 Some liquid crystal polymer structures: a) main chain; b) side chain; c) and d) other variations.

The effect of including mesogenic units in the main chain of a polymer is to force the alignment of the polymer chains and so produce extremely strong polymers [27-29].

In the side-chain polymer system there is a conflict between the aligning tendency of the mesogenic units and the random coiling of the backbone polymer [22,30,31]. The mesogenic units are connected to the backbone by a spacer unit which, if sufficiently flexible, may decouple the ordering of the mesogens from the backbone polymer conformations. In general, the conflict of properties leads to the mesogenic units in a side-chain polymer liquid crystal exhibiting a lower order parameter than their monomeric counterparts. However, the high viscosity of these materials leads to the mesogenic phases of the polymer being more stable than those of the monomer. Not only does the polymer exhibit mesogenic behaviour over a wider range of temperatures, but also a field induced alignment will persist after the field is removed, and this property has led to the investigation into the suitability of side-chain liquid crystal polymers as long-term optical data storage materials [32,33].

The general structure of the materials studied in this project is shown in figure 1.8. Some of these new materials were synthesised in the Chemistry Department of the polytechnic [34] and others were provided by a West German industrial consortium [35]. These materials comprise cyclic poly(dimethylsiloxane) backbones with side-chain mesogenic moieties attached via alkyl spacer units. Molecules were synthesised with a range of polymer ring sizes which may provide a variety of rigid and flexible backbone conformations. Molecules were also synthesised with different spacer lengths to alter the

a.

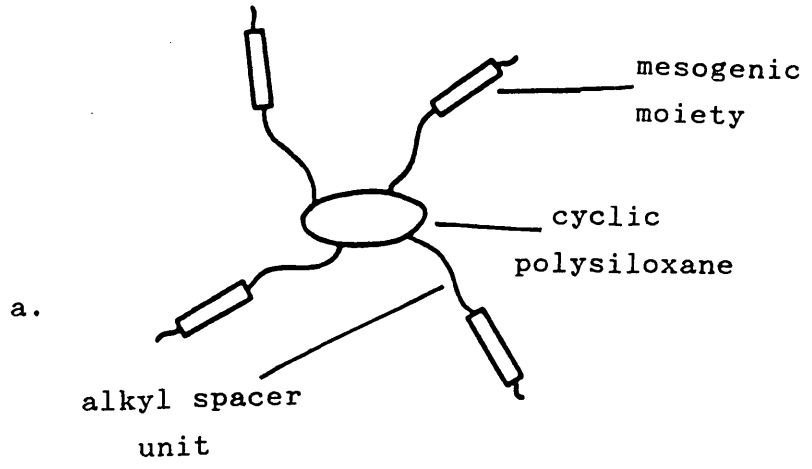

b.

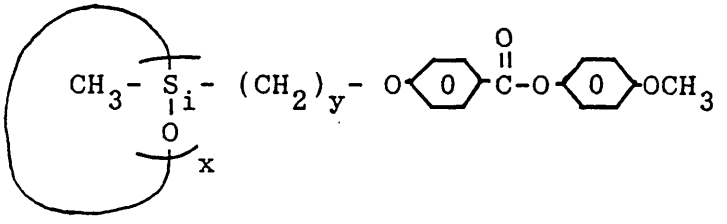

Samples were available with the following combinations of repeat units:

x = 4, y = 4;
x = 4, y = 6;
x = 5, y = 4;
x = 6, y = 4;
x = 7, y = 4.

Figure 1.8 The cyclic oligomer compounds studied: a) general physical structure; b) chemical structure.

degree of coupling between the backbone and the mesogenic moieties. Compounds have only been synthesised with a small number of repeat units in the backbone and so these low molecular weight polymers may be referred to as 'oligomers'.

Two theoretical techniques, the mean field approximation [13,36] and a Monte Carlo method [37-42] have been used in addition to experimental measurements in order to explore features of these molecules significant in the generation of liquid crystalline structures. The behaviour of these materials would be expected to be strongly dependent upon the nature of the coupling between the mesogenic moieties and the polymer ring backbone. A weak coupling should result in the formation of a conventional, calamitic (rod-like) nematic ordering of the mesogenic units. However, if the coupling is strong, the ring backbone will dominate the behaviour of the material. For example, if the mesogens are rigidly attached to the rings in a radial splay conformation, a discotic phase may be expected.

MONTE CARLO SIMULATIONS

A Monte Carlo technique [37-39,41] may be used to calculate the thermal average, or expectation value, of some thermodynamic property, A. In the canonical ensemble, the expectation value would be:

$$\langle A \rangle = \frac{\int\int_{\Omega} A \exp(-E(\Omega)/k_B T)\, d\Omega}{\int_{\Omega} \exp(-E(\Omega)/k_B T)\, d\Omega} \qquad 1.3$$

where $E(\Omega)$ is the total system energy and Ω represents the full system coordinates, chosen as appropriate for the system being modelled. For example, for a system of N mobile, non-spherical molecules, Ω would comprise three momentum coordinates, three positional coordinates, three orientational momentum coordinates and three orientational position coordinates for each molecule, making a 12N-fold phase space in total. For particles which interact via pair-wise potentials which are independent of velocity we may separate the kinetic and static contributions to the system energy and write:

$$E(\Omega) = \sum_{i}^{N} T_i + \sum_{i,j\ (j<i)}^{N} V_{ij} \qquad 1.4$$

where T_i is the kinetic energy of the i-th particle and V_{ij} is the pair interaction between the i-th and j-th particles.

The kinetic terms will cancel in the integrals in equation 1.3 if the thermodynamic property, A, is independent of the momenta of the particles:

$$\langle A \rangle = \frac{\int_{\Gamma} A \exp(-U(\Gamma)/k_B T)\, d\Omega}{\int_{\Gamma} \exp(-U(\Gamma)/k_B T)\, d\Omega} \qquad 1.5$$

where

$$U(\Gamma) = \sum_{i,j\ (j<i)}^{N} V_{ij} \qquad 1.6$$

and Γ represents the 6N positional and orientational coordinates of the system.

Owing to the large number of coordinates contained in Γ , it would be impossible to calculate the integrals for all but the simplest of systems. In a Monte Carlo method, this problem is overcome by the generation of configurations of the system of N particles. The expectation values of the configurational thermodynamic variables of the system may then be obtained by the weighted summation of the values of those same properties measured in the individual configurations.

A crude method of solution would be to generate configurations completely at random and weight them according to the Boltzmann probability factor, $\exp(-E(\Omega)/k_BT)$. However, the Boltzmann probability factor varies over many orders of magnitude and is sharply peaked in the region of the equilibrium configurations. Hence, most of the randomly generated configurations would possess an infinitesimally small weighting, making this summation method extremely inefficient.

The algorithm derived by Metropolis et al. [40] uses a technique known as 'importance sampling', where configurations are generated with a bias towards those near the maximum in the exponential terms in the integrals in equation 1.5.

The configurations are generated in the Metropolis method by creating a Markov chain of successive random alterations to the system of particles. The rules governing the alterations to successive configurations are chosen such that for an infinitely long Markov chain the asymptotic distribution of configurations is a canonical distribution at the specified temperature. The expectation value of a configurational property may then

be obtained as a simple average of the property over the configurations generated.

Several rules have been developed which generate configurations with the required distributions. We adopt the following method which is commonly used. A particle is chosen at random and its coordinates altered in some way. For example, it could be displaced by a small distance in some randomly chosen direction or rotated through a randomly determined angle. This attempted alteration (known as a 'move') is either accepted or rejected according to the following criteria:

i) the move is accepted if the resulting change in the system energy, ΔU, is negative.

ii) if the change in energy is positive, then the probability of the move being accepted is given by the Boltzmann factor, $\exp(-\Delta U/k_B T)$, and a comparison with a random number on the interval 0,1 determines whether the move is accepted.

The Metropolis Monte Carlo technique is usually very expensive in terms of computing time. Many thousands of attempted moves are required for the system to reach equilibrium at a given temperature and many thousands more are required to provide a valid canonical distribution of configurations from which the various properties may be measured. Care must be taken to ensure that the system does not lock itself into a non-equilibrium metastable state, from which it would be very difficult for the system to escape. In this case, the system may appear to have reached equilibrium and erroneous results might be obtained. However, to run the simulation on further to check whether true equilibrium has been reached may be prohibitively expensive in terms

of computing time.

The starting configuration for a run must be chosen carefully in order to minimise the likelihood of the system locking in such a non-equilibrium state. To ensure that the system reaches true thermal equilibrium, it is often necessary to allow the simulation to continue well after equilibrium appears to have been reached. Also, different starting configurations may be used in order to test whether the final equilibrium state is independent of the initial configuration.

The Monte Carlo technique is especially computationally intensive at very low temperatures, as few moves are accepted and consequently new configurations are generated inefficiently.

In many cases, including liquid crystal systems, the amount of change involved in a Monte Carlo move is an adjustable property and is often set so that the ratio of accepted to rejected moves is approximate unity as it is thought that this may allow the simulations to run most efficiently [38].

Monte Carlo simulations are invariably performed on systems of small numbers of molecules from a few tens to a few thousands. Hence comparison with macroscopic systems is not necessarily straightforward as there are of the order of 10^{23} molecules in a small sample real matter. Increasing the number of particles also increases the computing time required for the simulation, often as the square of the increase in the number of particles. For example, if the number of particles is doubled, we may expect a doubling in the computing time required to calculate the change in system energy for each attempted move. We might also expect to have to

attempt twice as many moves in order to reach thermal equilibrium, giving a four-fold increase in computing time altogether.

The usual way of mimicking a macroscopic system is to perform the simulation on a box of molecules with periodic boundary conditions such that the box is surrounded by identical boxes of molecules on each side. Interactions are then considered between one particle, i, and the closest replica of particle j. This technique is suitable for short range forces, where interactions with the next closest j-th molecule would be negligible. For molecules with longer range interactions, some adjustment may need to be made to the simulation or to its results in order to account for the omission of interactions beyond the closest of a pair of molecules. Also, it should be noted that these periodic boundary conditions introduce an unrealistic repetitiveness into the system.

Provided thermal equilibrium has been reached, the accuracy of a given measurement of a configurational property may be estimated from its fluctuations over the distribution of configurations. In fact, the fluctuations in some of the configurational properties may provide a means of calculating quantities such as the specific heat capacity, which cannot be measured directly from the configurations. However, such calculations are prone to large errors [38,41] owing to the loss of information about the partition function (the denominator in equation 1.3). One proposed solution to the problem has been to allow the volume of the box of particles to be one of the adjustable coordinates of the system and to perform the Monte Carlo simulation at constant pressure [42]. Such a simulation contains more information than the simulation in NVT canonical ensemble, allowing for the reliable calculation of the specific heat capacity

and the enthalpy etc.

The Metropolis Monte Carlo technique has been used to simulate a variety of physical systems [38,39], including classical fluids, many-body quantum systems and magnetic systems, as well as some simulations of simplified liquid crystal systems.

Various workers have undertaken Monte Carlo simulations of liquid crystalline systems in which the centres of mass of the molecules are constrained to a lattice [43,44,48-64]. This restriction results in a substantial saving in computing time for several reasons: moves involving the translation of a molecule are avoided; repulsive interactions, which would be necessary to prevent a translationally mobile system from collapsing, are no longer required; interactions can easily be limited to nearest neighbours only, simplifying the calculation of the change in energy involved in a move. Also, further savings in computing time may be made by restricting the orientations of the molecules to a limited number of discrete orientations. Of course, the restriction of the molecules to a lattice does place substantial limitations on the interpretation of the results. In particular, the fluid nature of any possible phases has been removed, prohibiting the formation of genuinely *liquid* phases. However, lattice models still retain orientational information and a useful comparison can be made between the results of these models and the true nematic to isotropic transition which involves only a change in the orientational ordering of the molecules. In fact, the simplifications involved in the construction of a lattice model may be used to advantage where the Monte Carlo technique is used to explore some specific restricted feature of liquid crystalline behaviour. For example, a lattice simulation may be used to assess the

validity of an analytic theory, such as a mean field approximation, in which no information is given concerning the spatial packing of the molecules.

The early uses of lattice Monte Carlo simulations of liquid crystalline systems were concerned with the comparison of an exact Monte Carlo model with the mean field approximation of Maier and Saupe. Lasher [43] and Lebwohl and Lasher[44], 1972, located a nematic to isotropic transition as a function of temperature in a lattice system of particles interacting via a potential which had the same orientational dependence as that used by Maier and Saupe in their mean field treatment [45-47]. The molecules were confined to a simple cubic lattice and energy calculations were restricted to nearest neighbour interactions. In the earlier model, the molecules were restricted to 12 discrete, evenly distributed, orientations, but were allowed to adopt any angle in the later model. In both cases a transition from the isotropic phase to the nematic was observed as the temperature was reduced (the terms 'isotropic' and 'nematic' used here somewhat loosely to define only the orientational ordering of the necessarily spatially ordered phases). Differences between the results of the two models were observed in the values of the transition temperature, the latent heat, and the change in the order parameter at the transition. In particular, the earlier, discrete, model grossly over-predicted the change in the order parameter at the transition. Quantitative agreement with the Maier-Saupe theory was also poor, although the change in the order parameter at transition was in better agreement for the simulation which had full orientational freedom. Further comparisons were made by Jansen et. al. [48] who investigated the Lebwohl-Lasher model more closely and confirmed that the observed nematic to isotropic transition was first order, as

predicted by the Maier-Saupe theory.

Luckhurst and co-workers have employed lattice Monte Carlo techniques in the systematic investigation of many liquid crystalline properties [49-61]. They have made comparisons with mean field calculations and extended the Lebwohl-Lasher model to include longer range interactions [49,50]. Other investigations include the simulation of systems of non-cylindrically symmetric molecules molecules [51], mixtures of rod-like and plate-like molecules [52], the effect of an external field on the alignment of phases [53], and pretransitional effects [54] (ie. the short-ranged ordering of nematogens in the isotropic phase just above the transition temperature). The transition from one smectic phase to another has also been modelled [55]. In this case the fixed spatial ordering of the lattice was an essential feature of the phases formed.

Another form of lattice liquid crystal model solved by Monte Carlo technique is that in which long semi-flexible molecules are represented by strings of adjacent squares or cubes on a simple grid in 2- or 3-dimensions. Attempted Monte Carlo moves are performed on individual segments of the molecules, with the rejection of moves that would involve the disintegration of an individual molecule. Such simulations have been used in the study of lyotropic mesogens in solution [65].

Hard repulsive interactions have often been used in the Monte Carlo simulation of liquid crystalline systems in which the molecules are given translational freedom [66-76]. These hard interactions are defined by assigning to the molecules some shape, such as that of a cylinder, and associating with that shape a pair-wise interaction in the form of a step function which becomes

infinite when any part of the two molecules overlaps, and which is zero otherwise. Hence, in the Monte Carlo simulation, any configuration generated in which any two or more molecules overlap is always rejected, and any configuration in which no molecules overlap is accepted. Consequently, the Boltzmann probability factor takes only values of one or zero, the result of which is that the state of the system is independent of the temperature. Phase transitions are, therefore, observed as a function of the density, rather than as a function of the temperature.

Simulations of hard particles can be relatively inexpensive in terms of computing time, provided a suitably simple shape is chosen for the molecules. In a large box of molecules most will not overlap and it is a straight-forward task to eliminate most pairs of molecules from the list of those which might possibly be overlapping. Efficient computing routines can be devised which are able to determine whether any of the remaining pairs of molecules overlap. However, performing Monte Carlo simulations on a system of anisometric molecules which have translational as well as orientational freedom is generally more expensive in terms of computing time than the simulation of molecules on a lattice. Consequently, simulations have been performed on systems of a few hundreds of translationally mobile molecules in comparison with the simulation of systems of several thousands of molecules confined to a lattice.

Many simulations of liquid crystalline systems have been performed using translationally mobile molecules of a variety of hard repulsive interactions. Viellard-Baron showed the transition from the crystalline solid to nematic fluid at high density and from nematic to isotropic fluid at lower density for a system of 170 hard

ellipses in 2-dimensions [66]. However, the extension of this work to hard spherocylinders (cylinders with hemi-spherical ends) in 3-dimensions did not yield an ordered liquid phase [67]. Since then other workers have employed a variety of hard shapes [68-75]: thin discs, oblate and prolate ellipsoids, cylinders and spherocylinders; and ordered phases have been located in 3-dimensional simulations. Nematic ordering has been observed for disc-like objects and studies on systems of uniaxial ellipsoids have shown an approximate equivalence in the phase behaviour of prolate and oblate ellipsoids which share the same axial ratio [72].

The study of hard-core particles has contributed to the debate as to the essential nature of the interaction between molecules which form liquid crystalline phases [74,77]. Short-range repulsive interactions have been shown to be sufficient to produce various smectic and nematic liquid crystalline phases [75]. However, the formation of a variety mesophases has also been successfully predicted by models which include only longer-ranged anisotropic forces, such as the various lattice Monte Carlo models and the Maier-Saupe mean field approximation. The debate as to whether the steric packing of hard-core particles dominates the behaviour of liquid crystalline materials is still active.

Relatively few Monte Carlo simulations have been undertaken on liquid crystalline systems in which the molecules, which have translational and orientational mobility, interact via pair-potentials with long-range attractive forces as well as short-range repulsive forces. The reason for this is that of the computing cost. The long-ranged attractive forces will necessitate the calculation of the interactions beyond the first shell of surrounding molecules. The pair interaction

itself will also be somewhat involved, comprising separation and orientational terms. However, the benefits of these simulations is in the use of more realistic interaction potentials and the retention of both spatial and temperature dependent effects.

One simulation of this type was that of Luckhurst and Romano [78] in which 256 translationally and orientationally free molecules interacted via a simple anisotropic pair potential based on the Lennard-Jones 12-6 potential. The system exhibited a weak first order transition from a nematic to an isotropic phase on increasing the system temperature.

We have used the Metropolis Monte Carlo technique to perform simulations on two models chosen to mimic the expected behaviour of the cyclic oligomer liquid crystals synthesised [79,80]. In both of these models, the molecules are allowed translational and rotational freedom and interact via anisotropic pair-potentials based on the Lennard-Jones 12-6 potential, thus comprising attractive and repulsive elements. Translational mobility was required in order to allow the possible formation of smectic or columnar discotic mesophases which might be expected to result from the complex nature of our molecules. In one of the models, the whole liquid crystal molecules are represented as soft disc entities and simulations of 50 discs in 2-D have generated partially ordered configurations in which the discs stack in columns. In the other model the cyclic backbones and the attached mesogens are represented individually and the simulations have exhibited a variety of phases dependent upon the temperature, density and, of particular interest, the strength of the coupling between the ring backbone and the attached mesogenic units.

Our application of the Monte Carlo method to the study of low molecular weight polymeric liquid crystal systems forms a natural progression from the study of monomeric liquid crystal systems, in parallel with the increased experimental interest in polymeric mesogens in recent years [5].

Another simulation technique which may be used in the study of fluids is that of 'molecular dynamics' [41]. The concept is very simple: the classical equations of motion for a box of N particles are repeatedly solved until the system reaches equilibrium. The real time path of the system is followed, unlike the artificial Markov process used in the Monte Carlo technique. Although the molecular dynamics approach has been applied to the study of some liquid crystal situations [81], the breadth of the application of this method has not been as wide as that of the application of the Monte Carlo technique to the study of liquid crystals [41]. Consequently, the Monte Carlo method seemed the more appropriate choice for our studies, providing us with a variety of documented applications of the technique from which to draw our inspiration and with which to make comparison. In particular, we have been able to compare our results with those of Luckhurst et.al. [78].

THE MEAN FIELD APPROXIMATION

The mean field approximation is a common first order approximation in the study of many body systems and has been applied to a variety liquid crystalline fluids [28,29,31,36,45-47,82-87]. In common with the Monte

Carlo method, the aim is the calculation of the expectation values of various properties of a system of particles interacting via a pair-wise potential, as given by equation 1.5, in which the kinetic energy dependence has been removed. Unlike the Monte Carlo method, an exact solution is not obtained, but rather the equation is reduced to a soluble form by the applications of successive averages and approximations.

Following the method outlined by P.J. Wojtowicz [13] we note that the pair interaction between axially symmetric molecules can be written as an expansion in spherical harmonic functions:

$$V_{ij} = 4\pi \sum_{L_i\ L_j\ m} U_{L_iL_jm}(r_{ij})\ \ Y_{L_im}(\theta_i,\phi_i)\ \ Y^*_{L_jm}(\theta_j,\phi_j) \qquad 1.7$$

where Y_{Lm} are the standard spherical harmonic functions and the angles are as defined in figure 1.9. For molecules with a mirror symmetry plane perpendicular to the rotational symmetry axis, the spherical harmonic terms with odd values of L drop from the series.

This pair-potential can be reduced to a single particle potential by the calculation of the potential experienced by particle i under the influence of the mean potential field created by the presence of all the other particles. Three averaging processes are involved. Firstly, the pair potential is averaged over all of the orientations of the relative position vector, $\underline{r}_{ij} = \underline{r}_i - \underline{r}_j$, with respect to the unique rotational symmetry axis of molecule i. Some assumption as to the distribution of these orientations is required, and that chosen here is that the orientations of the $\underline{r}_{ij}$ are evenly distributed

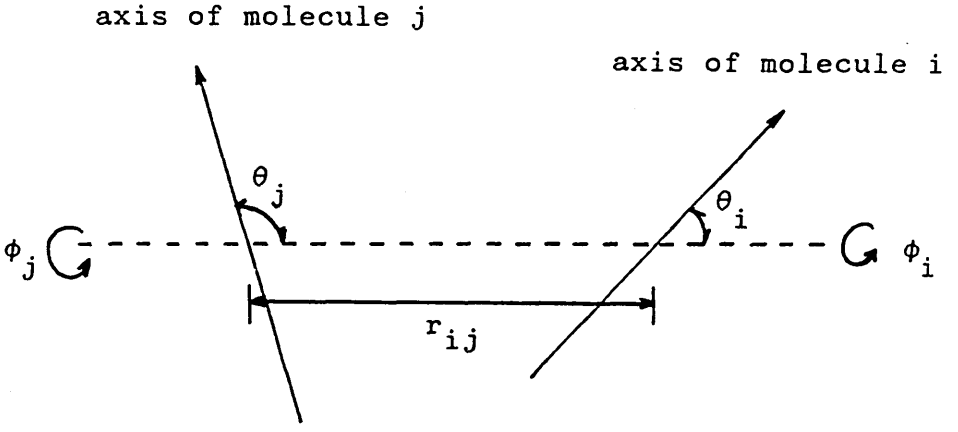

Figure 1.9 Full angular description of a pair of axially symmetric molecules.

on the surface of a sphere. This is a simplification of the real distribution present in a nematic fluid, which we might expect to possess cylindrical rather than spherical symmetry. This averaging process removes all terms in the interaction potential for which $L_i \neq L_j$.

The second average of V_{ij} is over all of the orientations of the unique symmetry axes of the molecules j with respect to the unique axis of molecule i. The potential resulting from these two orientational averages is:

$$\langle\langle V_i(\cos\theta)\rangle\rangle = \sum_L U_{LLm}(r) \langle P_L\rangle P_L(\cos\theta) \qquad 1.8$$

where θ is the angle between the unique axis of the i-th molecule and the director of the system, $\hat{\underset{\sim}{n}}$, and P_L are the usual Legendre polynomial functions.

Finally, an average is made over all values of the separation of the two particles, $|\underline{r}_{ij}|$ to give the following single particle potential:

$$V_i(\cos\theta) = \sum_L U_L \langle P_L\rangle P_L(\cos\theta) \qquad 1.9$$

where the U_L are given by

$$U_L = \sum_L \langle U_{LLm}(r)\rangle \qquad 1.10$$

and

$$\langle U_{LLm}(r)\rangle = \frac{1}{n}\int U_{LLm}(r)\, n_2(r)\, dr \qquad 1.11$$

where n is the number density of the molecules and $n_2(r)$ is the distribution function for the separation of pairs of molecules.

From equation 1.5 the expectation values of the P_L can be expressed in terms of the single particle potential in equation 1.9:

$$\langle P_L \rangle = \frac{\int P_L(\cos\theta)\, \exp(-V_i(\cos\theta)/k_BT)\, d\cos\theta}{\int \exp(-V_i(\cos\theta)/k_BT)\, d\cos\theta} \qquad 1.12$$

If N values of L are used in the original expansion of V_{ij} in equation 1.7 then there will be N equations of the form of equation 1.12 which will be self-consistent in the P_L and each of which will contain all the $\langle P_L \rangle$ within $V_i(\cos\theta)$ in the integrals on the right hand side. The simultaneous solution of these N equations at a given temperature yields the values of $\langle P_L \rangle$ at that temperature. Hence the temperature dependence of the $\langle P_L \rangle$ can be obtained, the solution for $\langle P_2 \rangle$ being the usual nematic order parameter. At some temperatures several solutions for the $\langle P_L \rangle$ are possible and in these cases it is necessary to calculate the free energies associated with these solutions to determine which one corresponds to the equilibrium state.

The results of the classic mean field theory of Maier and Saupe [45-47] may be obtained by using in the above derivation a pair-interaction potential which is dependent upon only the second order spherical harmonic functions. Only one self-consistent equation is obtained in this case:

$$\langle P_2 \rangle = \frac{\int P_2(\cos\theta)\, \exp(\nu P_2(\cos\theta)\langle P_2\rangle / k_B T)\, d\cos\theta}{\int \exp(\nu P_2(\cos\theta)\langle P_2\rangle / k_B T)\, d\cos\theta} \qquad 1.13$$

where ν is a measure of the strength of the pair-interaction.

The numerical solution of this equation yields three solutions for temperatures below $T = 0.22284\ \nu/k_B$ and just one solution, $\langle P_2 \rangle = 0$, above this temperature. These solutions are shown in figure 1.10. The solid lines represent the equilibrium solutions and the dashed lines the other solutions. The solution at low temperature is that of an ordered nematic, the order parameter of which, $\langle P_2 \rangle$, drops discontinuously from a value of 0.4289 to 0 at a critical temperature of $T_c = 0.22019\ \nu/k_B$.

The success of the Maier-Saupe theory lies in its prediction of a first-order transition from the nematic phase to the isotropic. However, quantitative comparisons with experimental measurements and Monte Carlo calculations have shown some discrepancies. For example, a comparison with a lattice model solved by the Monte Carlo technique [36] suggests that the transition temperature is too high in the Maier-Saupe theory by 17% and the spontaneous order parameter, $\langle P_2 \rangle$, at the transition too large by 25%. The entropy change at the transition was also found to be about a factor of four too large.

There has been some debate as to the source of the quantitative deficiencies of the theory [82-84]. It has been suggested that the prediction of a first-order transition is an artifact of the use of the mean field

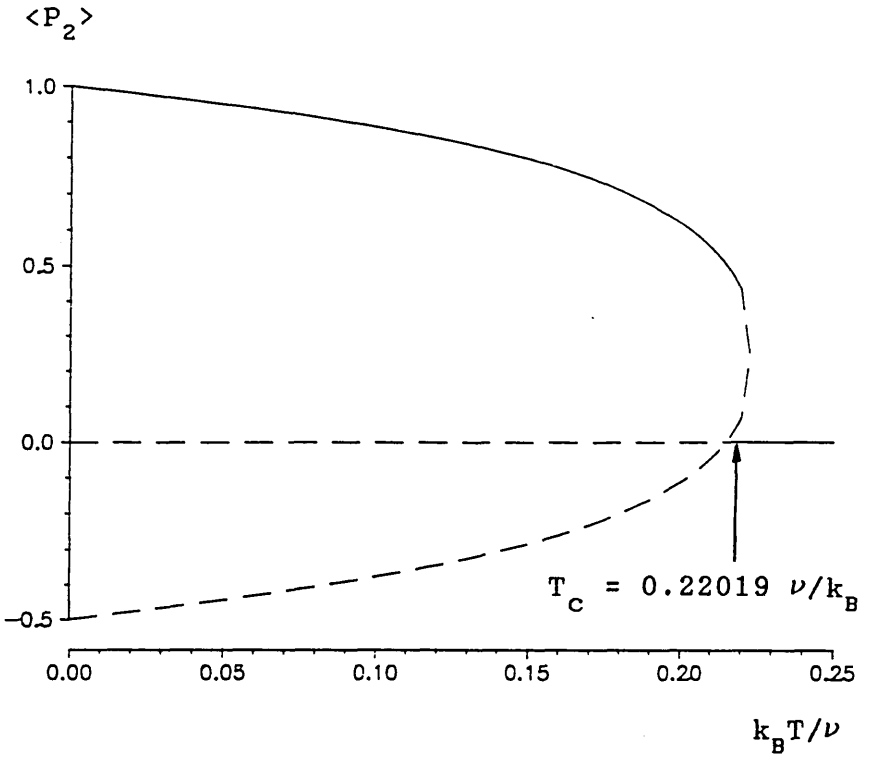

Figure 1.10 The solutions to the Maier-Saupe self consistent equation. The equilibrium solution is shown as a solid line.

approximation in the solution of the Maier-Saupe model [82]. Others, however, have extended the theory by the retention of the higher order, P_4, terms in the expansion of the pair potential and very good agreements with experimental data has been achieved in some cases [83].

In brief, the major limitations of the mean field approach in its application to the study of nematic liquid crystals lies in the neglect of short-range ordering and fluctuation effects. The loss of short-range ordering places too much emphasis on the longer range interactions, leading to an enhancement of the nematic ordering and the stability of the ordered phase. Pretransitional behaviour in the isotropic phase just above the critical temperature is precluded by these limitations of the mean field approximation.

Mean field calculations have been applied to a variety of liquid crystal systems more complex than that of rod-like nematogens. These have included the study of binary mixtures of rods and plates [85,86] and several polymer liquid crystal systems [28,29,31]. Of particular interest to us has been the work of Wang and Warner in which the uniaxial phases of comb-like liquid crystal polymers have been explored [31]. Various nematic phases were found in which either the polymer backbones or the rod-like side groups or both together exhibited positive ordering.

In parallel with our Monte Carlo models we have developed a further model of cyclic liquid crystal oligomers [87] which we have solve by means of a mean field approximation. We define a mean field which includes energy contributions for ring-ring, mesogen-mesogen, and ring-mesogen interactions. The uniaxial solution of this model has yielded two ordered phases: a

conventional calamitic nematic in which the rod-like mesogens align parallel and a discotic nematic in which it is the rings which tend to align parallel. The formation of these phases is dependent upon the relative strengths of the three energy contributions, the number of mesogens attached to a ring and temperature.

CHAPTER 2 MEASUREMENTS

INTRODUCTION

We have studied a series of oligomers which are the cyclic homologues of the linear side-chain liquid crystal polymers synthesized by Finkelmann et al. [88,89]. The chemical structure of these cyclic oligomers has been given in figure 1.8 in chapter 1. These comprise cyclic dimethylsiloxane backbones with biphenyl mesogenic units attached as side chains via alkyl spacer units. Samples of five liquid crystalline oligomers were available for investigation which allowed us to study the effects of altering the number of repeat units in the ring or the length of the alkyl spacer. An estimate of the relative sizes of the constituent parts of these oligomers has been made by the use of molecular graphics software. The over all phase behaviour of the materials was studied by optical microscopy and D.S.C. techniques, and the dielectric behaviour of the samples was studied in the temperature region of the mesogenic to isotropic phase transition.

For convenience, the cyclic liquid crystal materials will be referred to by abbreviations of the form DxCy where 'x' corresponds to the number of repeat units in the siloxane backbone and 'y' is the number of $-CH_2-$ units in the alkyl spacer. Table 2.1 lists the available materials using this notation, separating them into two homologous series according to variation in the spacer length and variation in the size of the cyclic backbone.

D4C4 D4C6	spacer variation
D4C4 D5C4 D6C4 D7C4	ring size variation

Table 2.1 The available cyclic liquid crystal oligomers, separated into two homologous series.

BOND LENGTHS:	C-C	1.54 Å
	C-C (benzene ring)	1.38 Å
	C=O	1.34 Å
	C-O	1.51 Å
	C-Si	1.87 Å
	Si-O	1.61 Å
	C-H	1.09 Å
	C-H (benzene ring)	1.02 Å
BOND ANGLES:	all Si, O, C	109°
	except:	
	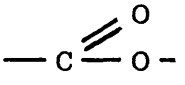	120° coplanar
	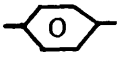	120° coplanar

Table 2.2 Bond lengths and bond angles used in the construction of the molecular graphics model of D4C4. Bond lengths obtained from covalent radii [90,91].

MOLECULAR DIMENSIONS

A molecular graphics package [90] has been employed in the construction of a model of a possible molecular structure of one of our oligomeric compounds, D4C4. Estimates of the dimensions of the major elements of the structure have been obtained from measurements made on this graphical model.

The bond-lengths used in the construction of the molecule were obtained from mean covalent bond radii [90,91] and are listed in table 2.2 together with the bond angles employed. In the construction of the mesogenic moieties, the benzene rings and the carboxyl group were constrained to be coplanar, with the 1-4 axes of the benzene rings parallel [92-94]. Other torsion angles about the bonds were chosen arbitrarily. The resultant mesogen and four membered alkyl spacer are shown in figure 2.1. A four membered ring of cyclic poly(dimethylsiloxane) was constructed in which the silicon atoms were fixed in one plane and the oxygen atoms fixed in a second plane parallel to the first, thus making a regular structure as shown in figure 2.2. Note that for the four membered ring oligomer, four of the $Si-CH_3$ bonds radiate from the ring structure in the plane of the Si atoms. The attachment of the alkyl spacers to the siloxane ring via these splay bonds results in the structure for the complete molecule given in figure 2.3.

Several points should be noted with regard to the construction of this molecule. The method of construction of this graphical model does not indicate the synthesis route used in the manufacture of the physical compounds [34,35]. The structure presented is just one of many possible conformations for these

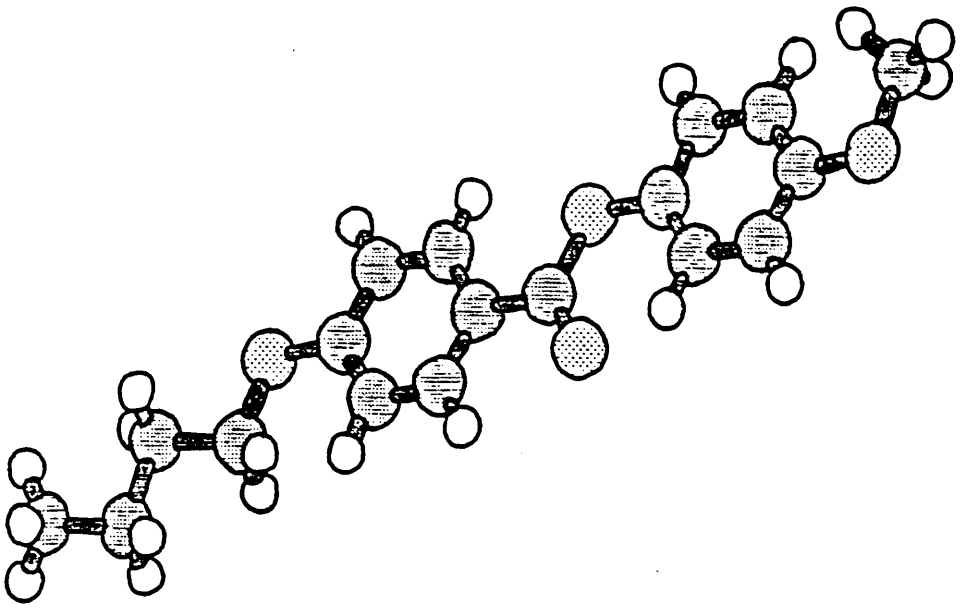

Figure 2.1 Molecular graphics model of the mesogen and four membered spacer: CH_3-$(CH_2)_3$-$OC_6H_4COOHC_6H_4)CH_3$.

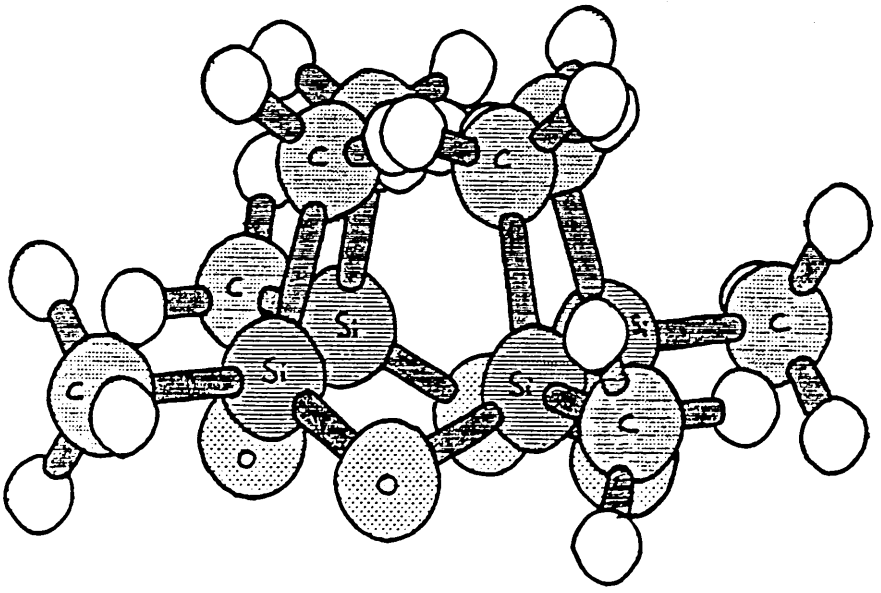

Figure 2.2 Molecular graphics model of cyclic $(dimethylsiloxane)_4$.

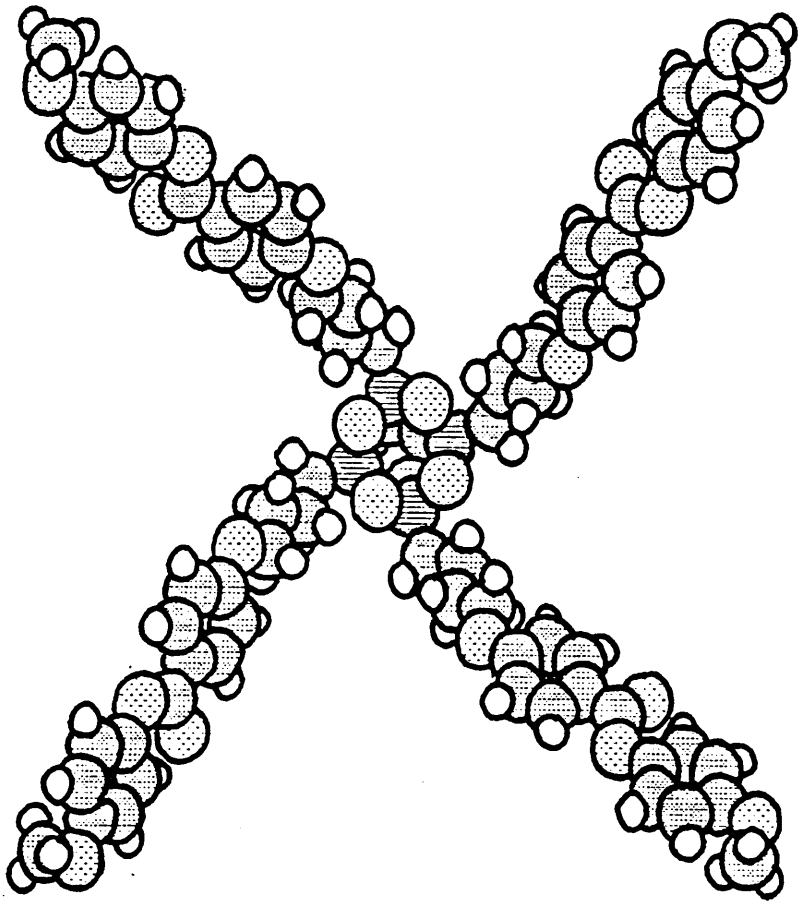

Figure 2.3 A molecular graphics construction of D4C4.

compounds and no minimum energy calculations have been involved in the construction. We expect the physical samples provided to contain a mixture of molecular conformations with only a proportion of the alkyl spacers attached to the siloxane rings in approximate splay conformations. The actual molecules will exhibit some flexibility, particularly in the alkyl spacer units and in the polymer ring backbone, dependent upon the number of repeat units in each [34]. We would expect the benzene ring pair, coupled by the carboxyl group, to provide an essentially rigid structure within the mesogenic moieties [92-94].

However, the molecular graphic model as constructed gives us insight into the interplay between the constituent parts of the molecules and their relative dimensions. If we consider as our simplified picture of the molecules a planar ring, with rod-like mesogenic units attached equidistant around the ring via spacer units, then we can make measurements on our graphical model to estimate the dimensions of the constituent parts of our idealised molecule. The relevant dimensions are the diameter of the central ring, the length of the spacer units and the length and diameter of the rod-like mesogens. The actual measurements made in three dimensions on the molecular structure are shown in figure 2.4. Owing to the possibility of other molecular conformations, these measurements should be treated as approximate.

From these measurements it is seen that the shape of the mesogenic part can be approximated to that of a rectangular prism some 13.2 Å long by 4.2 Å wide with a thickness of one atomic diameter, which we can take as approximately 1.5 Å. However, it is usual as a first approximation to reduce the shape of a nematogen to that

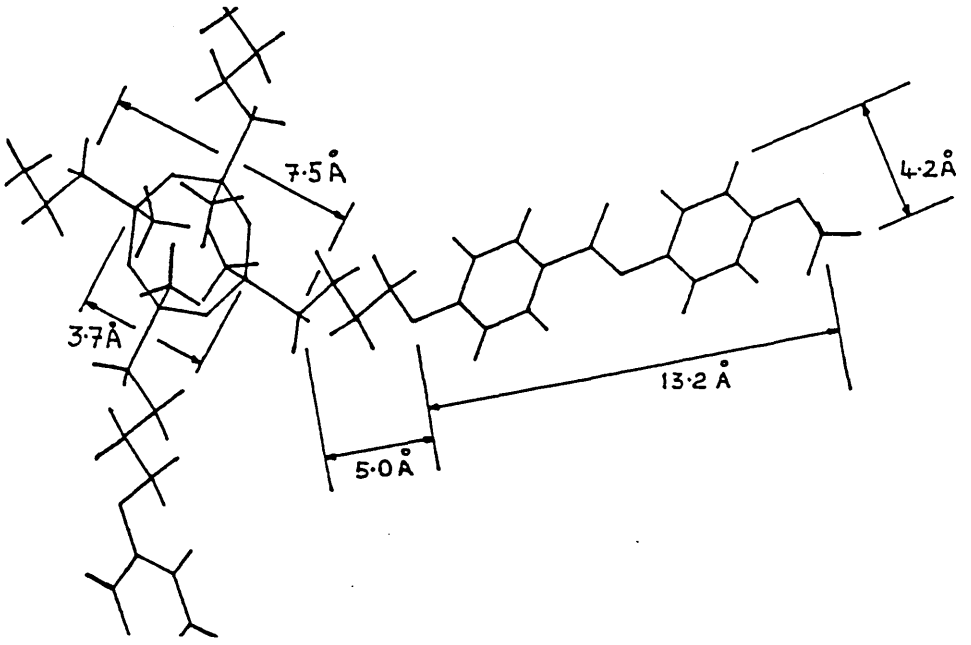

Figure 2.4 The distances measured from the model of D4C4.

MESOGEN	ROD LENGTH	13.2 Å
	ROD DIAMETER	4.2 Å
SPACER UNIT (length)	4-MEMBERED	5.0 Å
	6-MEMBERED	7.5 Å
RING DIAMETER	4-MEMBERED	5.6 Å
	5-MEMBERED	6.4 Å
	6-MEMBERED	7.1 Å
	7-MEMBERED	7.9 Å

Table 2.3 Approximate lengths of the basic units of the cyclic liquid crystal oligomers.

of a cylinder. Such a cylindrical shape may be obtained by the rotation of the lath-like mesogen about its long axis. The length of the $(CH_2)_4$ spacer is 5 Å, somewhat larger than one third of the length of the mesogenic unit. It is less clear how to define the diameter of the oligomer ring, and two measurements have been made: one the diameter of the circle of Si atoms and the other the diameter of the larger circle which includes the first C atoms of the flexible spacer when attached in a planar radial conformation. However, it is known that in the samples provided the spacer units will not all be attached to the backbone via radial bonds and so the mean of these two measurements, 5.6 Å, is adopted as the diameter of the idealised ring backbone.

Table 2.3 lists the approximate sizes the constituents of the idealised molecules for all of the compounds available. More involved calculations of the radii of gyration of cyclic dimethylsiloxane polymers have been undertaken [95,96], but these were for larger rings than in our oligomers. However, comparison the radius of gyration of an eight membered poly(dimethylsiloxane) ring is quoted as 4.5 Å, which compares well with the value of 4.4 Å as calculated by our method. It would be expected that our calculations would provide a reasonable estimate of the ring diameters for the smaller rings in which the number of available conformations is limited.

THERMAL AND OPTICAL MEASUREMENTS

Phase transition temperatures were measured by direct scanning calorimetry using a Mettler TA3000

scanner. These measurements were supported by optical observations using a polarising microscope with a hot-stage which had a temperature resolution of 0.1° Celsius.

The glass transition temperatures, T_g, and the clearing temperatures, T_c, are given in table 2.4 for the available materials. These were measured by D.S.C. calibration, cooling at a rate of 10°C/min from the isotropic phase. The clearing temperatures were confirmed by optical observation and for all of the materials the optical characteristics below T_c suggested possible nematic behaviour. In general the glass transition temperatures are about 10°C and the clearing temperatures about 90°C. In the case of D4C4, crystallites were seen to persist at temperatures above the clearing of the bulk of the fluid and to undergo a monotropic transition into the isotropic phase at 107°C. The density of the crystallites was increased when the sample was annealed for several hours at 50°C before heating beyond T_c on the optical stage. On cooling, a birefringent phase was not produced until the temperature dropped below 84°C. Repeated D.S.C. scans of D4C6 at 5°C/min indicated the formation of possibly crystalline forms at about 50°C for this material also. However, this form did not persist beyond the clearing temperature. Although further detailed examination of the phase behaviour of the other materials was not possible, these also may exhibit more than one phase between T_g and T_c. However, owing to the high viscosity of the materials, the exact form, or mixture of forms, would largely be dependent upon the thermal history of the sample.

compound	T_g (°C)	T_c(°C)
D4C4	8	84, 107 (see text)
D4C6	5	93
D5C4	6	83
D6C4	8	93
D7C4	13	92

Table 2.4 Glass transition temperature, T_g, and clearing temperature, T_c, of the cyclic oligomers.

compound	activation energy (eV)
D4C4	1.818
D4C6	1.572
D5C4	1.677
D6C4	1.740
D7C4	1.673

Table 2.5 Arrhenius activation energies of the cyclic oligomers.

Dielectric measurements were made using glass capacitance cells in a parallel plate configuration with a grounded guard-ring. The plates were kept 50 μm apart using mylar spacers and had an active area of one square centimetre. Electrical connections to the sample were achieved by an indium tin oxide coating and the plates were surface treated with Cr-complex to favour homeotropic alignment of the liquid crystals in the absence of an external aligning field. The cells were calibrated with air before filling with the oligomers by capillary action at a temperature a few degrees above the transition to the isotropic phase.

The capacitances of the filled cells were measured over the frequency range of 50Hz to 1MHz using a Hewlett Packard self balancing bridge HP4129A. The cells were held in a shielded holder and heated by a hot air temperature controller system. Homeotropic and homogeneous alignment were induced by a magnetic field of 1.5 T provided by a Newport electro-magnet with 7" diameter poles.

The method of measurement involved heating the filled cell into the isotropic phase and then applying the magnetic field to induce homeotropic alignment as the cell was cooled in stages into the liquid crystalline phase. Capacitances were measured over the full frequency range at each temperature. It was not generally possible to make repeatable measurements below 50° Celsius as it was found that the capacitances drifted indefinitely, probably due to the high viscosity of the materials and the possible formation of other crystalline forms at these temperatures.

After measurements had been taken at the lowest temperature the cell was heated again into the isotropic phase, turned through 90° to give homogeneous alignment, and measurements were again made as the cell was cooled in stages. Good alignment in the liquid crystalline phases was confirmed by the fact that the relaxations observed in the dielectric permittivities for homeotropic (parallel) alignment were not observed in the permittivities for homogeneous (perpendicular) alignment.

The measurements obtained from the bridge were the capacitance, C, and the quality factor, Q, of the equivalent parallel resistor-capacitor circuit. The real component of the complex dielectric permittivity, ε', was obtained from:

$$\varepsilon' = \frac{C}{C_0} \qquad 2.1$$

where C_0 was the capacitance of the cell when filled with air.

The resistive part of the circuit is related to the imaginary component of the complex dielectric permittivity, known as the dielectric loss, ε'', which was calculated from:

$$\varepsilon'' = \frac{\varepsilon'}{Q} \qquad 2.2$$

The parallel dielectric permittivities of D4C4 are given in figure 2.5 as a function of frequency. A single clear relaxation process is observed within the frequency and temperature ranges of the measurements. Corresponding peaks in the parallel dielectric loss are

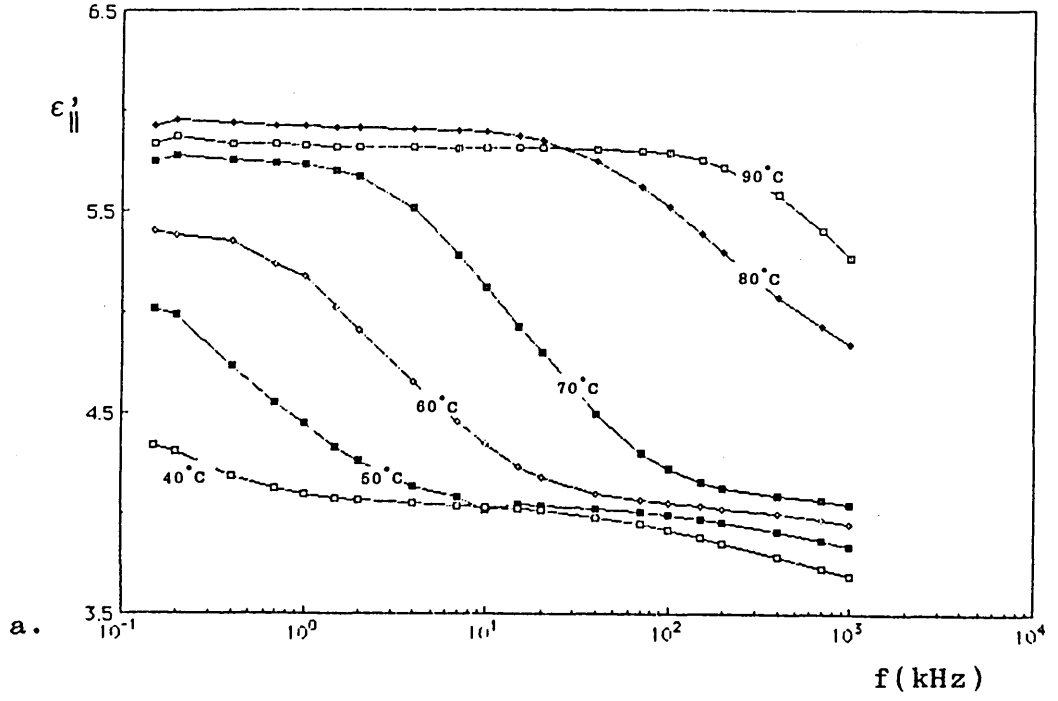

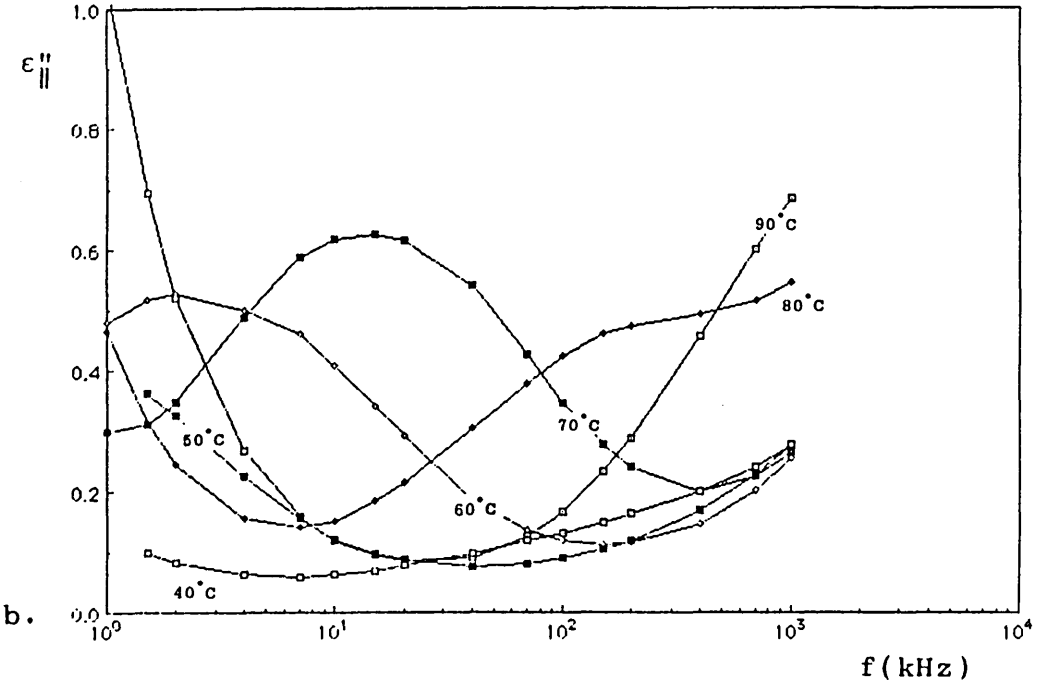

Figure 2.5 Parallel components of a) dielectric permittivity, $\epsilon'_{\parallel}$ and b) dielectric loss, $\epsilon''_{\parallel}$, plotted against frequency for the compound D4C4.

also observed and are shown separately in the same figure. The perpendicular dielectric permittivities of D4C4 shown in figure 2.6 do not exhibit relaxations over the same range of frequency and temperature as those for the parallel permittivities, and neither are there any peaks in the perpendicular dielectric loss. However, there is some fall off of the perpendicular permittivity at high frequency which may be the result of another relaxation process or possibly due to the finite resistance of the tin oxide conductor. This high frequency fall off is also observed in the parallel permittivity. The material is clearly dielectrically negative (ie. $\varepsilon'_{\parallel} - \varepsilon'_{\perp} < 0$), resulting from the large transverse component of the dipole in the mesogenic side chains [97]. The lack of a dominant longitudinal dipole in the mesogenic units prevented the simple estimation of the nematic order parameter from these dielectric measurements [17].

The existence of the relaxations only in the parallel permittivities confirms that good alignment was achieved for both orientations and suggests the δ-relaxation due to end to end motions of the mesogens.

The dielectric permittivities for the other materials showed qualitatively similar behaviour to that of D4C4.

The Debye theory of dielectric relaxation predicts a single relaxation frequency for dielectric material [98,99b]. The complex dielectric permittivity is given

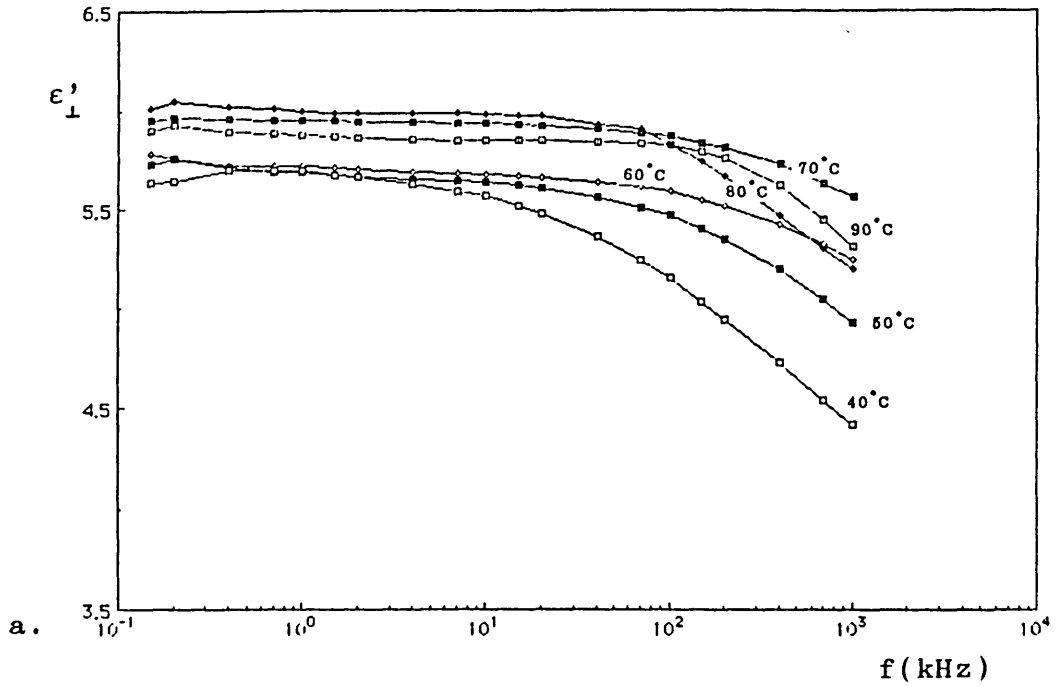

a.

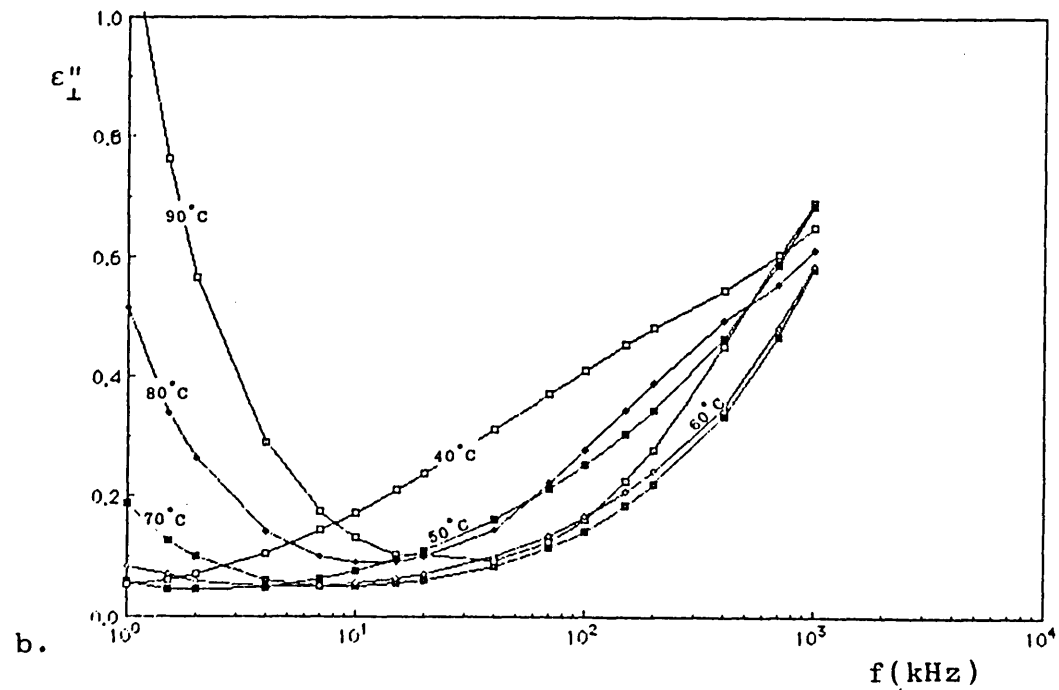

b.

Figure 2.6 Perpendicular components of a) dielectric permittivity, $\varepsilon'_{\perp}$ and b) dielectric loss, $\varepsilon''_{\perp}$, plotted against frequency for the compound D4C4.

as:

$$\underline{\varepsilon}(\omega) - \varepsilon'_\infty = (\varepsilon'_s - \varepsilon'_\infty) \frac{1}{1 + i\omega\tau_0} \qquad 2.3$$

$$i = \sqrt{-1}$$

where ε'_∞ is the dielectric permittivity at infinitely high frequency and ε'_s is the static dielectric permittivity. τ_0 is the relaxation time of the material and ω is the angular frequency of the measurement.

From equation 2.3 it can be shown that the plot of the dielectric loss against the real part of the complex dielectric permittivity is that of a semi-circle. The Debye theory has been extend by Cole and Cole to allow for a spread of relaxation times, in which case the equation for the dielectric permittivity becomes:

$$\underline{\varepsilon}(\omega) - \varepsilon'_\infty = (\varepsilon'_s - \varepsilon'_\infty) \frac{1}{1 + (i\omega\tau_0)^{1-\alpha}} \qquad 2.4$$

where τ_0 is here the mean relaxation time. The plot of ε'' against ε' is now part of a semi-circle, the centre of which is depressed below the $\varepsilon''=0$ axis. The parameter α is related to the amount by which the semi-circle is depressed below the axis and is a measure of the broadening of the relaxation. The minimum value of α is zero, which corresponds to a single relaxation time, and the maximum value is unity.

The Cole-Cole plots for the parallel permittivities of all of the materials were nearly semi-circular with the centre depressed below the ε'- axis, corresponding to broadened Debye-like relaxations. As an example, the Cole-Cole plot of D4C4 for 70°C is given in figure 2.7.

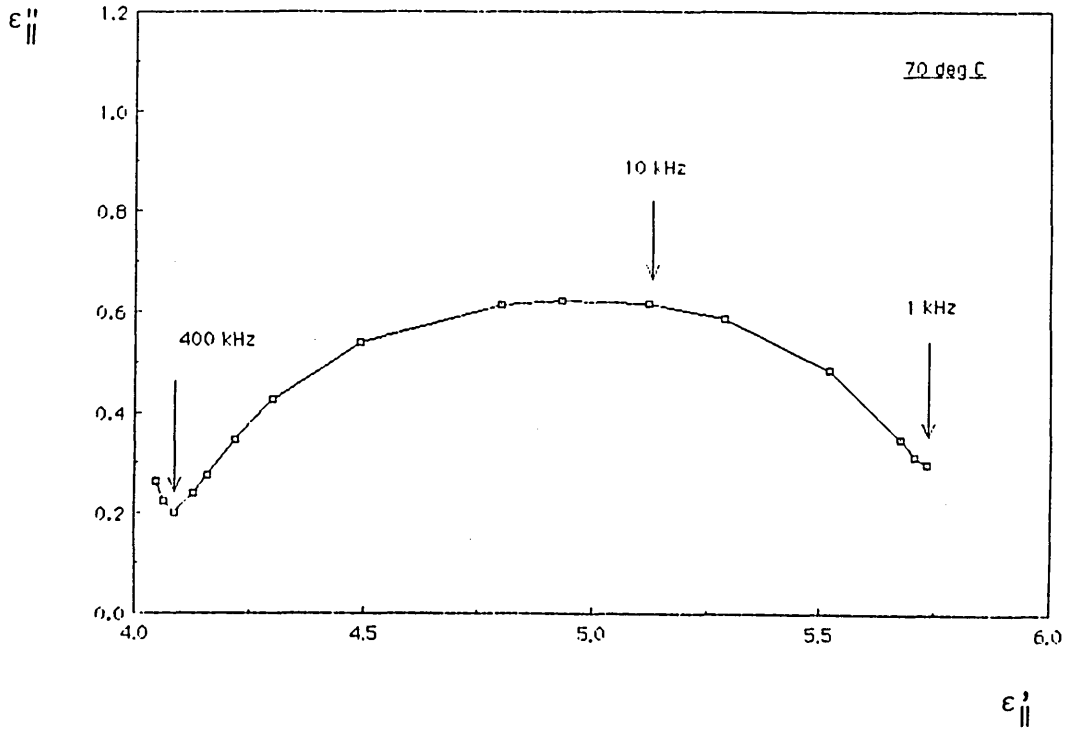

Figure 2.7 Cole-Cole plot for D4C4 at 70°C in parallel configuration.

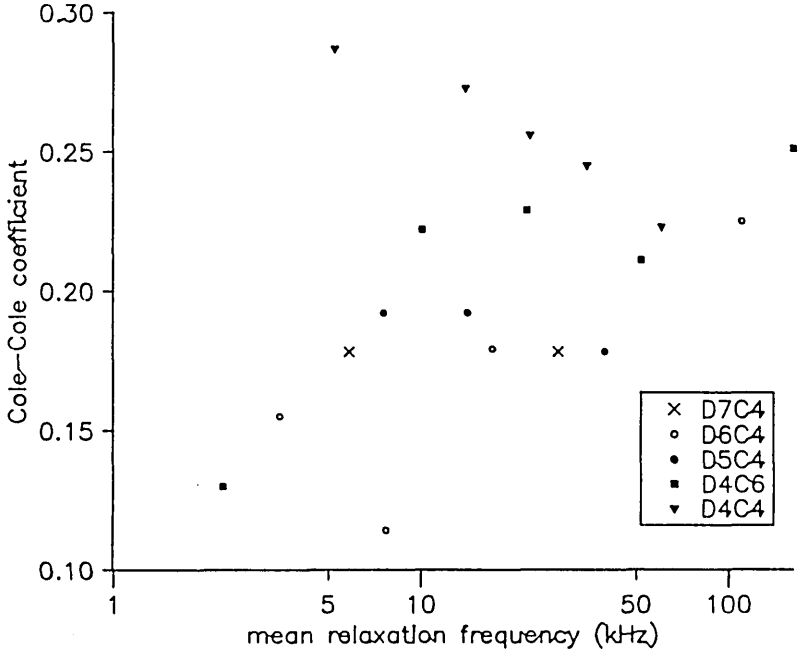

Figure 2.8 Plot of Cole-Cole broadening coefficient, α, against mean relaxation frequency for the five compounds.

Cole-Cole plots were constructed for all suitable relaxations of the materials and the broadening parameter, α, calculated from the depression of the semi-circle. These Cole-Cole parameters are plotted as a function of relaxation frequency in figure 2.8. The broadening is largest for D4C4, the molecule with the smallest ring and the shortest spacer, averaging $\alpha \approx 0.26$. For this material there is an apparent trend in which α diminishes as the relaxation frequency is increased. However, for the other materials, the α are scattered and show no clear trends. For D4C6 the average broadening parameter is $\alpha \approx 0.21$, 0.05 lower than that for D4C4. It would appear that the effect of lengthening the spacer by two $-(CH_2)-$ units is to increase the decoupling of the mesogenic units from the broadening effect of the ring backbone. The reduction in the α is even more pronounced as the number of repeat units in the ring is increased. The average of α for D5C4, D6C4 and D7C4 is about 0.18.

Another method of estimating the broadening of relaxation times was developed by Fuoss and Kirkwood, whose relation is [99b]:

$$\cosh^{-1}(\varepsilon''_{max}/\varepsilon'') = \beta \ln(f/f_0) \qquad 2.5$$

where ε''_{max} is the peak value of the dielectric loss and f_0 is the corresponding mean frequency of the relaxation. The Fuoss-Kirkwood coefficient, β, can be calculated from the slope of the curve $\cosh^{-1}(\varepsilon''_{max}/\varepsilon'')$ against $\ln(f)$. Such curves are shown in figure 2.9 for D4C4. The coefficient takes the value $\beta = 1$ for a pure Debye relaxation of a single frequency and lower values for broadened relaxations. The β were calculated for all the materials for all suitable loss peaks and figure 2.10 shows against f_0. Again, the largest broadening occurs

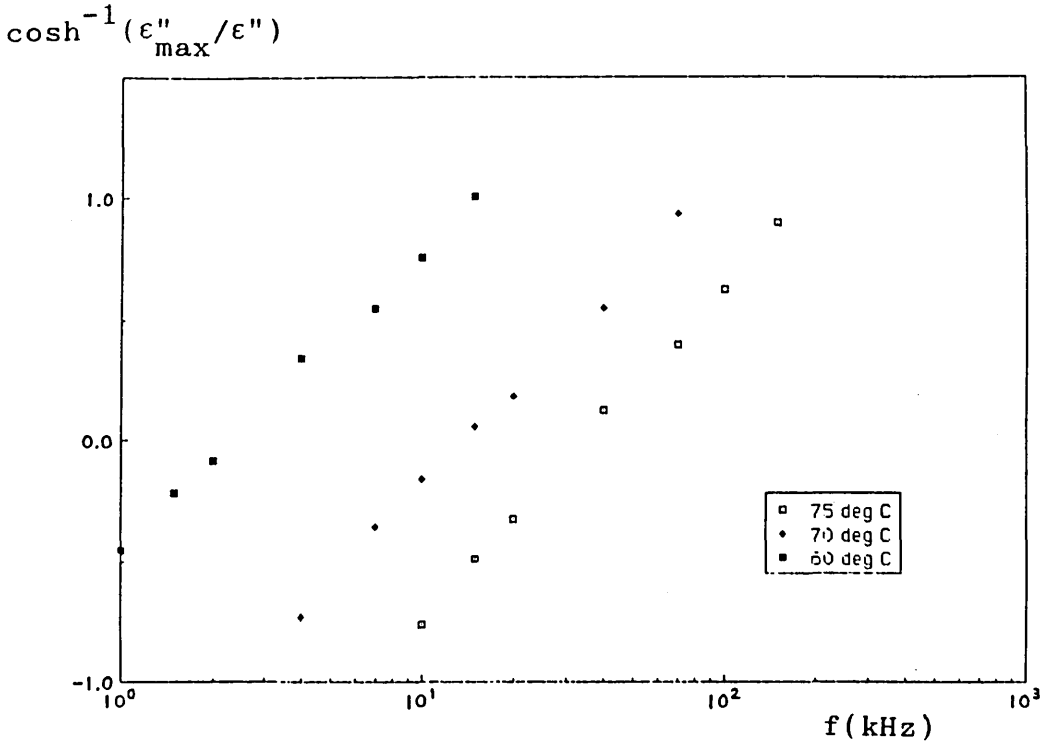

Figure 2.9 cosh$^{-1}(\varepsilon''_{max}/\varepsilon'')$ against frequency for D4C4.

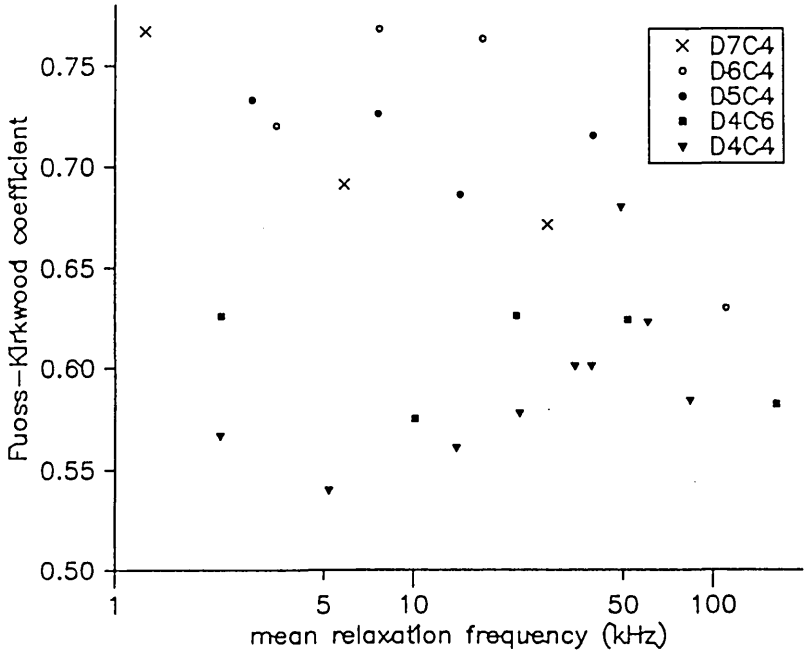

Figure 2.10 Plot of Fuoss-Kirkwood parameter, β, against frequency for the five compounds.

for D4C4, for which $\beta \approx .60$ is typical. The addition of two alkyl units to the spacers results in an increase in β to about 0.61 for D4C6. A more marked increase in β of approximately 0.12 is observed to correspond to an increase in the number of repeat units in the ring backbone. The average value for D5C4, D6C4 and D7C4 is $\beta \approx 0.72$.

Relaxation processes may also be modelled by a system with two energy states [99a] in which the mean relaxation frequency, f_0, is related to the potential energy barrier, ΔW, separating the two states:

$$f_0 = A \exp(-\Delta W/k_B T) \qquad 2.6$$

where A is some constant. A measure of the activation energy, ΔW, can be therefore be obtained from the slope of the plot of $\ln f_0$ against $1/T$; such a plot is known as an Arrhenius plot. Figure 2.11 gives the Arrhenius plot for the relaxations in the homologous series of molecules of increasing ring size. There is a linear dependence of the relaxation frequencies on the inverse temperature, with a slight curvature in D4C4 at high temperature as the isotropic phase is approached. The slope of the linear part of the D4C4 plot is clearly greater than that of the molecules with larger rings, and the activation energies as calculated from the slopes are given in table 2.5. There is clearly a general reduction in the activation energy as the size of the polymer ring increases. This could be explained by a decrease in the rigidity of the ring as the number of repeat units is increased resulting in the ring playing a less dominant part in the relaxation processes. The Arrhenius plots for the homologous series with the spacer length increasing are given in figure 2.12. Again a linear relation is observed and the slope for D4C4 is larger

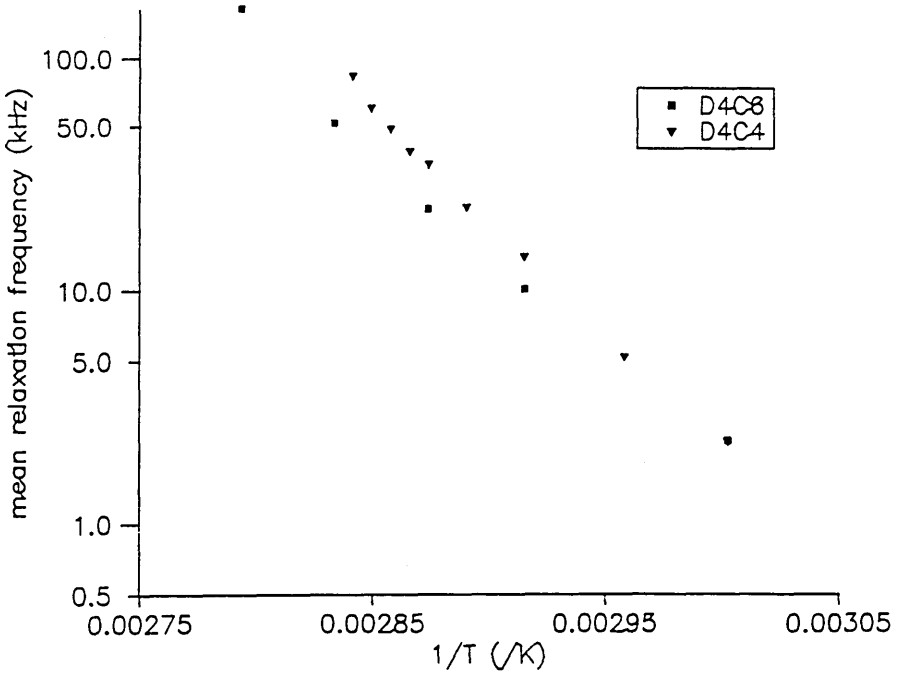

Figure 2.11 Arrhenius plot for D4C4 and D4C6.

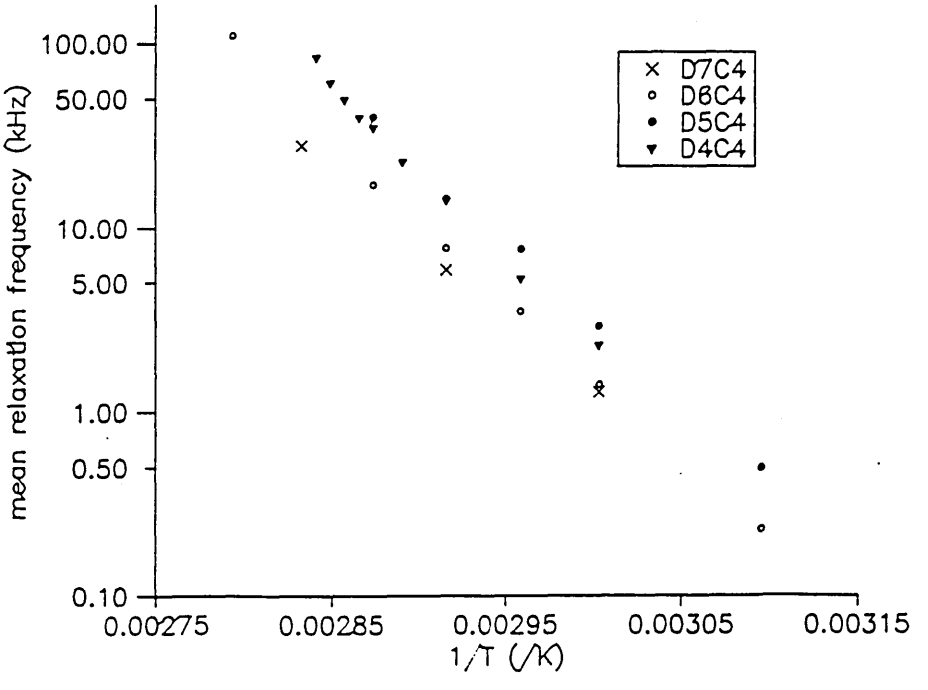

Figure 2.12 Arrhenius plot for D4C4, D5C4, D6C4, D7C4.

than that for D4C6. The corresponding activation energies are given in table 2.5. The decoupling of the mesogenic unit from the ring by the lengthened spacer results in a substantial decrease in the activation energy for D4C6 when compared to D4C4.

As the polymer ring size or alkyl spacer length is increased the spread in the relaxation times becomes narrower. This effect is more marked for changes in ring size. Conversely, the decrease in the activation energy is larger for the increase in spacer length than for the increase in ring size. The rigidity of the alkly spacer makes the dominant contribution to the potential barrier associated with the relaxation of the rod-like mesogenic units. However, it is the polymer ring environment which mostly affects the broadening mechanism.

CONCLUSIONS

A molecular graphic representation of the compound D4C4 has been constructed and from which the approximate dimensions of the molecular building blocks of these materials has been measured. We have shown that the side chains may be attached to a four membered poly(dimethylsiloxane) ring by means of radially splay bonds although in the physical samples supplied we expect a variety of bond angles. However, we suggest that it should be possible to synthesise a molecule with short alkyl spacers in which the mesogens adopt a fairly rigid planar splay conformation. Such a material might be expected to exhibit discotic mesogenic behaviour.

The five cyclic oligomers examined exhibit one or

more mesophases between the glass transition temperature and the clearing temperature. Two of the compounds, D4C4 and D4C6, have been shown to exist in at least two forms in the liquid phase below their respective clearing temperatures and it is likely that the other compounds may also exhibit more than one birefringent phase under normal laboratory conditions. From optical observations it is suggested that the phase dominant just below the clearing temperature is nematic for all of the materials, although this would need to be confirmed by, for example, X-ray diffraction.

Dielectric studies have revealed a clear relaxation in the parallel component of the dielectric permittivity present in the temperature range 50°C to 100°C for all of the samples. This relaxation is not pure Debye, but is broadened and the amount of broadening has been quantified in terms of the Cole-Cole parameter, α, and the Fuoss-Kirkwood coefficient, β. The broadening is most pronounced for the compound whose molecules have the smallest ring backbone and the shortest length of alkyl spacer between the backbone and the mesogenic units, namely D4C4. From Arrhenius plots, activation energies have been calculated for the relaxations and D4C4 has the highest activation energy. The activation energy is sensitive to the length of the alkyl spacer unit, the molecule with the longer spacer exhibiting a lower activation energy, although the size of the cyclic backbone also affects the activation energy of the relaxation.

CHAPTER 3 SOFT DISC MODEL

THE MOLECULAR INTERACTION POTENTIAL

This model was developed to investigate by Metropolis Monte Carlo simulation the properties of a system of cyclic liquid crystal oligomer molecules represented by a simple intermolecular potential.

In this model, each complex, multi-component, oligomeric liquid crystal molecule is represented as a single entity by a pair interaction potential. A spherical Lennard-Jones 12-6 potential is used to model the cyclic polymer backbone and the average effect of splay conformations of the attached mesogenic moieties is provided by the addition of a ring of softer potential in the form of an angular dependent r^{-9} term. This gives an essentially disc-like object as shown in figure 3.1.

The interaction between rod-like liquid crystal molecules is commonly represented as an intermolecular potential which depends solely upon the separation of the molecules and the angle between their symmetry axes [43-47,78]. However, this angular simplification leads to some unrealistic packing properties of the molecules as shown, for example, in figure 3.2. In order to allow the construction of an interaction potential which gives more realistic treatment to the two disc configurations shown in the figure, a fuller angular description of the molecular relationships is required, such as that given in figure 1.9 in chapter 1.

As discussed in the introduction, the interaction

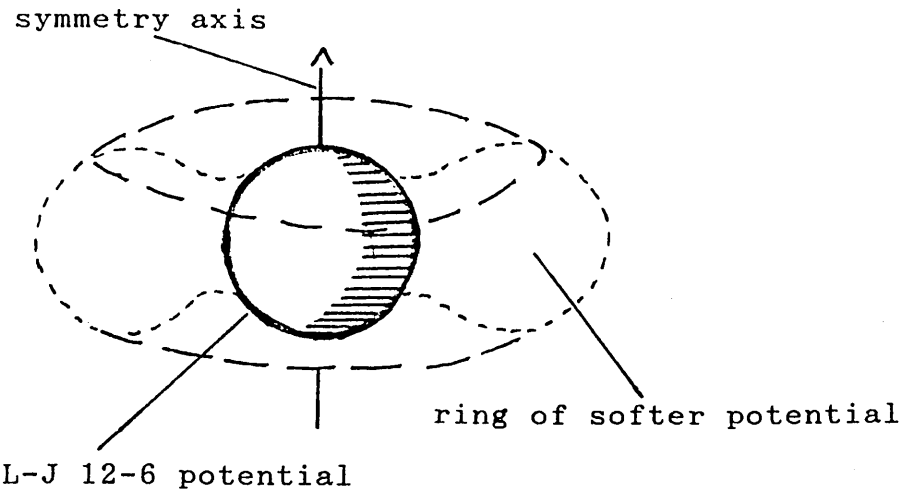

Figure 3.1 The approximate shape of the molecules in the Soft Disc model.

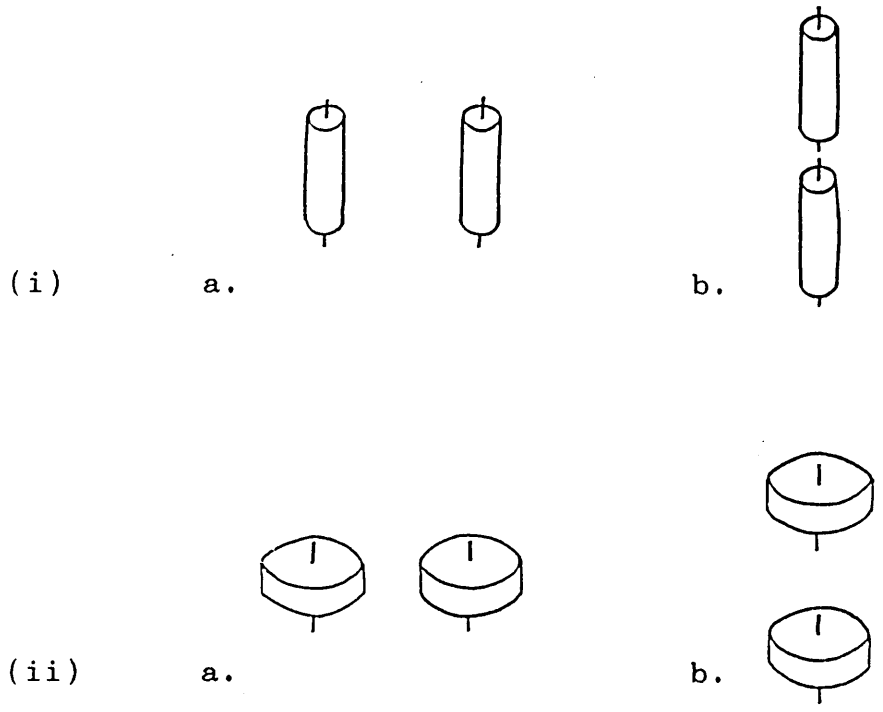

Figure 3.2 Parallel configurations of two i) rod-like and ii) disc-shaped molecules. Configurations (a) and (b) have the same energy at equal separations if the interaction potential is angularly dependent only on the angle between the molecular symmetry axes.

potential for a pair of axially symmetric molecules can be represented in the following standard expansion [13]:

$$V_{ij} = 4\pi \sum_{L_i\ L_j\ m} U_{L_iL_jm}(r_{ij})\ \ Y_{L_im}(\theta_i,\phi_i)\ \ Y^*_{L_jm}(\theta_j,\phi_j) \qquad 3.1$$

where Y_{Lm} are the usual spherical harmonic functions and the angles are as defined in figure 1.9.

For molecules with a mirror symmetry plane perpendicular to the rotational symmetry axis, the spherical harmonic terms with odd values of L drop from the series, and our interaction potential is represented as such a series of spherical harmonic terms truncated after the second order terms.

The modified Lennard-Jones potential used was taken to have the following form:

$$V_{ij} = 4\ \varepsilon \left\{ \left(\frac{\sigma}{r_{ij}}\right)^{12} - \left(\frac{\sigma}{r_{ij}}\right)^{6} + F(\theta_i,\phi_i,\theta_j,\phi_j) \left(\frac{\sigma}{r_{ij}}\right)^{9} \right\} \qquad 3.2$$

The values of $F(\theta_i,\phi_i,\theta_j,\phi_j)$ were calculated to give the proposed separations of the molecules in specific configurations of two molecules which are shown in figure 3.3. The expansion (equation 3.1) was then equated to the modified Lennard-Jones interaction (equation 3.2) in these configurations to determine the coefficients of the spherical harmonic terms. The potential was simplified by the omission of the ϕ_i,ϕ_j dependence in order to make efficient use of computing time. The resulting potential

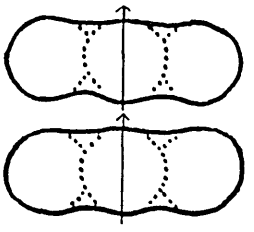

A. equilibrium separation = a_0

$\theta_i = 0^\circ$, $\theta_j = 0^\circ$

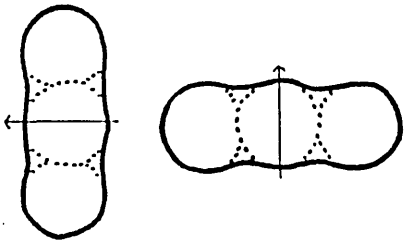

B. equilibrium separation = 2 a_0

$\theta_i = 0^\circ$, $\theta_j = 90^\circ$

C. equilibrium separation = 4 a_0

$\theta_i = 90^\circ$, $\theta_j = 90^\circ$

Figure 3.3 Specific equilibrium configurations of the molecules used to define the Soft Disc pair interaction potential. a_0 is the equilibrium separation for the standard Lennard-Jones 12-6 potential.

used in the simulations is given by:

$$V_{ij} = 4\,\varepsilon \left\{ \left(\frac{\sigma}{r_{ij}}\right)^{12} - \left(\frac{\sigma}{r_{ij}}\right)^{6} + \left(\frac{\sigma}{r_{ij}}\right)^{9} \cdot \left(\frac{85}{2} - \frac{71}{2} \left(\cos^2\theta_i + \cos^2\theta_j \right) + \frac{57}{2} \cos^2\theta_i \cos^2\theta_j + \frac{35}{2} \sin^2\theta_i \sin^2\theta_j \right) \right\} \qquad 3.3$$

Contour diagrams and isometric projections of this potential are presented in figure 3.4 for specific configurations of the molecules.

COMPUTING DETAILS

Simulations were performed with the centres of the molecules constrained to lie in a plane, but still allowed free translational motion in 2-D and rotational freedom in 3-D. The restriction to a plane increased the speed of the simulation and allowed configurations to be presented in a simple diagrammatic form, from which the ordering in the system could be observed. The simulations were performed in the NVT ensemble as, in general, the volume change at the nematic to isotropic phase transition is known to be small [67,100].

New configurations were obtained by choosing a molecule at random and moving it in one of two ways, a translation or a rotation. For a translational move, the

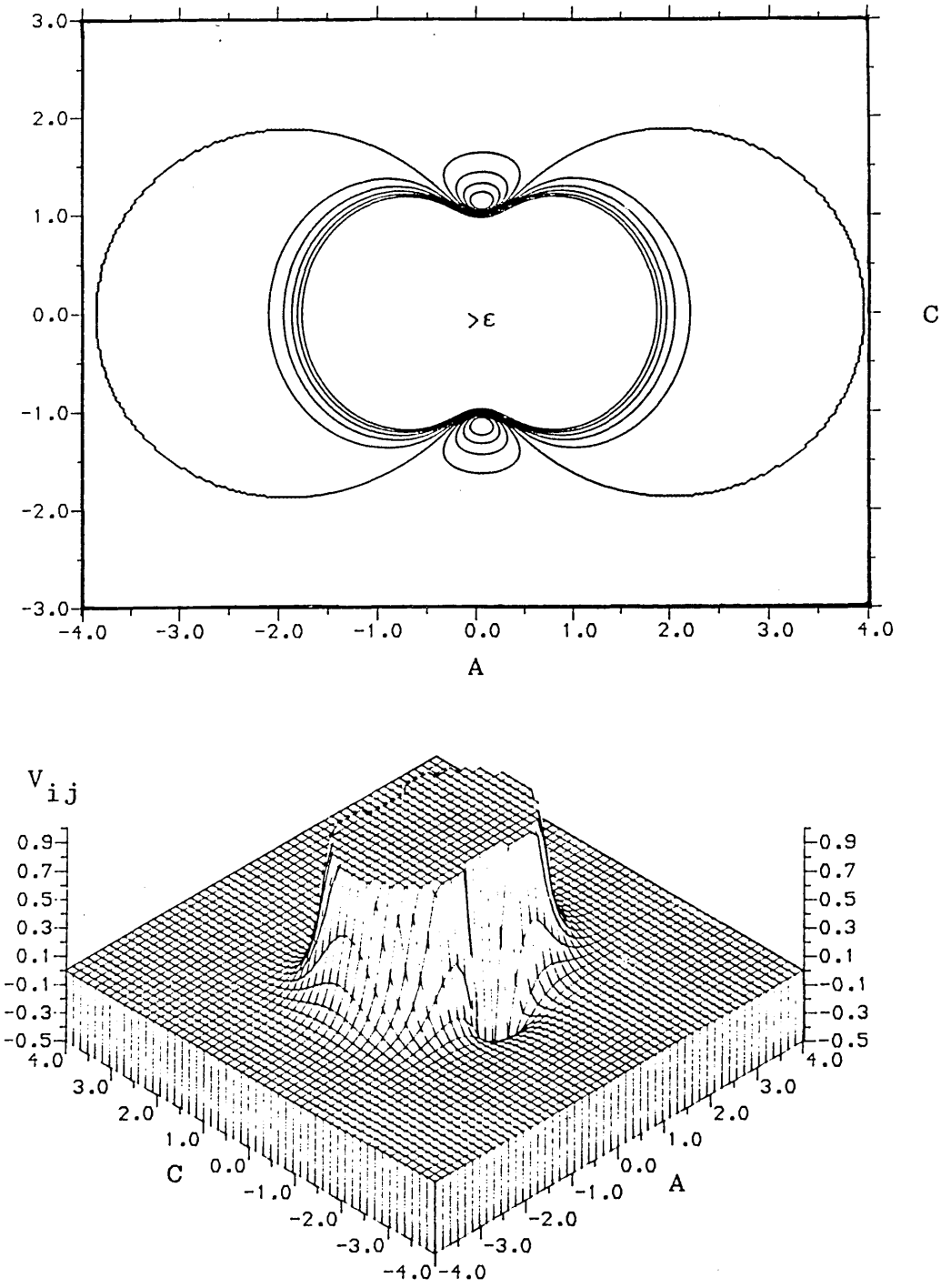

Figure 3.4 Contour diagram and isometric projection of the Soft Disc interaction potential. Contour intervals of 0.2ε, spatial dimensions in units of σ, values only shown for $V_{ij} \leq \varepsilon$. The labels A, B, C refer to the configurations in figure 3.3.

a. molecules parallel, $\theta_i = \theta_j$.

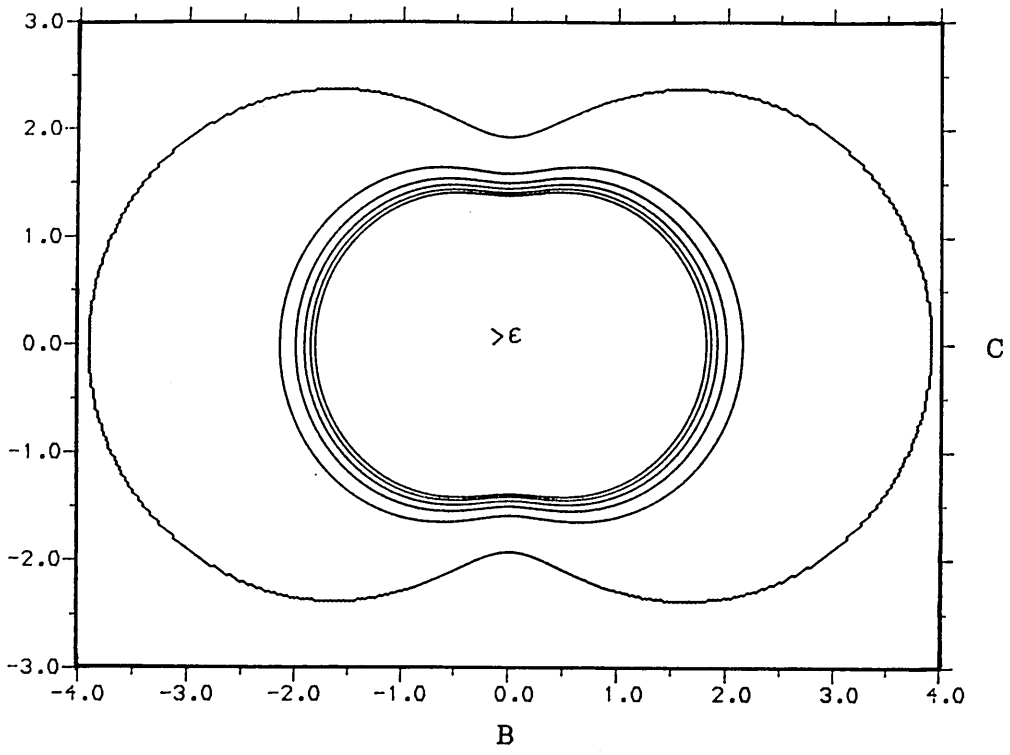

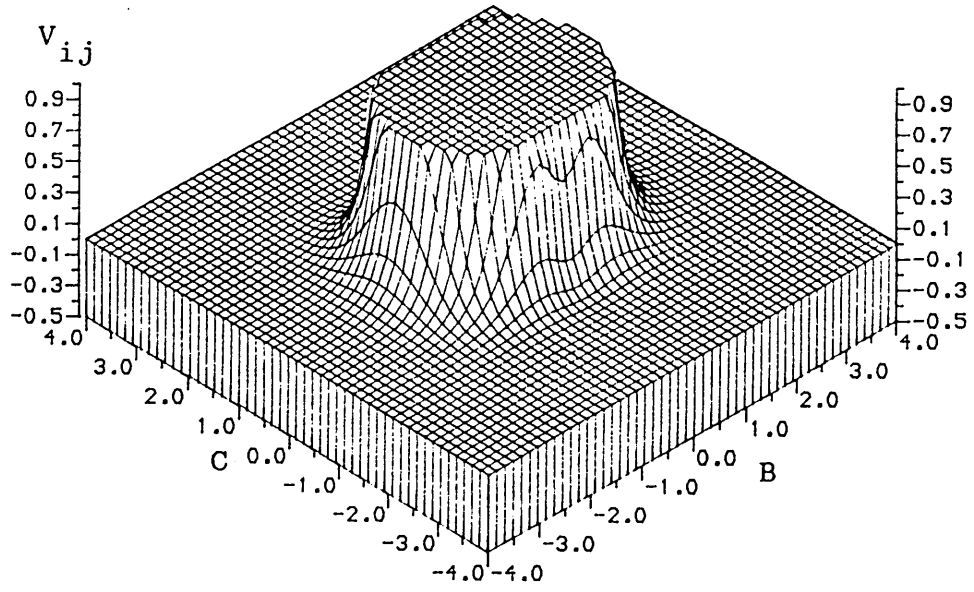

Figure 3.4 b $\theta_j = 90^\circ$.

molecule was moved along a randomly chosen direction by a random amount, up to a maximum, Δ_t. For a rotational move, one of the laboratory axes was chosen at random and the symmetry axis of the molecule rotated randomly about this chosen axis by a randomly determined angle, $\delta\phi$.

$$\delta\phi = \frac{1}{2} \Delta_r (2\Re - 1) \qquad 3.4$$

where $\Re$ is a pseudo-random number on the interval 0,1 and Δ_r is the maximum rotation. After each move, the change in interaction energy for the whole system was calculated and the new configuration was accepted or rejected according to the usual Monte Carlo criteria [40]. The magnitude of Δ_r and Δ_t were adjusted between simulations to give approximately equal occurrence of accepted and rejected moves.

A minimum molecular separation was defined in order to eliminate overflow errors in the calculation of the interaction potential. The effect of this was to introduce a small spherical region of infinite potential at the centres of the molecules. this minimum separation was set low enough to just eliminate all possible overflow errors, and in practice less than one in 200 000 moves needed to be rejected for this reason. Hence, the simulation was not greatly affected by this additional procedure.

Simulations of a system of fifty particles were started from a random configuration at high temperature and, as the temperature was reduced, the final configuration of a run at one temperature became the starting configuration of the run at the next lower temperature. The simulations were performed overnight on the IBM 4341 mainframe computer at the polytechnic. Owing to low computing demand at this time, about four

hours of CPU time were available for these simulations each night, which, it was estimated, was enough time to allow for thermalisation of the system at one temperature. Subroutines were written to allow a configuration to be stored on computer disk and then picked up in a subsequent run, allowing a simulation to continue over several nights. The results of these simulations are presented as diagrams of the molecular positions and orientations which were obtained from the final configurations of the simulations at each temperature.

The reduced temperature, T^*, and density, ρ^*, used in these simulations are given:

$$T^* = \frac{k_B T}{\varepsilon} \quad ; \quad \rho^* = \frac{N\sigma^2}{A} \qquad 3.5$$

where N is the number of discs in the 2-D box which has area A.

An overnight simulation at one temperature involved 250 000 attempted moves of each type and typically used some 256 minutes of central processor time.

RESULTS

In the diagrams presented, the projections of the unique symmetry axes of the disc-like molecules onto the plane are represented by the lengths of the lines. The attached circles indicate the upper end of the axes.

Figure 3.5 shows configurations of three simulations at the same temperature, but with different densities.

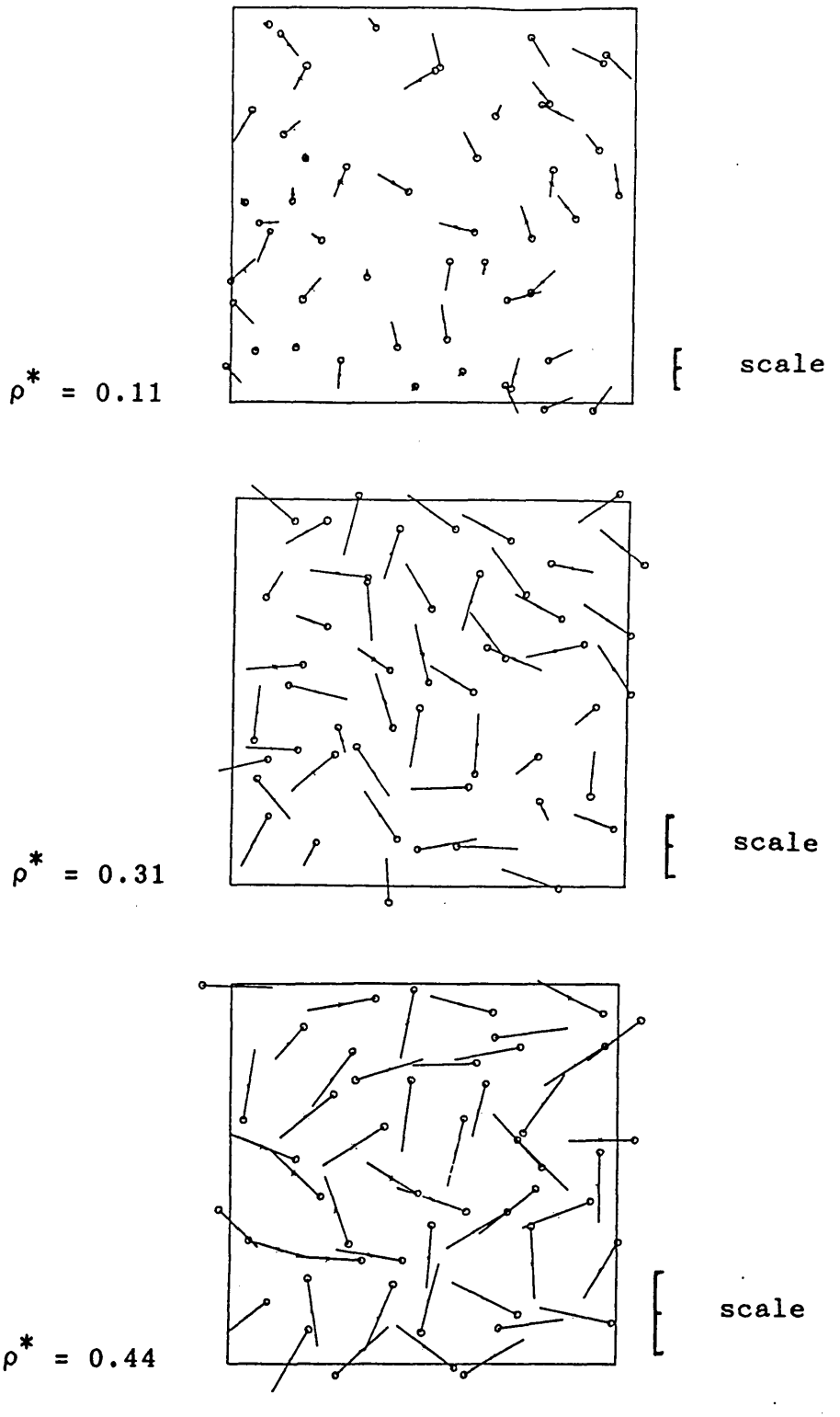

Figure 3.5 Typical configurations from the Soft Disc model at a reduced temperature of T^*=1.43.
The scale indicates the length of an axis parallel to the plane.

It can be seen that as the density is increased, the molecules pack more evenly to reduce the system internal energy. Furthermore, at the highest density, there is a tendency for the discs to be perpendicular to the plane rather than lie flat in it. This is indicated in the diagrams by the longer axis lines.

Figure 3.6 shows configurations at a relatively high density of 0.39. It can be seen that as the temperature is reduced, the molecules tend to align themselves with one another to produce localised columnar stacking in domains. This stacking is typical of discotic liquid crystalline behaviour [8]. The simulations did not produce any configurations with an overall uniform ordering, and it it thought that this may be due to the restriction to two dimensions [57]. No attempt was made to quantify the ordering of the molecules in this model.

The above simulations have generated configurations showing typically discotic ordering and have shown the applicability of the Metropolis Monte Carlo method to the modelling of these cyclic liquid crystal oligomer systems. However, the simple potential used here does not offer scope to examine the interplay between the polymer rings and the attached mesogens. A more complicated model which reflects the multi-component nature of the liquid crystal oligomer molecules was, therefore, developed and simulated in three dimensions.

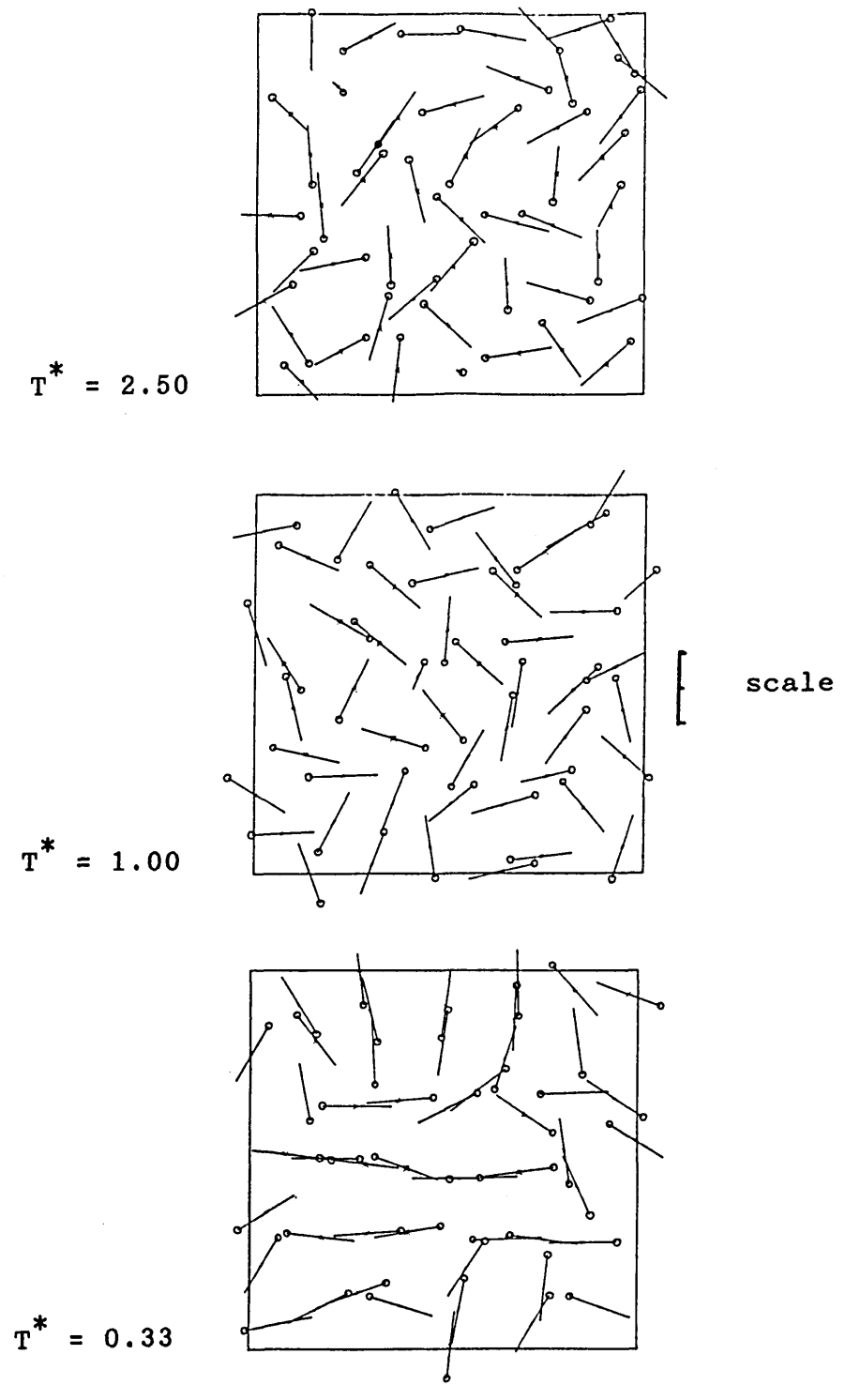

Figure 3.6 Typical configurations from the Soft Disc model at a reduced density of $\rho^* = 0.39$.
The scale indicates the length of an axis parallel to the plane.

CHAPTER 4 THE MULTI-MESOGEN RING MODEL

The multi-mesogen ring (m.m.r.) model was developed to investigate the effects of altering the internal structure of the cyclic oligomeric liquid crystalline molecules. The cyclic polymer backbone and the mesogenic moieties are given separate representations, thus allowing the behaviour of the molecules to be observed as the coupling strength between the rings and the attached mesogens is varied.

THE MOLECULAR INTERACTION POTENTIAL

In the m.m.r. model, the individual mesogenic units are represented separately, with a mesogen-mesogen interaction potential chosen for the interaction between these rod-like moieties. The cyclic polymer backbones are simply represented as a constraint on the relative motions of the attached mesogens. Figure 4.1 shows the general structure of the model. The cyclic backbones are taken to have a planar ring conformation and the mesogen centres of mass are placed at sites equal distances apart on this rigid ring. The flexibility of the coupling between the mesogens and the rings is incorporated by means of a restriction on the orientations which the mesogens may have with respect to the ring axes. An axis may be imagined to pass through the centre of the ring and the centre of mass of a mesogen. The mesogen is then only allowed to adopt orientations for which the angle between this imagined axis and the long axis of the mesogen is less than some

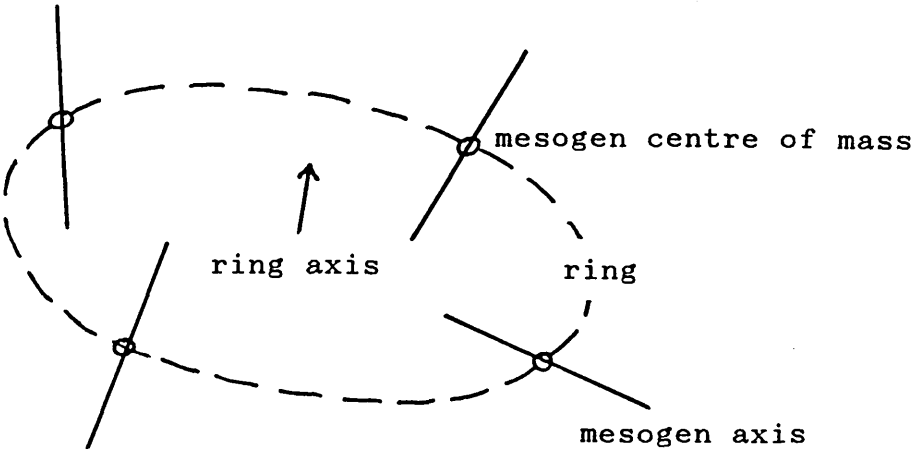

Figure 4.1 The structure of the multi-mesogen ring model.

maximum, referred to as the flex angle. Any attempted Monte Carlo move of the mesogen which would cause the mesogen to be orientated outside the cone defined by this flex angle is rejected.

By suitable choice of parameters, this model can represent a range of molecular structures. These adjustable parameters are the ring size, the number of attached mesogens and the ring-mesogen coupling flexibility via the flex angle. Also, the interaction potential to describe the mesogens can be chosen to have an appropriate form.

The mesogen-mesogen interaction potential adopted for use in this model is that developed by Luckhurst et. al. [78] for their simulation of rod-like molecules in the NPT ensemble. This potential contains both attractive and repulsive contributions, allowing the study of the temperature dependent behaviour of the translationally mobile molecules. The pair potential was constructed by the addition of an anisotropic term to the usual, spherical, Lennard-Jones 12-6 potential:

$$u_{ij} = u_0 + u_a$$

where

$$u_0 = 4\varepsilon \left\{ \left(\frac{\sigma}{r_{ij}}\right)^{12} - \left(\frac{\sigma}{r_{ij}}\right)^{6} \right\}$$

and

$$u_a = -4\ \varepsilon\ \lambda_a \left\{ \left(\frac{\sigma}{r_{ij}}\right)^{12} + \left(\frac{\sigma}{r_{ij}}\right)^{6} \right\} P_2(\cos \beta_{ij})$$

4.1

where β_{ij} is the angle between the unique symmetry axes of the two mesogenic moieties and λ_a is a measure of the anisotropy of the interaction.

This potential was chosen for two reasons. Firstly, Luckhurst et. al. had already shown the applicability of the potential to the simulation of rod-like mesogens using the Metropolis Monte Carlo technique, observing a transition from a nematic phase to isotropic fluid. We might also expect a similar transition for our molecules in the case of full flexibility, and the use of the same mesogen interaction potential would allow for a comparison between our results and those of Luckhurst et. al.. Secondly, owing to the complexity of the Monte Carlo moves involved in the simulation of our multi component molecules it was essential to use a relatively simple mesogen-mesogen interaction potential in order to minimise the necessarily large computing time required for the simulations. The potential proposed by Luckhurst et. al. has an angular dependence which is dependent only upon the angle between the long axes of the mesogens, and consequently is simpler to calculate than the interaction potential used in the soft disc model which had a fuller angular description.

The choice of an interaction potential whose angular dependence is limited to the angle between between the unique axes of the mesogens results in a somewhat unrealistic symmetry. A pair of molecules which maintain the same angle between their unique axes will interact with a reduced form of the potential which is independent of the orientation of the relative position vector, $\underline{r}_{ij}$. For the interaction potential adopted by ourselves and Luckhurst et. al., two molecules which maintain the same relative orientations will 'see' each other as Lennard-Jonès spheres. These Lennard-Jones

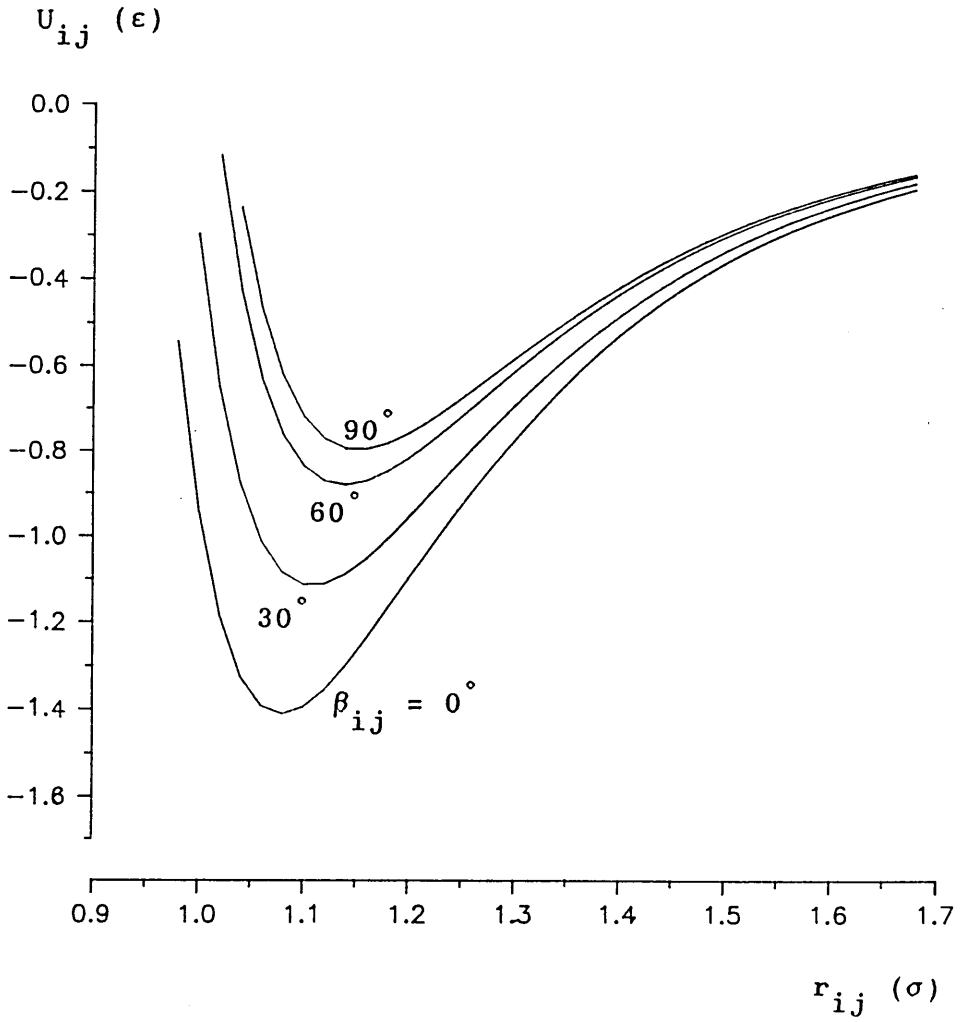

Figure 4.2 The mesogen interaction potential for fixed angles β_{ij} between the axes of the pair of mesogens. λ_a = 0.15.

functions are shown in figure 4.2 for our potential with an anisotropy of λ_a = .15 over a range of fixed angles between the unique axes of the mesogens.

For the Lennard-Jones curves we define two characteristic values: the depth of the well, U_0, and the separation, r_{eqm}, corresponding to this minimum in the potential energy. It can be seen that for our potential r_{eqm} is increased by approximately 7% as the molecules turn from parallel to perpendicular alignment. This is accompanied by a reduction in the well depth of nearly 50%.

Owing to the small size of the variation in r_{eqm} we may expect our mesogenic moieties to exhibit spatial packing analogous to that of simple Lennard-Jones spheres of a radius of approximately $r_{eqm} = 1.1\ \sigma$. The interpretation adopted by Luckhurst et. al. for this packing behaviour is that the pair interaction may be associated with highly ordered clusters of rod-like molecules, the clusters being considerably less anisometric than their constituent rod-like molecules. This interpretation is not applicable to our molecules because we define the interaction potential to act between a pair of individual mesogens. However, a variety of models of mesogenic behaviour have made use of interactions which posses the same angular dependence as equation 4.1. These models include many lattice based Monte Carlo simulations and the classic Maier-Saupe theory. Consequently we believe that the interaction potential chosen contains the essential features required for the representation of the mesogens in the m.m.r. model.

The simulations were performed with a mesogen anisotropy of λ_a= 0.15. Preliminary calculations were

also performed with a higher anisotropy, but it was found that the degree of order obtained was persistent up to high temperatures, in agreement with the results obtained by Luckhurst et. al. for their monomeric rod-like mesogens.

COMPUTING DETAILS

The Metropolis [40] Monte Carlo technique was used to simulate a system containing N_r molecules in which the mesogenic units were attached four to a ring. The simulations were performed in the NVT ensemble and each molecule was allowed free translational and rotational motion in 3-dimensions. For most of the simulations N_r was given the value 15, as detailed in the results section of this chapter.

The simulations were performed subject to the usual periodic boundary conditions. In order to prevent the interaction of mesogen i with more than one duplicate of mesogen j, the pair interaction potential was discontinuously reduced to zero at a distance equal to half of the length of the sides of the cube containing the molecules. This cut-off distance will, therefore, vary between simulations performed on molecules in boxes of different size. However, the majority of results presented are for boxes with the same density of molecules and the same number of molecules in the box. For these simulations the size of the box and range of the interaction potential are constant.

As in the soft disc model, a small central region of infinite potential was included in the mesogen

interaction to prevent computer overflow should two molecules get too close. However, this condition never occurred in practice in the simulation of the m.m.r. model.

The structure of the molecules allowed for just three types of Monte Carlo move: ring translations, where the attached mesogens were moved by the same translational increment, maintaining their relative positions; ring rotations, in which the ring-mesogen entity was rotated as a rigid body; mesogen rotations where an individual mesogen was rotated with respect to the ring. The directions and amounts of these motions were chosen in the same random manner as used in the simulation of the soft disc model described in chapter 3. The number of accepted moves of each type was recorded and the nominal move size adjusted between simulations to achieve an approximately equal frequency of accepted and rejected moves for each type.

Output from the model consisted of the reduced internal energy, E^*, two order parameters describing the ordering of the rings and two order parameters describing the ordering of the mesogens.

The internal potential energy of the system was calculated from the simple sum of the mesogen pair interactions, averaged over the Monte Carlo configurations generated after the system had reached equilibrium:

$$E = \left\langle \sum_{i=1}^{N} \sum_{j=i+1}^{N} u_{ij} \right\rangle \qquad 4.2$$

where N is the number of mesogenic units in the system

and the angled brackets, '<...>', represent the thermal average over the Monte Carlo configurations. The values are presented in the form of a dimensionless reduced energy, E*:

$$E^* = \frac{E}{\varepsilon N} \qquad 4.3$$

The mesogen order parameters were obtained by first calculating the following order tensor [100]:

$$\underline{Q} = \begin{vmatrix} \langle x_i x_i \rangle & \langle x_i y_i \rangle & \langle x_i z_i \rangle \\ \langle y_i x_i \rangle & \langle y_i y_i \rangle & \langle y_i z_i \rangle \\ \langle z_i x_i \rangle & \langle z_i y_i \rangle & \langle z_i z_i \rangle \end{vmatrix} \qquad 4.4$$

where x_i is the x-component direction cosine of the i-th mesogen and the angled brackets represent the average over all molecules as well as Monte Carlo configurations. This tensor was diagonalised to yield three eigenvalues, Q_1, Q_2, and Q_3. In the uniaxial state, one of these eigenvalues, Q_1, is different from the other two, which are equal. The usual uniaxial order parameter (as given in equation 1.1 in chapter 1) is then

$$S_m = \frac{1}{2} (3\ Q_1 - 1) \qquad 4.5$$

However, for the composite m.m.r. molecules the formation of biaxial phases is possible, in which case no two eigenvalues are the same. Such a biaxial phase indicates the tendency of the unique axes of the mesogens to align with a secondary preference along an axis perpendicular to the primary director, the ordering of this phase being described by the three

eigenvalues of $\underline{Q}$. The tensor $\underline{Q}$ has unit trace and so only two of the eigenvalues are independent. The problem, therefore, is how to present the two values in a meaningful form. Based on the results of Luckhurst et. al. we expected the formation of uniaxial phases at low temperatures for some of the systems of our molecules. Therefore, we attempted the calculation of a uniaxial order parameter in all cases. Where all three eigenvalues differed, Q_1, was taken as that eigenvalue most different from the other two and the usual uniaxial order parameter was calculated from Q_1. A biaxiallity order parameter, B_m, was then calculated from the difference in the other two eigenvalues [103]:

$$B_m = \frac{3}{2} \mid Q_2 - Q_3 \mid \qquad 4.6$$

This biaxiallity parameter can take values from zero for uniaxial phases up to 0.5 for a phase with maximum biaxiallity.

The order parameters for the ring normals were calculated in an analogous manner.

The reduced temperature, T^*, and reduced volume, V^*, used in the simulations are defined as:

$$T^* = k_B T/\varepsilon \quad ; \quad V^* = V/N_m\sigma \qquad 4.7$$

where ε and σ are from the definition of the pair interaction potential and N_m is the number of mesogens in the system.

The model was programmed in PASCAL and run on the CRAY X-MP/48 at the Atlas Centre of the Rutherford Appleton Laboratory. A variation of the main programme was also developed in order to explore the behaviour of a

system of lone mesogens in the NVT ensemble. The same mesogen pair interaction potential was used as in the m.m.r. model, allowing for comparison with the results of the simulations of the ring molecules and comparison with the results of Luckhurst et.al. which were performed in the NPT ensemble. The programme for the mesogen only model was derived from the m.m.r. programme by the addition of mesogen translational moves and the removal of the procedures pertaining to the rings.

The programmes were developed on the IBM 4341 mainframe computer at the Polytechnic and all of the computational routines, such as the diagonalisation of the order tensors, were coded into the programme in preference to accessing library routines. This was to allow the programme to be portable between different computers. The only exception to this was the use of the random number generator as provided on the computer, as the change from the use of one generator to another was generally quite straightforward.

Two series of runs were performed. The first series involved only the model for the lone mesogens. As explained above, this allowed us to compare our results to Luckhurst's and to assess the effect of using the NVT ensemble rather than the NPT ensemble. In the second series the m.m.r. model was employed to explore the effect of altering the coupling between the mesogens and the rings by means of adjusting the flex angle. A run of the lone mesogens model was included in this second series for comparison.

In the second series of runs the system consisted of sixty mesogens attached four to a ring. The ring radius was chosen by considering two competing requirements. The first requirement was that the rings should be

substantially smaller than the box in which they were contained so as to minimise any unwanted effects which might result from the combination of large rings and the periodic boundary conditions. The other requirement was that the rings should be large enough such that interactions between neighbouring mesogens on a ring would not outweigh all other interactions between pairs of mesogens. The ring radius was chosen such that the interaction between a pair of neighbouring mesogens on the ring could adopt any relative orientation without forcing the pair interaction between them into the repulsive region of the modified Lennard-Jones curve. The combination of these requirements provided a ring radius of 0.76 σ, which was used throughout.

The programmes were divided into several nesting levels, each level comprising a number of repeats of the next, inner level and usually some data processing as appropriate to the level. The number of repeats required for each level was estimated from preliminary calculations as indicated in the discussion of the programme structure given below. The numbers quoted apply to the runs of the m.m.r. model, although similar numbers of repeats were used in the simulations of the lone mesogens. The nesting structure is summarised in figure 4.3.

SHUFFLE level.

The shuffle level consisted of a number of attempted Monte Carlo moves. These comprised one attempted ring rotation, one attempted ring translation and four attempted mesogen rotations. Preliminary simulations of mesogens alone and rigid rings (flex angle = 0°) suggested that this ratio of ring to mesogen moves should cause the ring and mesogen elements to equilibrate at

```
for TEMPERATURE = START_TEMP to END_TEMP do
 begin
 for SECTION = 1 to 5 do
  begin
  for COUNT = 1 to 10 do
   begin
   MACROSTEP
   write macrostep averages of E*, Sm, Sr, Bm, Br
   accumulate running totals of E*,Sm, Sr, Bm, Br
   end (for COUNT)
  average E*, Sm, Sr, Bm, Br
  write section averages of E*, Sm, Sr, Bm, Br
  if SECTION ≥ 3 then {ie. "production" stage of run}
    begin
    accumulate running totals of E*, Sm, Sr, Bm, Br
    end (if SECTION)
  end (for SECTION)
 average E*, Sm, Sr, Bm, Br
 write "production" averages of E*, Sm, Sr, Bm, Br
 end (for TEMPERATURE)
```

```
MACROSTEP
 for COUNT = 1 to NSUBMACROSTEPS do
   begin
   SUBMACROSTEP
    for COUNT = 1 to NSTEPS do
      begin
      STEP
       for COUNT = 1 to NSHUFFLES do
         begin
         SHUFFLE
          RING rotation
          RING translation
          for COUNT = 1 to 4 do
            begin
            MESOGEN rotation
            end

         end
      calculate E* and order tensors
      accumulate running totals of E* and
              order tensors
      end

   calculate Sm, Sr, Bm, Br
   accumulate running totals of Sm, Sr, Bm, Br
   end
```

Figure 4.3 The nesting structure of the programme used in the simulation of the m.m.r. model.

approximately the same rate. For each move a new ring or mesogen was chosen at random.

STEP level.

The step level consisted of a number of repeated shuffles. Measurements on the final configuration generated in each step contributed to the average values of the various properties. A requirement for the Monte Carlo technique is that the configurations from consecutive steps should not be correlated.

A method of estimating the number of Monte Carlo moves required to satisfy this criterion has been suggested by Binder [38]. A 'guess' is made at the required number of moves and Monte Carlo runs of different length are performed on an equilibrated system. If the configurations generated are not correlated then the product of the length of the run and the statistical error in some configurational property of the system will be independent of the length of the run. This technique was applied to the lone mesogens version of our model and measurements of the variance in the internal energy of the system suggested the number of Monte Carlo moves required per step was of the order of 2.4 N_m, where N_m is the total number of mesogenic units in the system. Similar calculations on rigid rings did not yield clear results, probably because of the relatively small number of rings in the system. The configurations appeared to be uncorrelated even for steps of a few Monte Carlo moves. The number of shuffles in a step was therefore chosen as 36 in accordance with the requirement for the mesogens, given that there are four attempted mesogen moves per shuffle.

SUBMACROSTEP level.

The submacrostep consisted of 20 steps, at the end of which the order parameters were calculated from the order tensor averaged over those steps. The number of repeated steps in the submacrostep was chosen such that the drift in the directors during the submacrostep was less than one degree. This was confirmed by observation of the drift in the directors in simulations of lone mesogens and rigid rings in equilibrated systems at a temperature just above the critical temperature. A substantial drift in the directors during a step would result in the calculation of inaccurate order parameters from the averaged order tensor.

MACROSTEP level.

Each macrostep comprised 35 submacrosteps, at the end of which the averages of the order parameters and the internal energy were calculated.

SECTION level.

Each section consisted of 10 macrosteps. Statistics were performed on the values of the energy and the order parameters calculated at each macrostep to yield mean values and standard deviations.

The whole of a run was divided into five sections. The first two sections were discarded as equilibration and the final three sections provided the average values of the order parameters and energies for plotting in the figures. However, close to the transitions it was found that longer than usual equilibration was required in some cases. Here the plotted results were obtained from just one or two sections as appropriate.

The length of run required for the equilibration of the system and for the collection of data from the configurations was estimated from the variations in the internal energy and order parameters for extended simulations of lone mesogens and rigid rings. Adequate equilibration was checked in the rest of the simulations by inspection of the mean values calculated at each section and at each macrostep.

The difficulties involved in estimating the required run lengths can be gathered from figure 4.4. The variations in the two uniaxial order parameters and the internal energy are plotted throughout a run of the m.m.r. model in which the flex angle is 60°. The system is in a fluctuating state just above the clearing temperature and the plots are dominated by a substantial scatter in the measured values which are shown for every macrostep. The solid lines drawn correspond at each macrostep to the average of the given properties over the whole of the run up to that macrostep. From these lines we can estimate the length of the data collection part of the runs required. At the start of the simulations the running averages are dominated by the initial values. The influence of the early values is mostly lost by about one fifth of the total run length, with the running average settling by just over half of the total run length. Hence a production run length of at least one fifth of this total run length would be required to provide reliable estimates of the configurational properties. A more reliable measurement would be obtained from a production run length of just greater than one half of the total. Owing to the substantial scatter in the values at each macrostep it is more difficult to estimate the length of run required for equilibration. In the example given the system appears

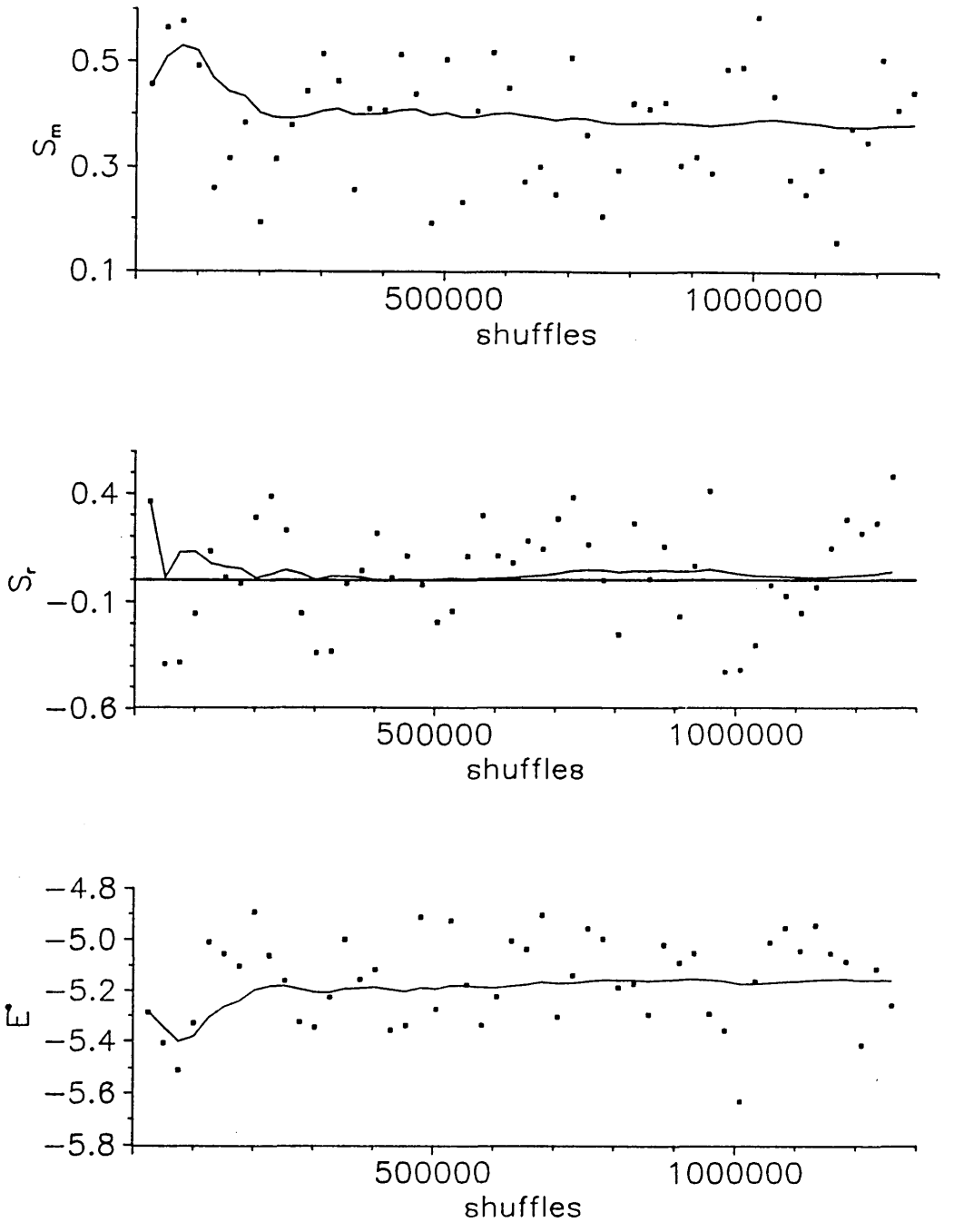

Figure 4.4 The development of S_m, S_r and E^* during a run of the m.m.r. model at a reduced temperature of $T^* = 1.0$ and with a flex angle of 60°. The symbols represent the values averaged at each macrostep and the solid line represents the cumulative average.

to have settled into an equilibrium state by the first one fifth of the total run length at most. This was confirmed by inspection of the values averaged over each section, which showed no general drift.

In the simulation of the m.m.r. model, 1 260 000 shuffles were performed at each temperature. The first two fifths of the configurations generated were discarded for equilibration except in those cases near to a phase transition in which inspection of the section averages suggested that longer equilibration was required.

The simulations were started from a random configuration at high temperature and as the temperature was reduced, the final configuration at one temperature became the initial configuration for the next, lower, temperature. For a typical simulation of the m.m.r. model involving 23 temperatures, a total of about 14 hours of CRAY central processor time were required. In total over 300 hours of CRAY processor time were used in this project.

Results of preliminary simulations of the m.m.r. model have already been published [79,80].

Copies of the source code of the implementation of the m.m.r. model have been deposited with the applied physics department of the Polytechnic.

RESULTS

i) Simulations of Lone Mesogens

First a comparison is made with the results of the

simulation of the monomer mesogens by Luckhurst et al. [78] to assess the effects of the use of the NVT ensemble and the size of the system of molecules.

Luckhurst's results were obtained by the simulation of a system of 256 rod-like mesogens in the NPT ensemble. The simulations were started from an ordered phase at low temperature and a first order transition into the isotropic phase was observed as the temperature was increased. The temperature of the transition was estimated as $T^*_{NI} = 1.13 \pm 0.02$, at a reduced volume of $V^*_{NI} = 1.334 \pm 0.004$.

We have also performed a simulation of a system of 256 lone mesogens, in our case in the NVT ensemble. The reduced volume was set at 1.334 in agreement with the critical volume observed by Luckhurst et. al. and the simulations were started from a random configuration at high temperature with 6.16 million moves attempted at each temperature as the temperature was reduced. We also performed a simulation of 60 lone mesogens at the same reduced volume, with 1.44 million attempted moves at each temperature.

The uniaxial mesogen order parameters for these three simulations are plotted against temperature in figure 4.5. In contrast with the first order transition observed in the NPT ensemble, a continuous transition from a disordered to an orientationally ordered phase is observed for both of the simulations in the NVT ensemble. At high temperature, the order parameters for the two simulations of 256 mesogens are equal. However, at low temperature, the order parameters obtained in the NVT ensemble are much lower than those from the simulation in

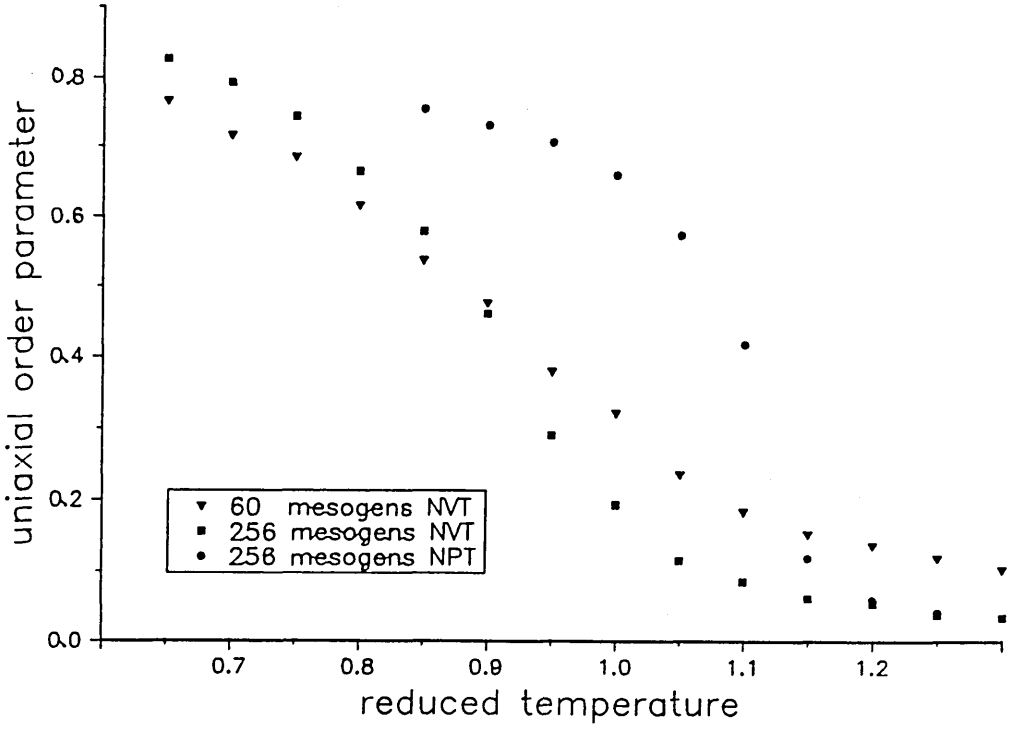

Figure 4.5 The uniaxial order parameter for simulations of lone mesogens in the NVT and NPT ensemble. Data for the NPT ensemble from Luckhurst et. al. [78].

the NPT ensemble. Owing to the continuous nature of the transition in the NVT ensemble it is difficult to ascribe a single temperature to the transition, although it is clear that the transition occurs over a range of temperatures lower than T^*_{NI} for the transition in the NPT ensemble. It would appear that the removal of the volume as a variable coordinate of the system has the effect of weakening the strength of the transition.

The difference in the transition temperatures may result from hysteresis in the system in the NPT ensemble. Simulations from low temperature to high temperature have shown that there is no hysteresis in the transition in the NVT ensemble. However, it is possible that the first order phase transition in the NPT ensemble exhibits some hysteresis resulting in the transition temperature being higher than that which would have been observed if the simulation had been undertaken from high temperature to low temperature.

The major difference between the two simulations in the NVT ensemble is in the slope of the transition in the order parameters. The reduction in the number of mesogens in the simulation causes an increase in the order parameter at high temperature and a decrease in the order parameter at low temperature. The actual temperature of the transition, if taken as the mid-point of the slope, is unchanged.

Localised pre-transitional ordering in the isotropic phase above the transition will make a larger contribution to the overall order for the smaller system of molecules. This results in the larger order parameter observed at high temperature in the simulation of 60 mesogens. The relatively low order parameter observed at high temperatures in this smaller simulation may be

caused by the shorter cut-off length in the pair interaction potential necessitated by the smaller box.

In summary, a continuous transition in the uniaxial order parameter is observed for the simulation of the monomeric mesogens in the NVT ensemble, where as a first order transition had been observed in the NPT ensemble. Whether there is also a difference in the transition temperature is uncertain owing to the lack of data for the reverse transition in the NPT ensemble. A shallower transition is observed for the simulation of a smaller number of molecules in the NVT ensemble.

ii) Simulations of the M.M.R. Model

The simulations of the multi-mesogen ring model were started from a random configuration at a reduced temperature of $T^* = 2.0$ and cooled in stages of $T^* = -0.1$ down to $T^* = 1.3$ with 1.26 M shuffles at each temperature as detailed earlier. The systems were then cooled more slowly in 15 stages of $\Delta T^* = -0.05$, with the disorder-order transitions occurring in this lower temperature range. The initial random configuration at high temperature was chosen by placing the rings at randomly chosen positions in the box and at randomly chosen orientations with respect to the axes of the box. The mesogens were placed on the rings in planar radial splay conformations in this starting configuration. Thermalisation at high temperature allowed the mesogens to adopt less rigid relations to the rings in the cases of finite flex angle.

It was decided to cool the system from a temperature of $T^* = 2.0$ because earlier simulations starting from a lower temperature only produced partially ordered phases

at low temperature for rigid rings. For consistency, the same method of cooling was adopted for all of the simulations, regardless of the flex angle.

A reduced volume of $V^* = 1.4$ was used in these simulations. In simulations of rigid rings at a lower reduced volume the extent of pretransitional ordering and fluctuations were increased, reducing the definition of the transition. However, in simulations at a reduced volume larger than $V^* = 1.4$ the definition of the transition was not improved further, but the transition temperature was depressed.

We look first at the simulation of rigid rings in the m.m.r. model, that is molecules with a flex angle of 0°. The ring uniaxial order parameter and biaxiallity parameter are plotted against reduced temperature in figure 4.6. At high temperature the uniaxial ordering of the rings averages at about $S_r \approx 0.25$ with substantial fluctuations as indicated by the error bars which correspond to one standard deviation in the values obtained at each macrostep. At lower temperatures there is a region of higher order, $S_r \approx 0.5$, and substantial fluctuations. This region corresponds to the local pretransitional ordering typically observed in mesogenic systems just above the transition temperature. In our system of just 15 rings, the local ordering of just a few rings could make a substantial contribution to the measured order parameter.

As the temperature is reduced further to $T^* \approx 0.9$ a transition is observed in the ring order parameter to $S_r = 0.95$, accompanied by a sharp reduction in the size of the fluctuations. A transition is also observed in the ring biaxiallity which drops from a value of about 0.18 to about 0.04. The ordering of this phase is

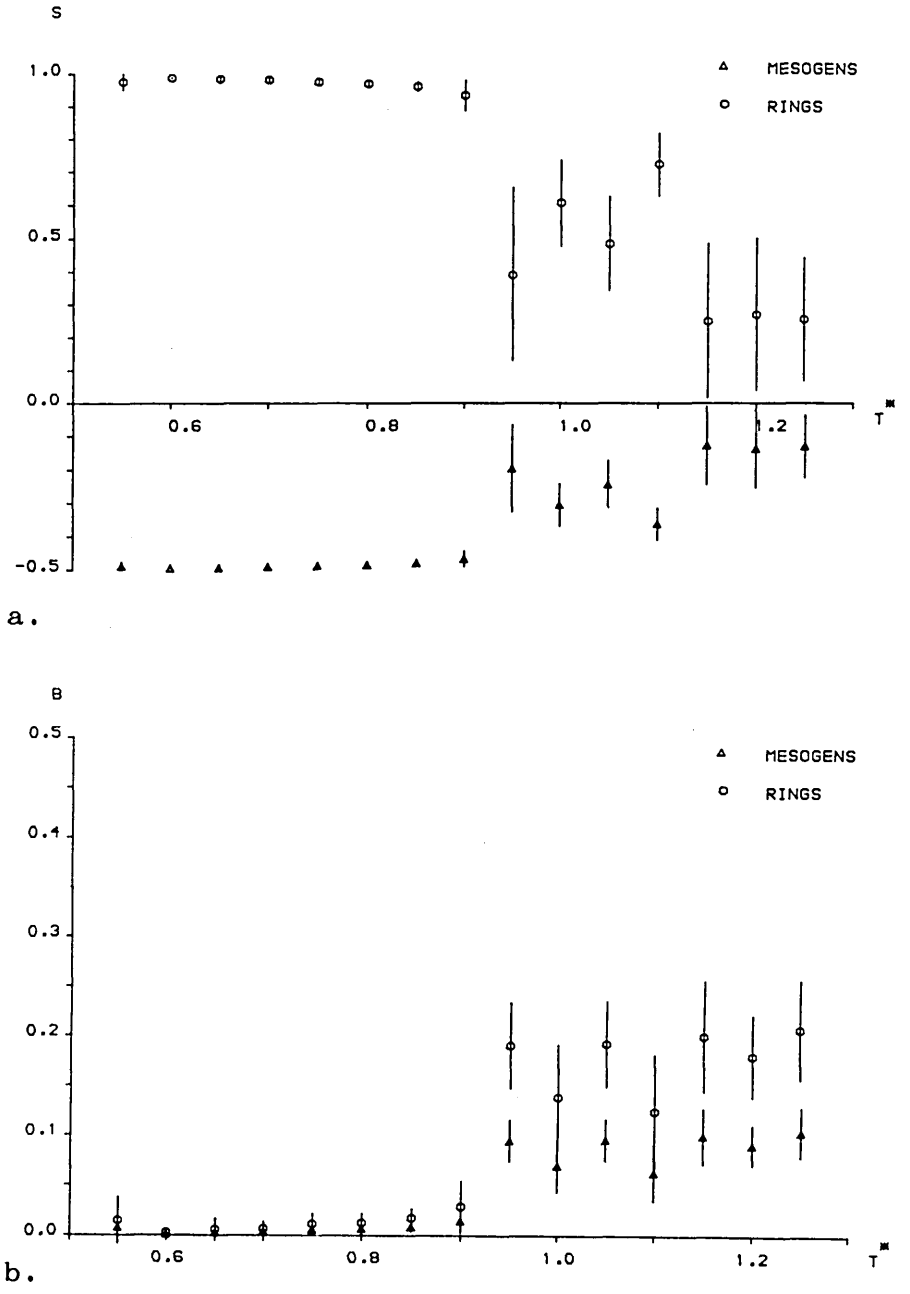

Figure 4.6 Order parameters for the ring and mesogen systems of the m.m.r. model with a flex angle of 0°. a) uniaxial order parameters; b) biaxial order parameters. The error bars indicate one standard deviation fluctuation.

stabilised at lower temperature with an increase in the uniaxial order parameter to 0.98 and a further reduction in the biaxiallity to very nearly zero.

For this rigid case the mesogen order parameters are directly related to the ring order parameters:

$$S_m = -0.5\ S_r$$

$$B_m = 0.5\ B_r \qquad 4.8$$

The internal energy of the system, E^*, and the specific heat capacity, C_v, are plotted in figure 4.7. The specific heat capacity was obtained from the gradient in the reduced internal energy:

$$C_v = \frac{dE^*}{dT^*} \qquad 4.9$$

The gradient at each temperature was obtained by fitting a cubic polynomial to four adjacent values of E^*. Estimates of the specific heat capacity were also attempted by the measurement of the fluctuations in the reduced energy during the simulation [51], but these values showed too much scatter to be of any use. A clear discontinuity in the reduced energy is seen in the figure between the temperatures of $T^* = 0.95$ and $T^* = 0.9$. This is accompanied by a sharp peak in C_v at $T^* = 0.925$.

A reverse simulation was also performed starting from the ordered state at $T^* = 0.55$ and increasing the temperature. The uniaxial order parameter and the reduced energy for this reverse simulation are given in figure 4.8. Here the transition appears to occur at a slightly lower temperature between $T^* = 0.85$ and $T^* = 0.9$. However, other, preliminary, simulations of systems of rigid rings showed the transition temperature to be

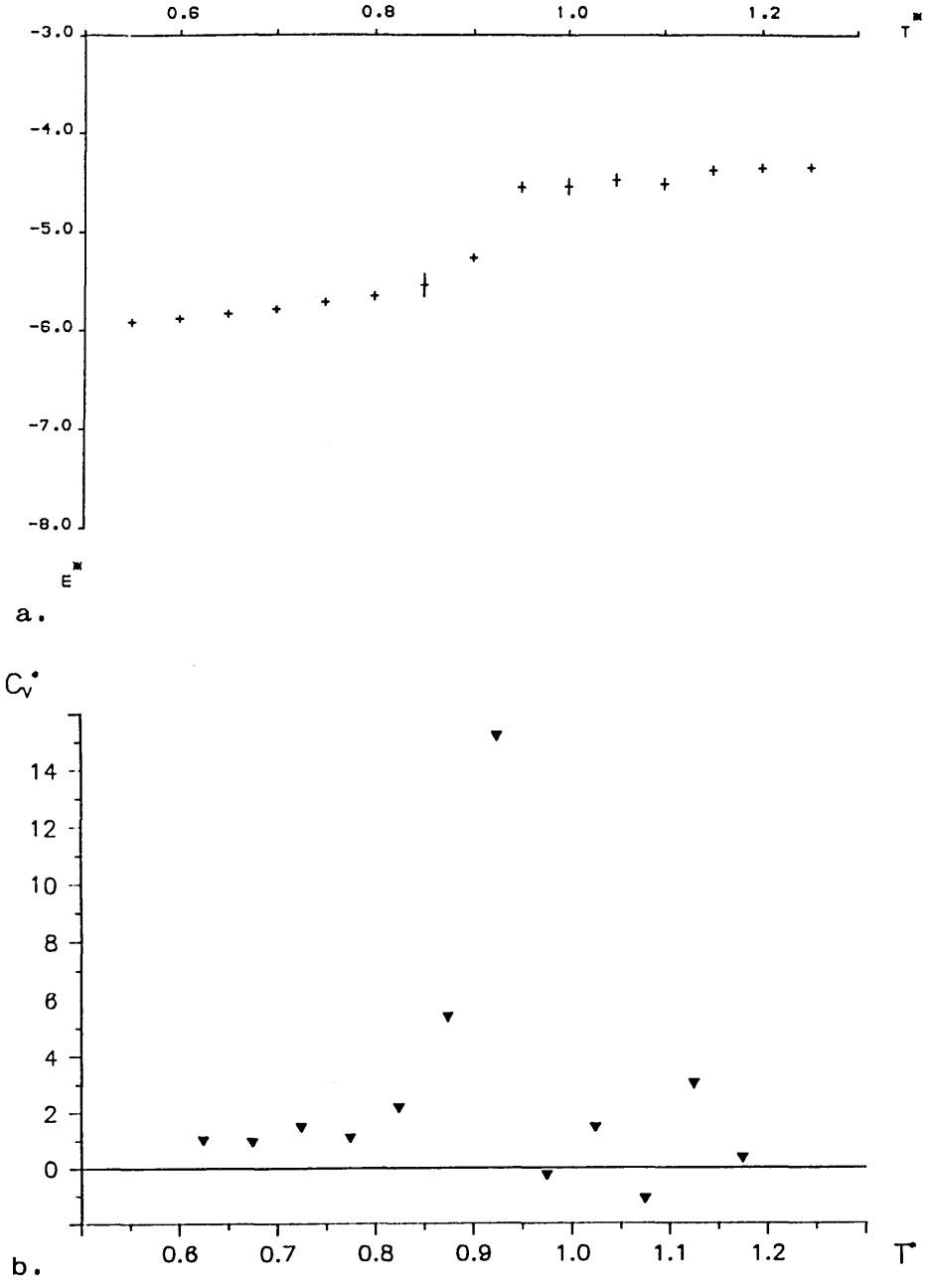

Figure 4.7 a) The reduced internal energy and b) the reduced specific heat capacity for the m.m.r. model with a flex angle of 0°.

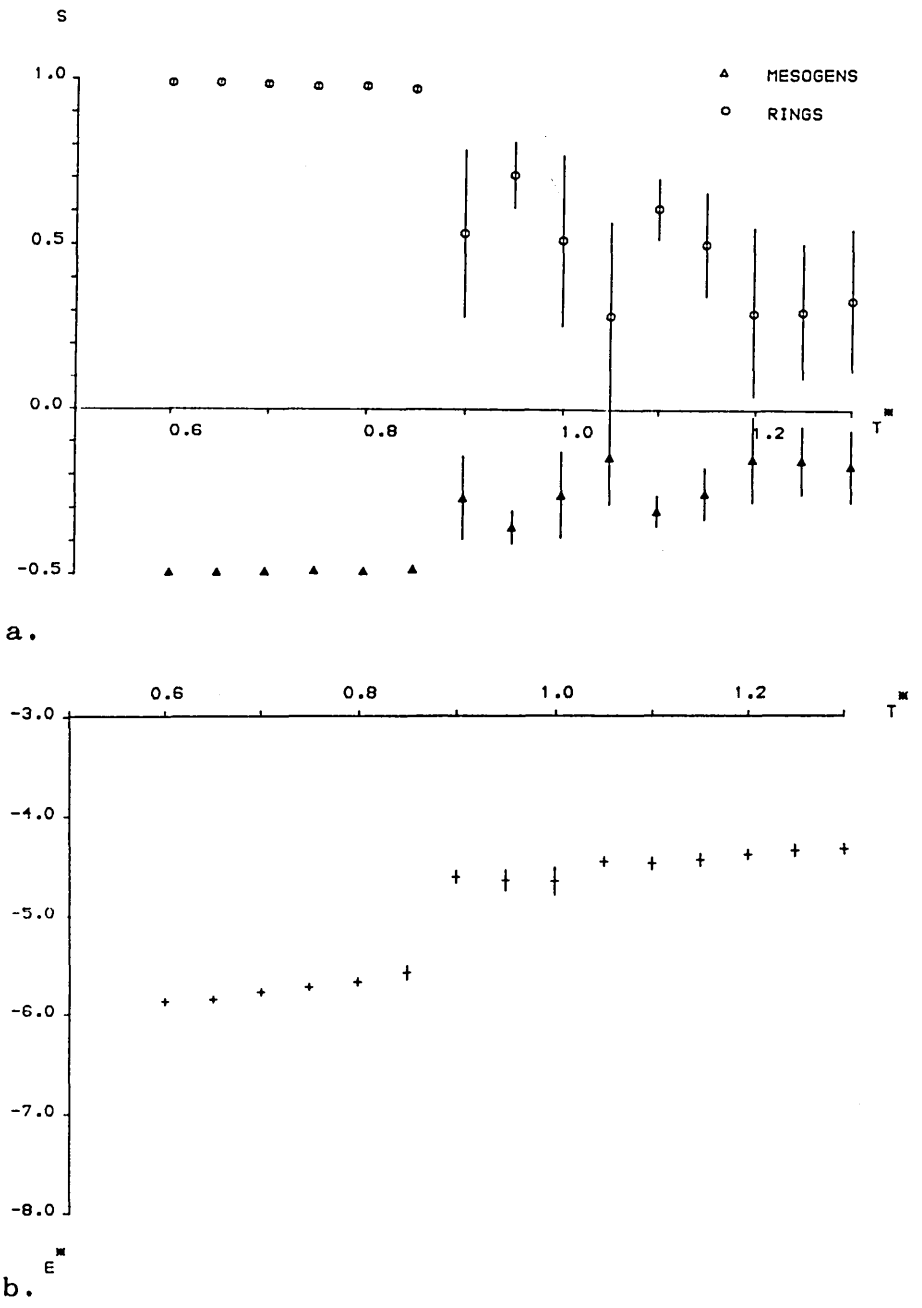

Figure 4.8 The simulation of the m.m.r. model with a flex angle of 0°. Reverse simulation from the ordered phase at low temperature. a) uniaxial order parameters; b) reduced internal energy.

slightly higher for the simulation from low to high temperature than for the simulation of decreasing temperature. It would appear that the exact transition temperature for the rigid rings is somewhat uncertain owing to the large fluctuations in the order parameters in the pretransitional region. There is insufficient evidence to suggest any genuine hysteresis in the transition.

From the combination of the 'forward' and 'reverse' simulations the transition temperature is estimated at $T^* = 0.9 \pm 0.25$.

We have explored further the effect of the use of a small number of molecules on the behaviour in the region above the transition. Simulations have been performed at a reduced volume of $V^* = 1.4$ on systems of 60 and 15 lone mesogens. At temperatures above the transition the smaller system does exhibit order parameters and fluctuations larger than those for the 60 mesogen system. However, these values are much lower than those observed in the pretransitional region of the rigid ring simulation. Therefore the size of the fluctuations in the pretransitional region for the rigid m.m.r. molecules does not result solely from the smallness of the system.

In figure 4.9 is shown a frequency diagram of the uniaxial ring order parameters calculated at each macrostep in the production part of the simulation of the rigid rings at a reduced temperature of $T^* = 0.95$ in the pretransitional region. There is a clear bistability in the system with preferred uniaxial order parameters centred about $S_r \approx 0.28$ and $S_r \approx 0.58$. Fluctuations between the two preferred states contributes to the uncertainties in the measured order parameters and the

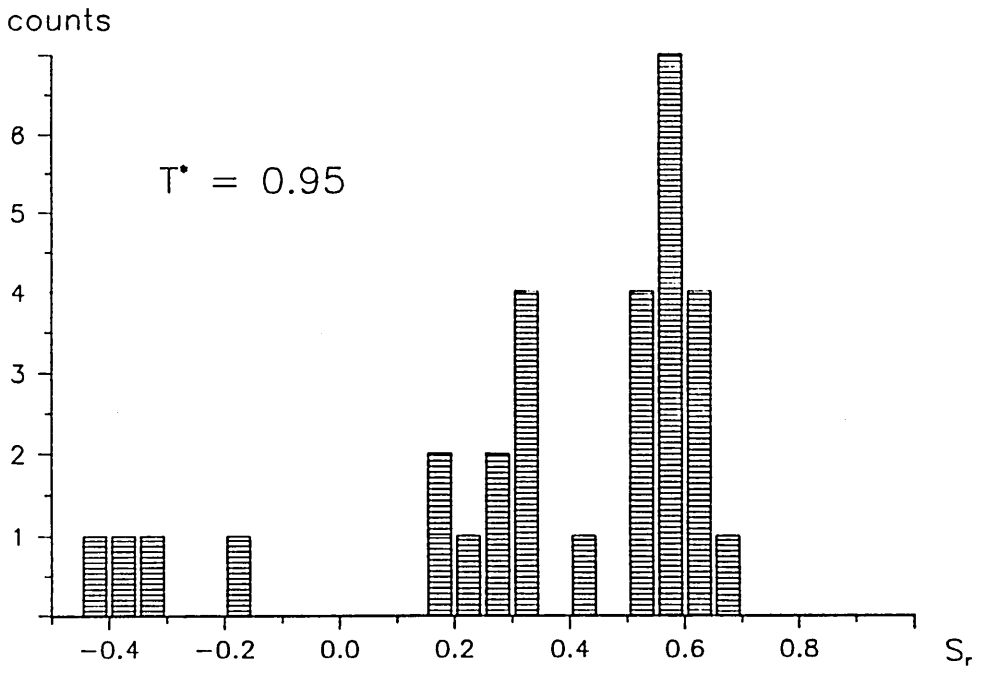

Figure 4.9 Frequency diagram of the values of S_r calculated at each macrostep during the production stage of the simulation of the m.m.r. model with a flex angle of 0° at a temperature of $T^* = 0.95$.

difficulties in locating the exact position of the transition.

Note the occasional excursions into negative order. This results from the definition of the uniaxial order parameter in the case of finite biaxiallity and only moderate uniaxial order. The biaxiallity of a phase has a maximum possible value equal to the magnitude of the uniaxial order of the phase according to the manner of calculation described earlier in this chapter. As the limiting value of biaxiallity is approached the three eigenvalues of the order tensor become evenly spaced in value and there is ambiguity as to whether the largest or smallest eigenvalue should be adopted in the calculation of the uniaxial order parameter. Although in the simulations this limit is never achieved exactly, the biaxiallity may increase as if to cross the limit, in which case there is a change in the sign of the uniaxial order parameter accompanied by a change in the choice of director. Consequently, a small continuous change in the ordering of a system may produce a large discontinuous change in the measured uniaxial order parameter. Some other workers [58] have adopted other methods of calculating the uniaxial order parameter, but these also have had drawbacks. In particular, if the uniaxial order parameter is defined solely in terms of the largest eigenvalue of the $\underline{Q}$ tensor it can never take negative values. We have adopted our method of calculation because it correctly measures strong uniaxial order, both positive and negative, and the simple relations between the mesogen and the ring order parameters (equation 4.8) are preserved for rigid rings. Cases in which the uniaxial order parameter frequently changes sign may be identified by the average in the biaxiallity parameter being larger in value than the average uniaxial order parameter.

As a control, a system of m.m.r. molecules in which the anisotropic mesogen pair interaction has been replaced by a simple spherical Lennard-Jones potential has also been simulated. From this simulation, the contribution made by steric interactions to the ordering of the rings may be gauged, in the absence of the aligning forces of the attached mesogens. The uniaxial and biaxial order parameters, and the internal energy for this simulation are given in figure 4.10. There is a transition to partial uniaxial ring ordering at $T^* \approx 0.62$, accompanied by an increase in the biaxiallity of the ring system. The transition is first order, with a discrete change in the internal energy. The transition is different from that of the rigid rings in several respects. The transition occurs at a much lower temperature and produces only a partially ordered biaxial phase. Also, there is a lack pretransitional ordering at temperatures above the transition.

It would appear that the anisotropic contribution to the mesogen interaction potential is essential for the formation of a uniaxial phase of the rigid ring m.m.r. molecules at a temperature of $T^* \approx 0.9$, and also for the production of localised pretransitional ordering above this temperature.

In the simulation of a small system of molecules, such as ours, it is difficult to determine whether the observed phase transitions are first order or continuous. Similarly the extrapolation of the transition into a macroscopic system is non-trivial and therefore it is not possible to state with certainty the expected nature of the discotic nematic to isotropic fluid transition in a macroscopic system of rigid m.m.r. molecules. According to Binder [38] some finite hysteresis may be observed in

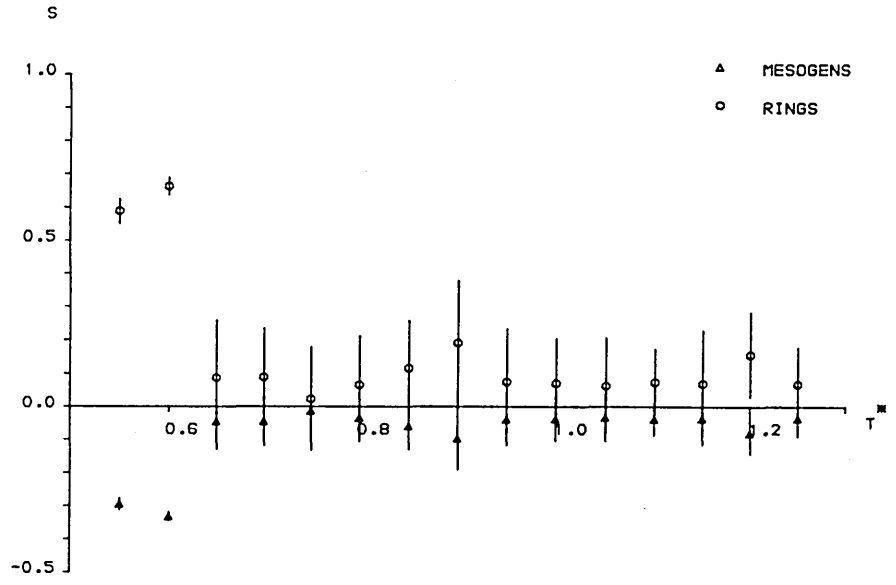

a.

Figure 4.10 a) the uniaxial order parameters; b) the biaxial order parameters and c) the reduced internal energy for the m.m.r. model with zero mesogen anisotropy ($\lambda_a = 0$).

continued over...

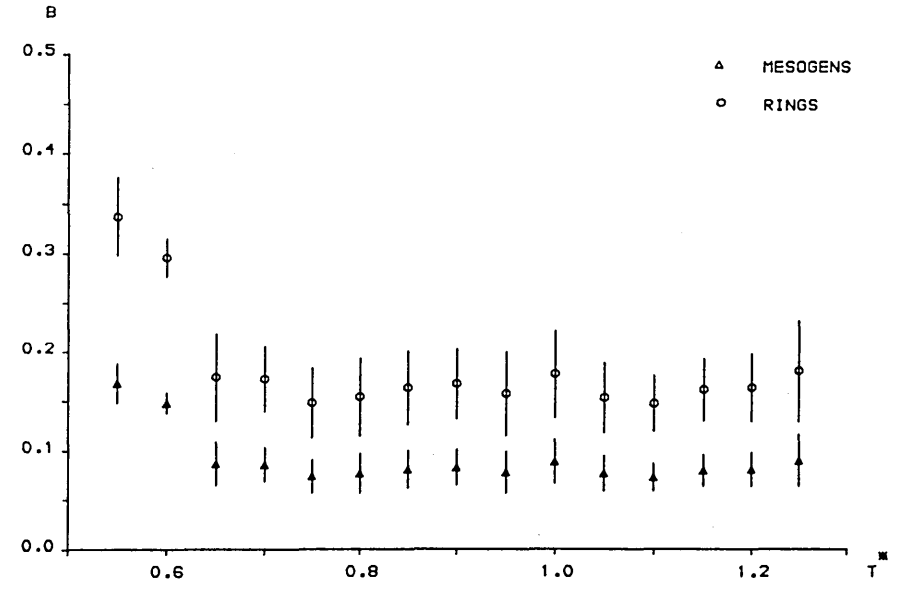

b.

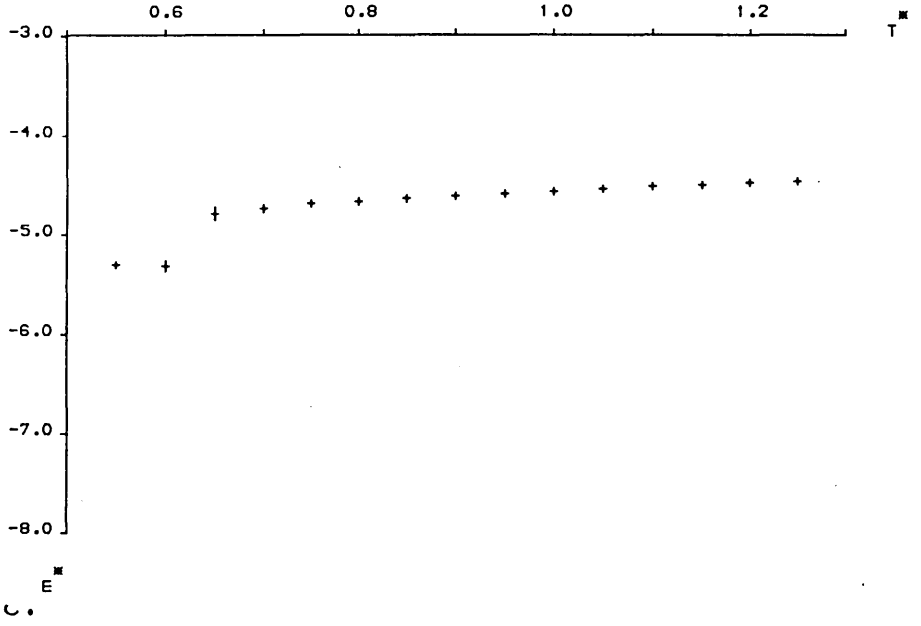

c.

Figure 4.10 b) and c).

the Monte Carlo simulation of both first order and second order transitions owing to the finite sampling of phase space. However, in practice, strong hysteresis has been taken as an indication of a first order transition [104]. Although no clear hysteresis is observed in our simulation of rigid m.m.r. molecules the bistability observed in the pretransitional region indicates that the transition may first order. Localised pretransitional ordering is a characteristic of the first order nematic to isotropic transition for rod-like molecules, although for non-mesogenic systems pretransitional behaviour is more generally associated with continuous transitions [13]. The sharp discontinuities in the order parameters and the sharp peak in the specific heat capacity also indicate that the transition observed for our rigid m.m.r. molecules may be first order [100].

We summarise the behaviour of the rigid ring m.m.r. model. At high temperature the system is in the isotropic phase. Owing to the small number of molecules in the system, the statistical fluctuations in the orientations of the molecules produce finite uniaxial and biaxial order parameters. As the temperature is lowered an increase in the uniaxial ring order parameter is observed, which we identify as a region of localised pretransitional ordering and bistability. A transition into a strongly uniaxial ring ordering is observed as the temperature is further reduced below $T^* = 0.9$. The strong uniaxial ring ordering forces a reduction in the biaxiallity of the system and also forces the mesogen system into negative uniaxial order. The transition is identified as probably first order.

The m.m.r. model has also been explored for finite values of the flex angle. Owing to the multi component nature of the systems and the complicated phases

produced, a nomenclature has been developed to summarise the phases formed. This is explained by example. For the above rigid ring simulation the ordered phase at low temperatures is described by:

$$M^{-}_{b-} \quad R^{+}_{b-}$$

The letters M and R refer to the mesogen and ring systems respectively. The superscripts refer to the uniaxial ordering of the phase. A '+' indicates a positive uniaxial order parameter and a '-' a negative order parameter. The lack of a superscript indicates a low uniaxial order parameter, not significantly different from that in the high temperature isotropic phase. The subscript b indicates a change in the biaxiallity from that observed in the isotropic phase. The '+' or '-' indicate an increase or a decrease in the biaxiallity respectively. The lack of a subscript indicates no change in the biaxiallity from isotropic.

The order parameters and internal energy are plotted in figure 4.11 for the simulation of the m.m.r. molecules with a flex angle of 15°. As the temperature is reduced there is a general increase in the uniaxial ring order parameter until a discontinuous transition to $S_r \approx 0.87$ is observed at a reduced temperature of $T^* = 0.775 \pm 0.025$. The transition in S_r is accompanied by a small discontinuous fall in the ring biaxiallity. The mesogens are still strongly coupled to the rings and are forced into a negative uniaxial order, although little change is observed in the mesogen biaxiallity which hovers about its high temperature background level of 0.1 at all temperatures. The transition is accompanied by a discrete change in the internal energy of $E^* = -0.50 \pm 0.17$ and is probably first order. We identify the phase at low temperature as $M^{-} R^{+}_{b-}$ in our

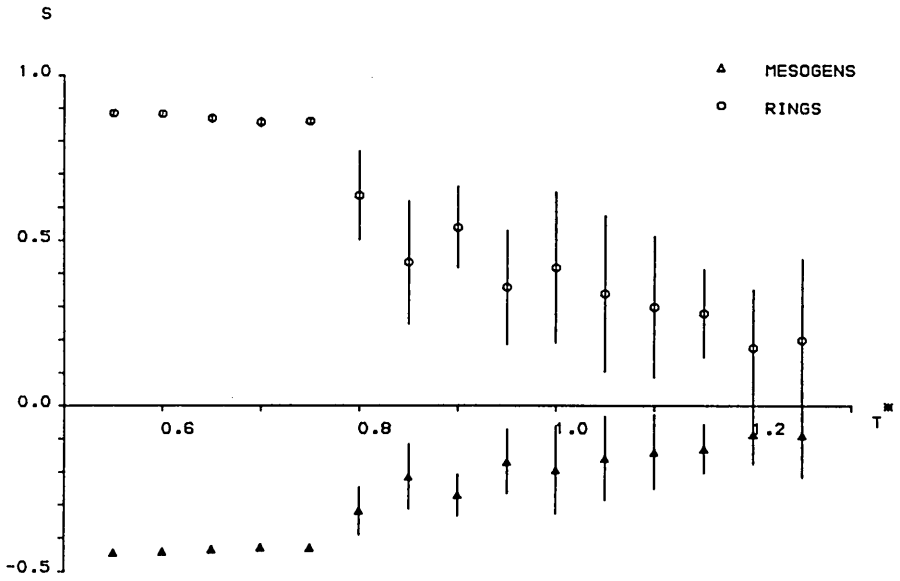

a.

Figure 4.11 a) the uniaxial order parameters; b) the biaxial order parameters and c) the internal energy for the simulation of the m.m.r. model with a 15° flex angle.

continued over...

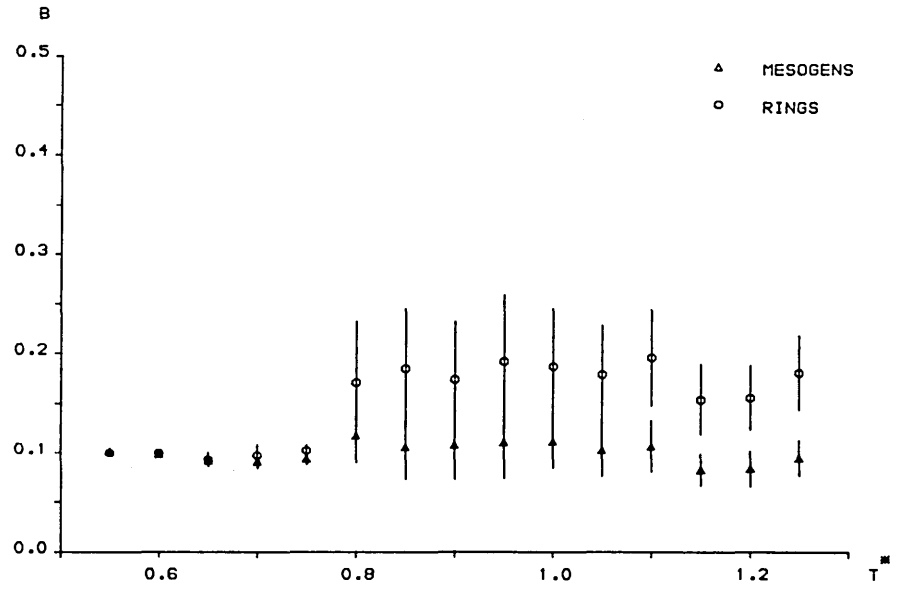

b.

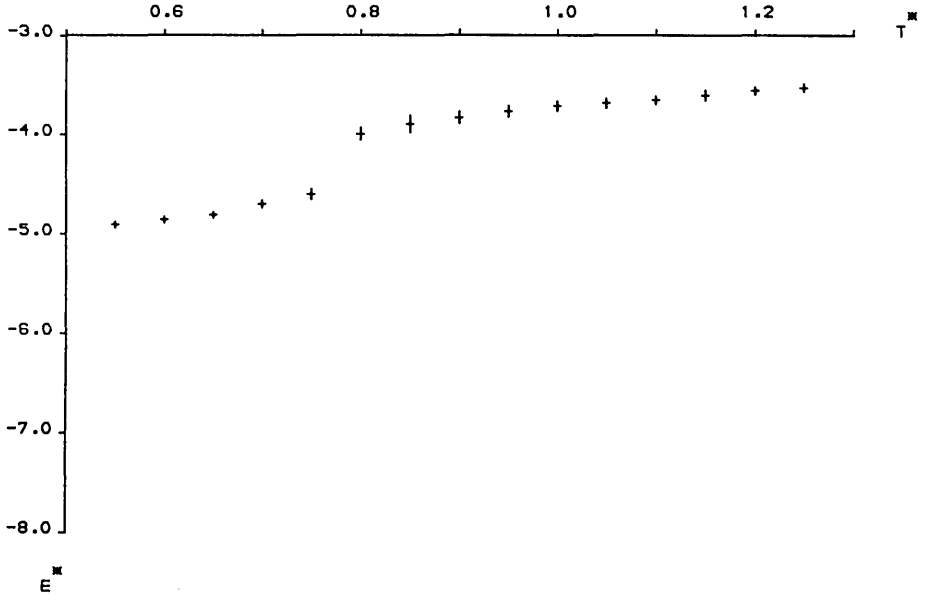

c.

Figure 4.11 b) and c).

notation.

The behaviour of the uniaxial order parameters is similar to that of the rigid rings except that the transition occurs at lower temperature and the order parameters change more smoothly in the pretransitional region. It would appear that the increase in the orientational freedom of the mesogens allows the ring dominated system to drift more smoothly between the isotropic and the ordered states. The change in the biaxiallity is less marked than for the rigid ring system.

For the system with a 30° flex angle we found a low temperature state of positive uniaxial mesogen ordering and negative ring ordering at low temperature when the system was cooled in the usual manner. However, preliminary investigations had predicted a low temperature state in which both the mesogens and the rings were positively ordered and so the simulation was re-run with a slower cooling rate of $\Delta T^{*} = -0.025$ over the region of the transition. The order parameters and the internal energy of the system are plotted in figure 4.12. A discrete increase in S_{m} is observed at a reduced temperature of $T^{*} \approx 0.79$, accompanied by a small decrease in the internal energy and a drift in S_{r} into negative order. At a lower temperature of $T^{*} \approx 0.74$ the ring system becomes quite strongly positively ordered, accompanied by a further increase in the mesogen order parameter and a decrease in the internal energy. Little change is observed in the biaxiallity order parameters between the high and low temperature states, although there are some small discrete changes associated with the transitions in the uniaxial order parameters.

We identify the phases as M R (isotropic) at high

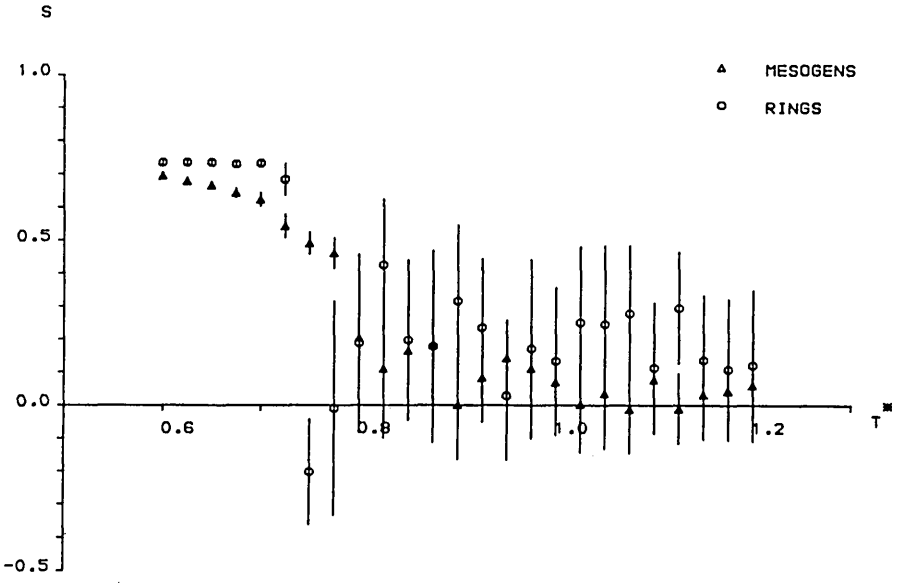

a.

Figure 4.12 a) the uniaxial order parameters; b) the biaxial order parameters and c) the internal energy for the simulation of the m.m.r. model with a 30° flex angle. slower cooling in stages of $\Delta T^* = -0.025$.

continued over...

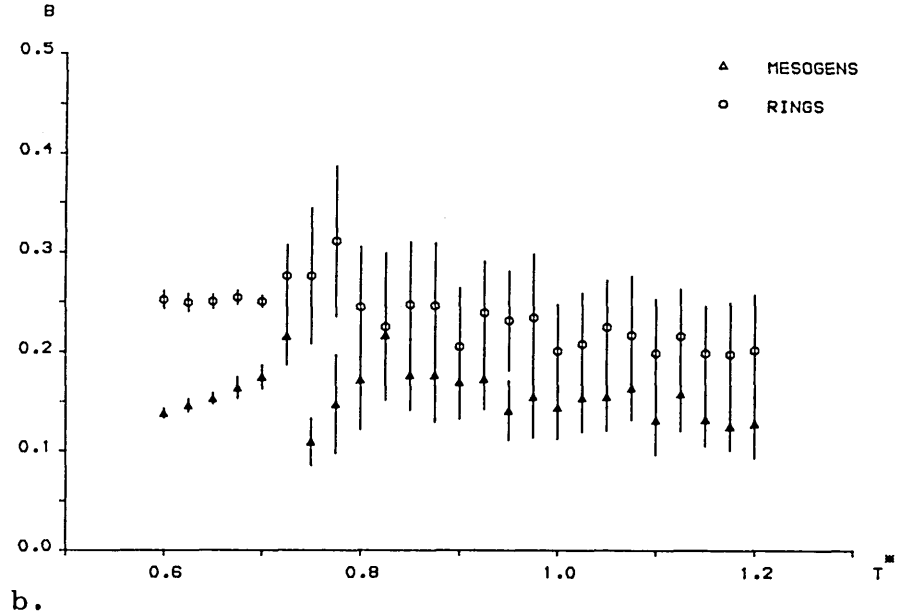

b.

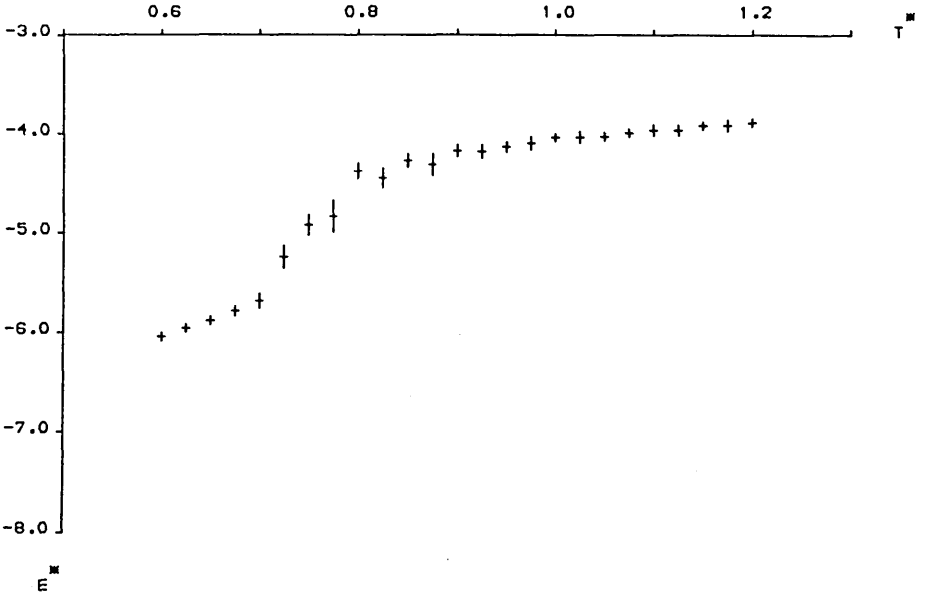

c.

Figure 4.12 b) and c).

temperature, M^+R^- at lower temperature and M^+R^+ at even lower temperature. However, considering the results obtained at the usual, faster, cooling rate we cannot identify with certainty which of the states is the true equilibrium state at low temperature. It is clear that at this flex angle of 30° the system is in a region of transition from ring dominated ordering, for smaller flex angle, to mesogen dominated ordering, for larger flex angle. In such a region close to a triple point it may be expected that the transition temperatures would be difficult to locate exactly, a problem exacerbated by the use of such a small system of molecules [38,102].

The results of the simulation with a flex angle of 45° are given in figure 4.13. There is a sharp transition in the uniaxial mesogen order parameter from low order at high temperature to $S_m \approx 0.8$ at a reduced temperature of $T^* = .925 \pm .025$. This transition is accompanied by a fall in the mesogen biaxiallity, an increase in the ring biaxiallity and a discontinuous decrease in the internal energy. There is an apparent transition in S_r at the lower temperature of $T^* \approx 0.625$, but there is no associated change in the internal energy. However, in the temperature region between this apparent transition and the transition identified in S_m, the ring system is highly biaxial and the fluctuations in S_r are large, as indicated by the error bars. In this region S_r is fluctuating between moderate positive and negative order as may be expected for a highly biaxial system. The magnitude of the instantaneous ring uniaxial order parameter must be as large as B_r, ie. $|S_r| \approx 0.4$. The apparently large transition in the rings at $T^* \approx 0.625$ merely corresponds to a small increase in magnitude of the uniaxial order parameter, which forces S_r to be always positive rather than fluctuating between positive and negative values. Consequently, there is only one

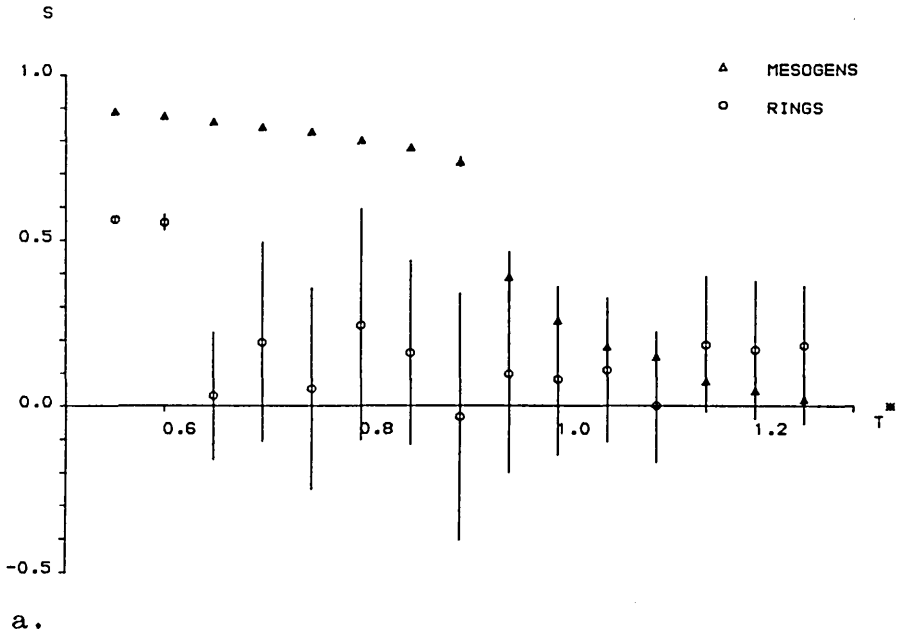

a.

Figure 4.13 a) the uniaxial order parameters; b) the biaxial order parameters and c) the internal energy for the simulation of the m.m.r. model with a 45° flex angle.

continued over...

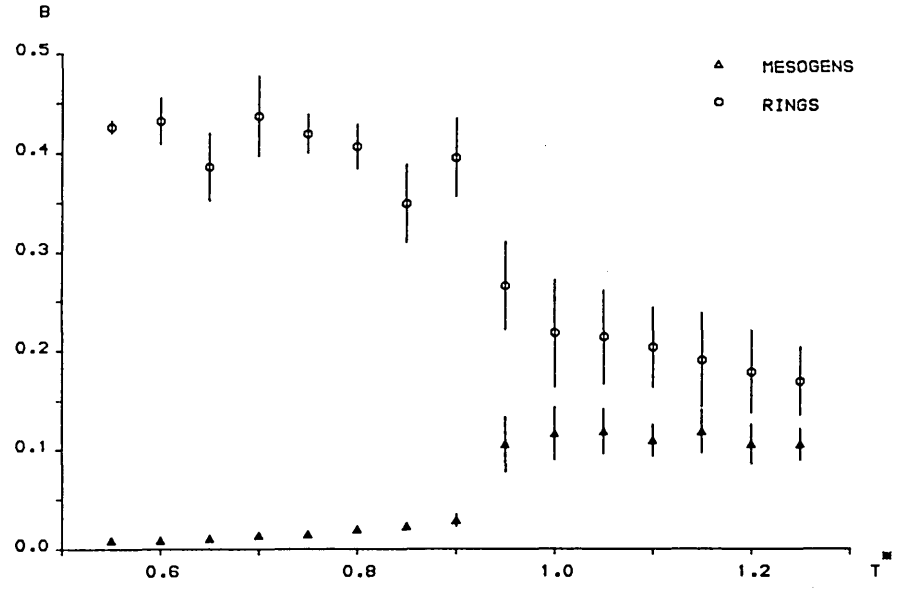

b.

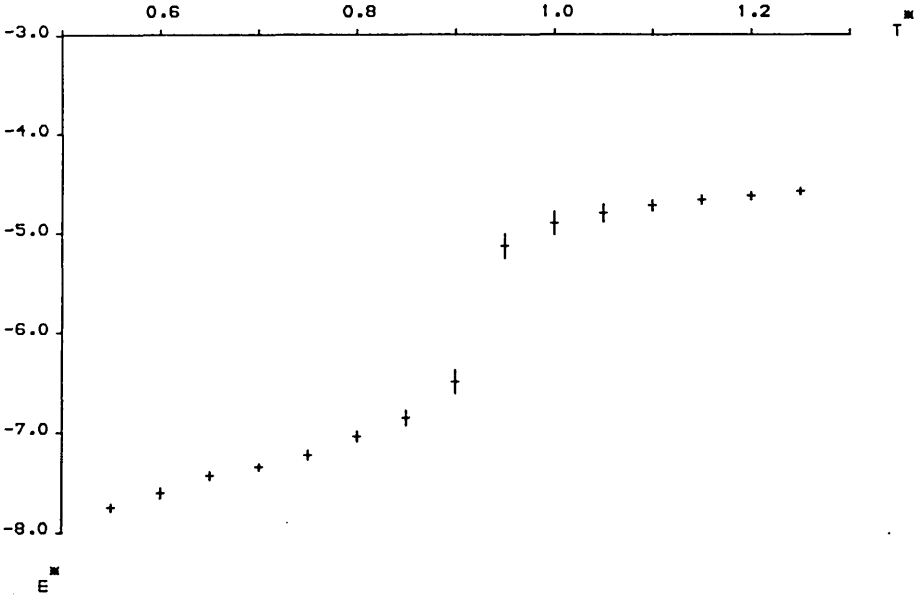

c.

Figure 4.13 b) and c).

true transition in the system, which is from isotropic to $M^{+}_{b-}R^{+}_{b+}$.

The order parameters and internal energy are presented in figure 4.14 for the system of m.m.r. molecules with a flex angle of 60°. A single sharp transition is observed at a temperature of $T^{*} = 0.975 \pm 0.025$. There is a large discontinuous increase in S_r and S_m as the temperature is reduced, which is accompanied by decreases in both of the biaxiallity parameters. There is a large discontinuous decrease in the internal energy of $E^{*} = -1.64 \pm 0.36$ strongly suggesting a first order transition. The state at low temperature is highly uniaxially ordered in respect of both the rings and the mesogens and is classified as $M^{+}_{b-}R^{+}_{b-}$. A simulation with 60° flex angle was also performed from low to high temperature, in which case the transition to the isotropic phase from the ordered phase was observed at a reduced temperature of $T^{*} = 1.075 \pm 0.025$, indicating some small hysteresis in this transition.

There is a significant ordering of the mesogens at temperatures just above the transition, not seen also in the rings, which indicates that the ordering mechanism is mesogen dominated. However, it is clear that the coupling between the mesogens and the rings is strong enough to encourage the rings to align whilst not so strong that the high degree of uniaxial mesogen ordering inhibits the formation of a strongly ordered ring system, as was observed in the cases of 30° and 45° flex angle. For the 60° flex angle simulation, the temperature of the transition is relatively high and the uniaxial ordering of the state at lower temperature is especially strong for both the mesogens and the rings. At this strength of coupling, the mesogens and the rings reorientate in a

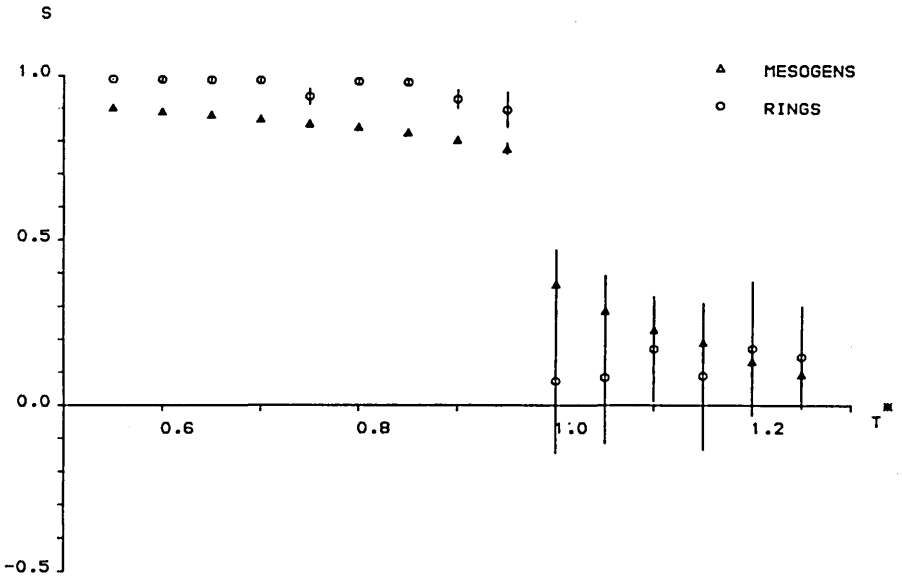

a.

Figure 4.14 a) the uniaxial order parameters; b) the biaxial order parameters and c) the internal energy for the simulation of the m.m.r. model with a 60° flex angle.

continued over...

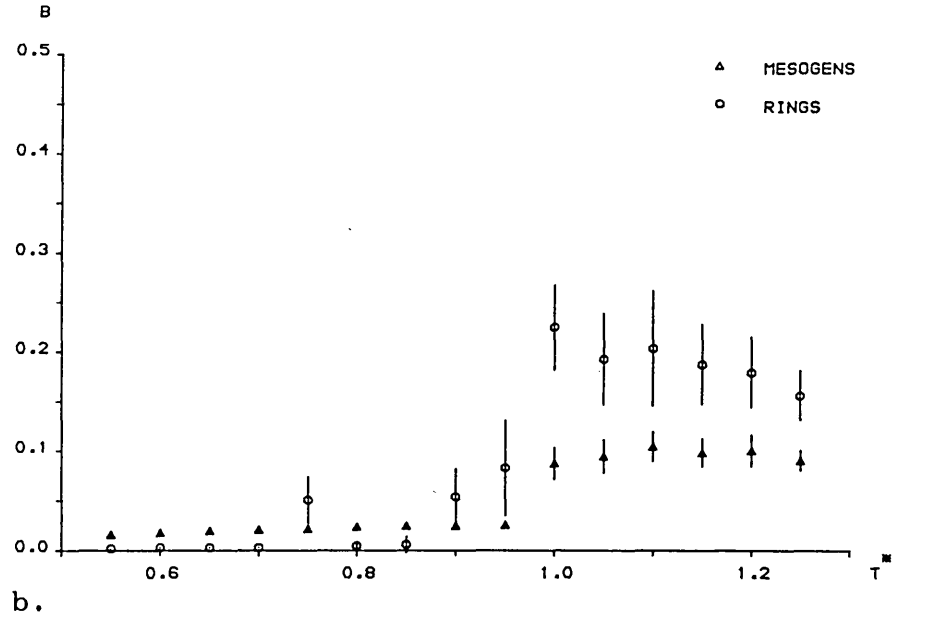

b.

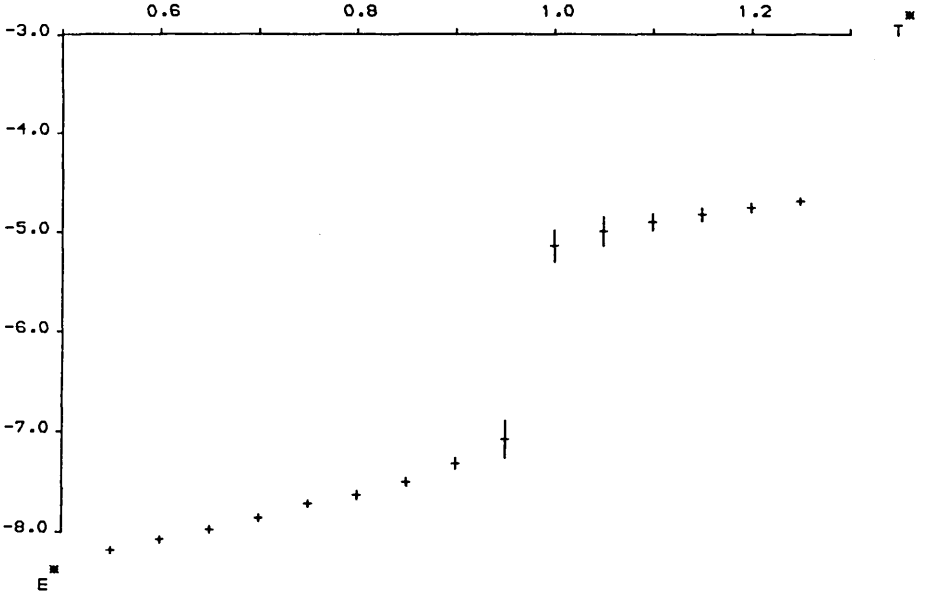

c.

Figure 4.14 b) and c).

cooperative manner to produce a stable and highly ordered phase.

Figure 4.15 gives the order parameters and the internal energy for a system of m.m.r. molecules with a 75° Flex angle. The variation in the uniaxial mesogen order parameter with temperature is mostly continuous, although two small discrete increases may be identified at $T^* \approx 0.925$ and $T^* \approx 0.825$. Small changes in the internal energy are also seen at these temperatures, although the fluctuations in the energy are of a similar magnitude. There is a distinct increase in S_r at the lower of the two temperatures. An increase in the ring biaxiallity is observed at the lower temperature of $T^* \approx 0.7$, and associated with this is a temporary fall in the uniaxial ring order parameter and a change in the gradient of the internal energy. The following phases are identified: isotropic to $M^+_{b-}R$ down to $M^+_{b-}R^+$ and further down to $M^+_{b-}R^+_{b+}$. However, it is again likely that the exact phase behaviour has been obscured by too rapid cooling, possibly inadequate thermalisation at low temperature and poor statistics due to the size of the system. The observed sequence of phases may be simplified were the simulation performed on a much larger system, cooled more slowly.

The order parameters for the simulation with a flex angle of 90° are given in figure 4.16. The transitions in the mesogen order parameters are continuous, with the uniaxial order parameter becoming large as the temperature is reduced. At low temperature S_r is low with some scatter and the associated ring biaxiallity is large. The change in the internal energy is mostly continuous with a distinct drop at a temperature of $T^* = 0.775 \pm 0.025$. Comparison between the change in the ring biaxiallity and the change in slope of the uniaxial

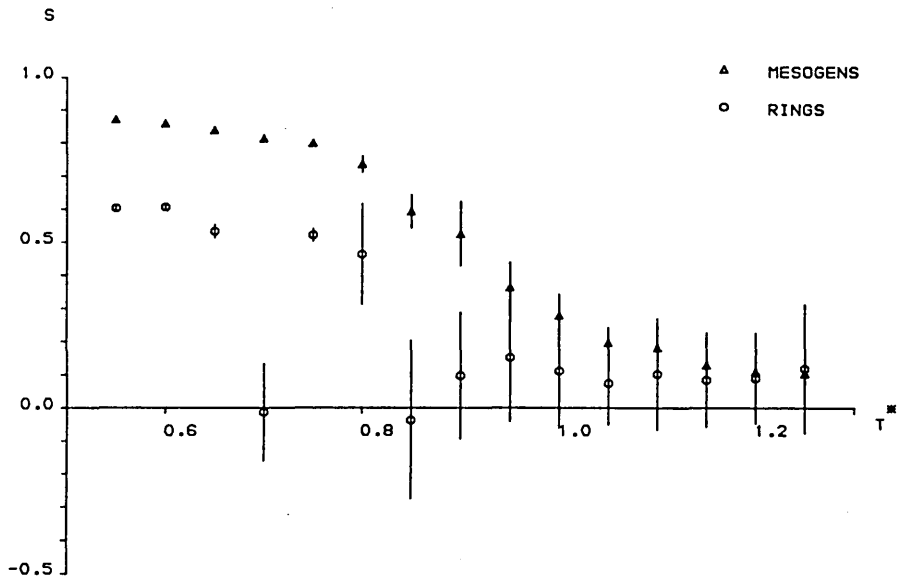

a.

Figure 4.15 a) the uniaxial order parameters; b) the biaxial order parameters and c) the internal energy for the simulation of the m.m.r. model with a 75° flex angle.

continued over...

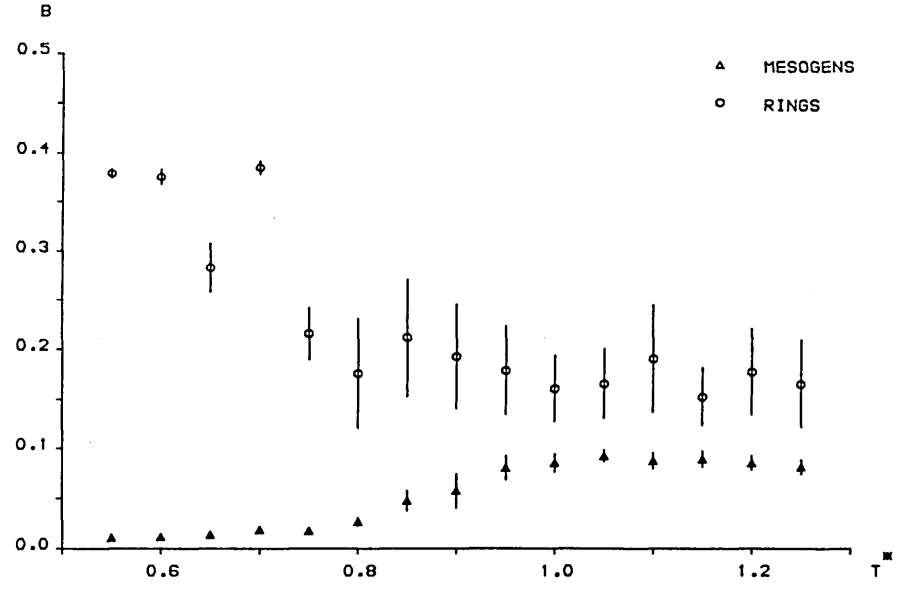

b.

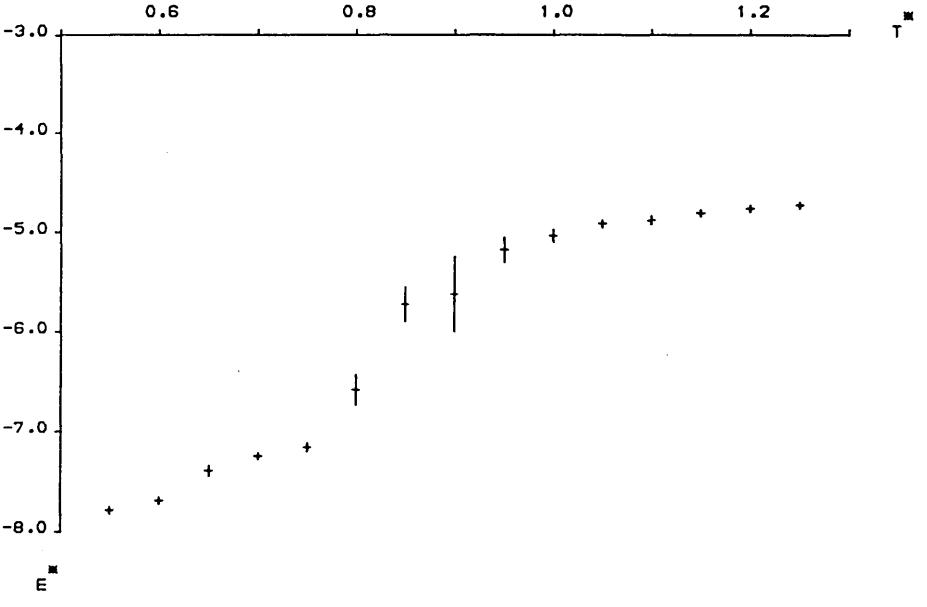

c.

Figure 4.15 b) and c).

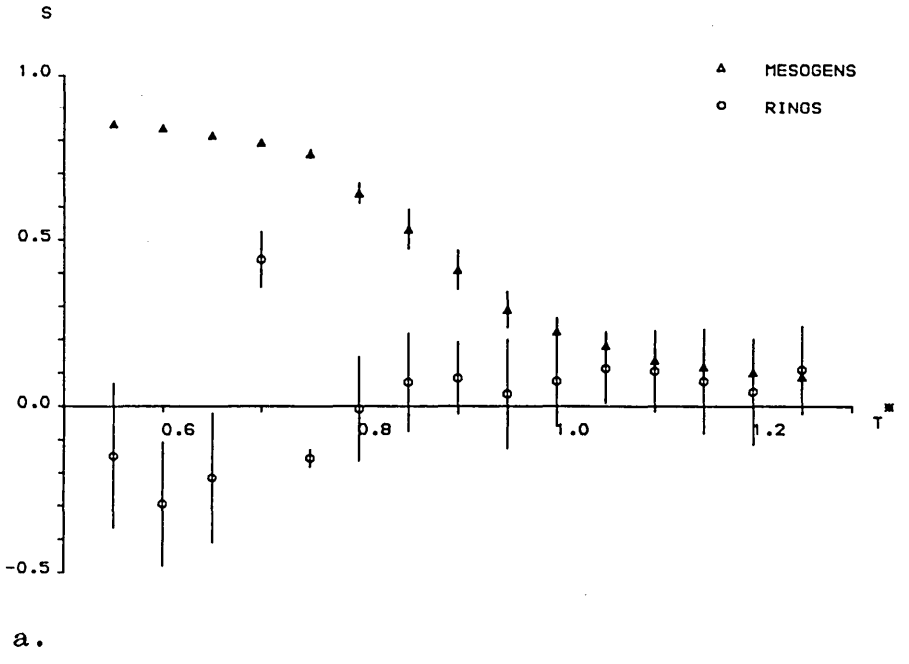

a.

Figure 4.16 a) the uniaxial order parameters; b) the biaxial order parameters and c) the internal energy for the simulation of the m.m.r. model with a 90° flex angle.

continued over...

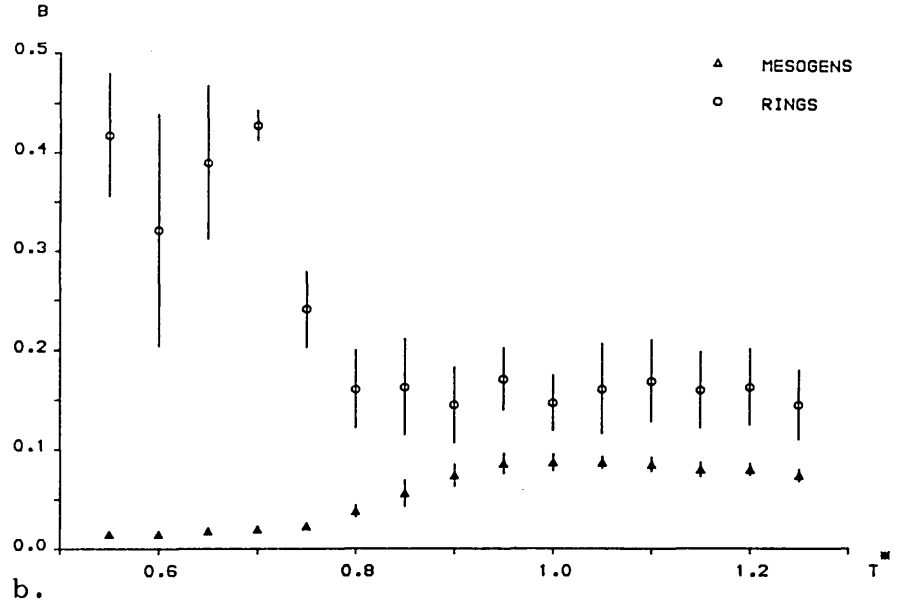

b.

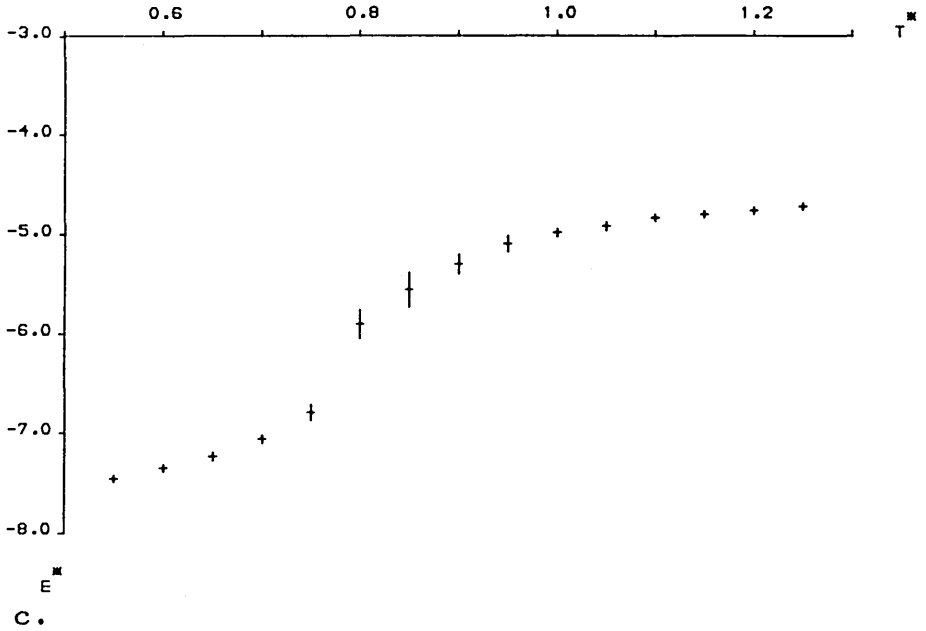

c.

Figure 4.16 b) and c).

mesogen order parameter suggest a single transition at T^* $\approx$ 0.75 from the isotropic phase to $M^+_{b-}R^-_{b+}$.

The results of the simulation for the flex angle of 180° are given in figure 4.17. The uniaxial order parameter for the mesogens increases continuously as the temperature is reduced, with a discontinuity in the slope at $T^* \approx 0.75$, which corresponds with a small drop in the internal energy and an increase in the ring biaxiallity to about $B_m \approx 0.2$. The phase behaviour is therefore similar to the simulation with a flex angle of 90°, except that for the simulation with the larger flex angle the increased decoupling of the mesogenic units from the ring backbones results in a lower B_r in the low temperature ordered phase. S_r remains low throughout the temperature range and B_m falls from its high temperature statistical value as the mesogens adopt uniaxial order. A single transition from isotropic to $M^+_{b-}R^+_{b+}$ is identified.

A simulation of 60 free mesogens has also been performed at a reduced volume of $V^* = 1.4$. In figure 4.18, a comparison is made between S_m for the 180° flex angle m.m.r. system and the mesogen only system. At high and low temperature, the mesogen order parameters are closely similar. However, in the region of the transition, the m.m.r. model exhibits a higher order parameter, indicating that the presence of the rings stabilises the mesogen phase to a small extent.

The phases observed are summarised in table 4.1 and the changes in the internal energy and the order parameters on the transition from high to low temperature are tabulated in table 4.2.

By considering only isotropic phases and the final

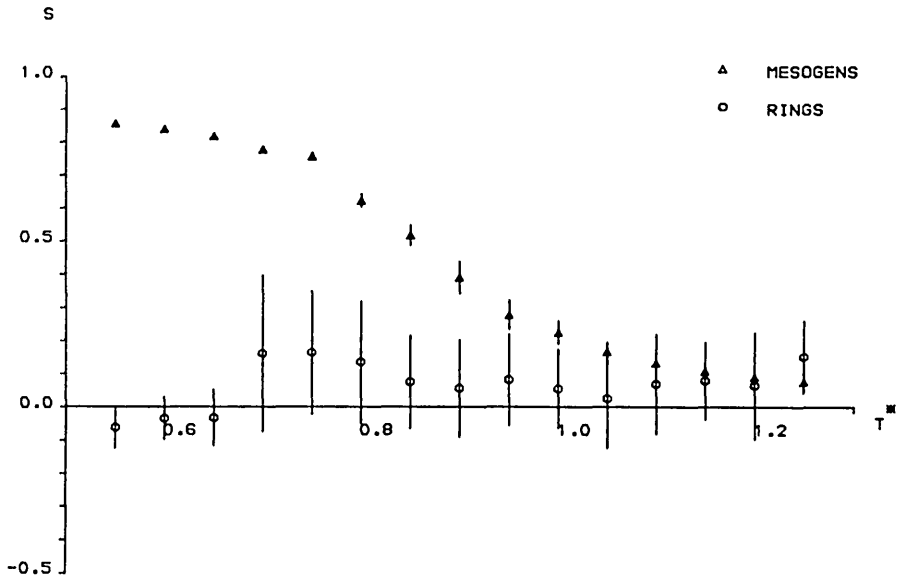

a.

Figure 4.17 a) the uniaxial order parameters; b) the biaxial order parameters and c) the internal energy for the simulation of the m.m.r. model with a 180° flex angle.

continued over...

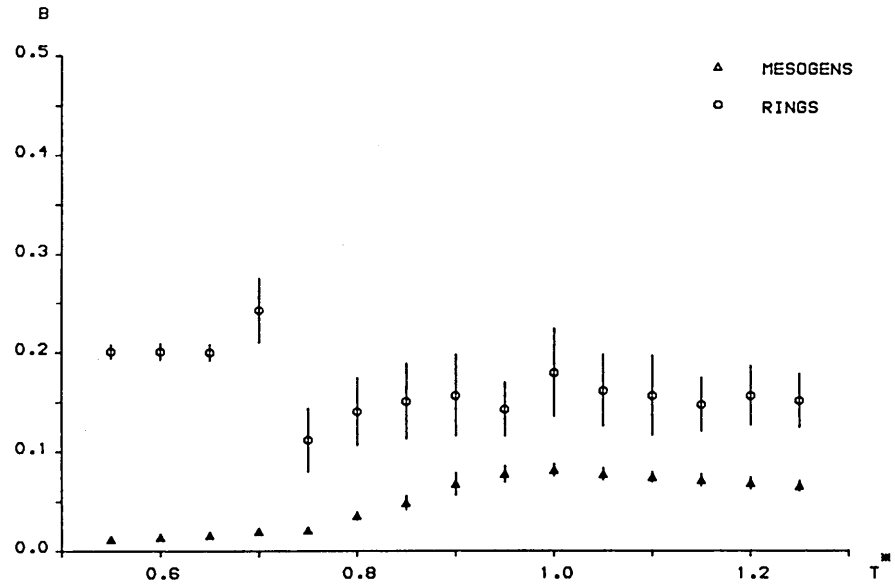

b.

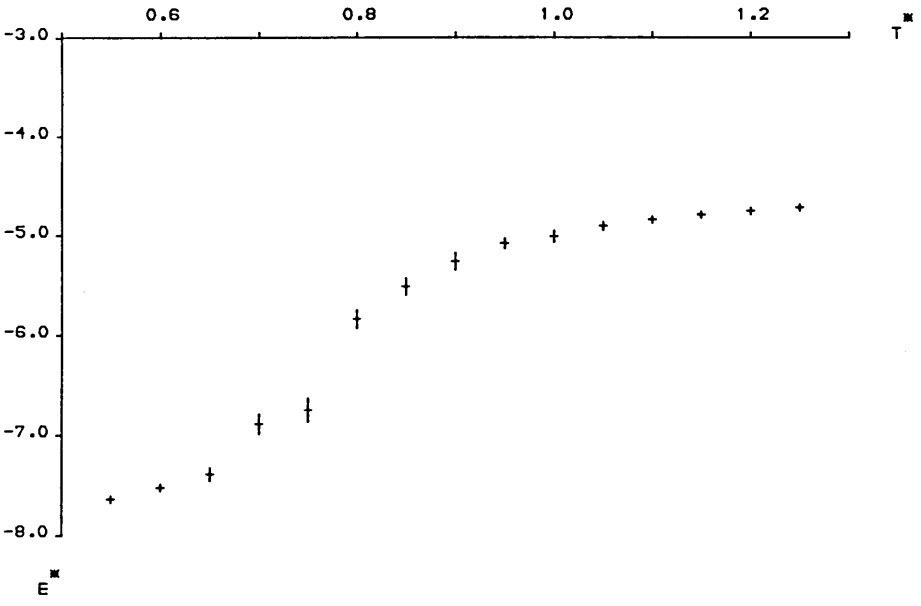

c.

Figure 4.17 b) and c).

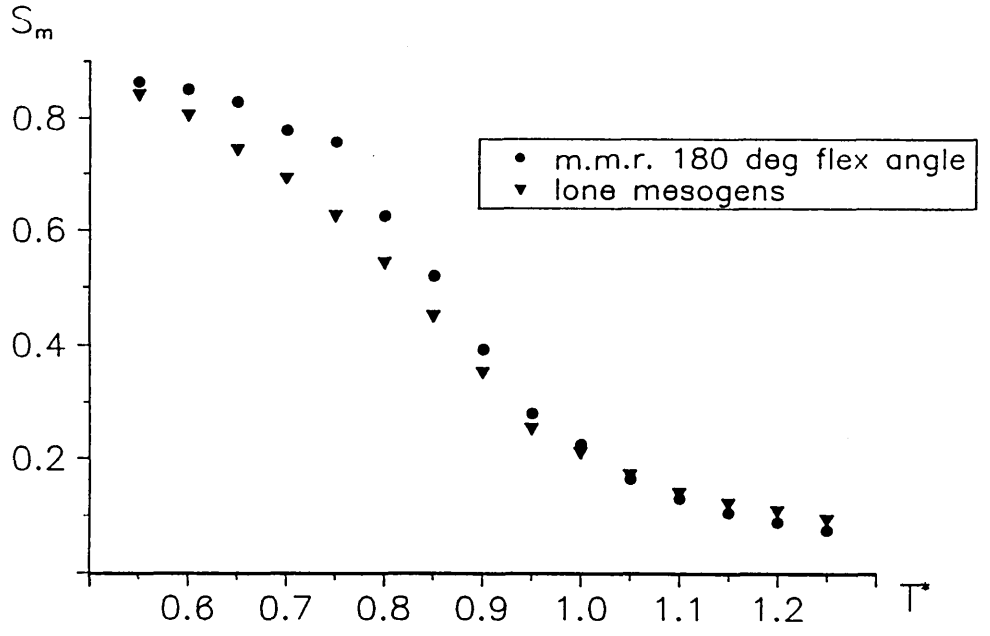

Figure 4.18 The uniaxial order parameters from the simulation of 60 lone mesogens and the simulation of the m.m.r. model with a flex angle of 180°.

flexangle	phase changes on reduction of temperature
0°	$I \xrightarrow{T^* = 0.9} M^-_{b-}\ R^+_{b-}$
15°	$I \xrightarrow{T^* = 0.775} M^-\ R^+_{b+}$
30°	$I \xrightarrow{T^* = 0.79} M^+\ R^- \xrightarrow{T^* = 0.74} M^+\ R^+$
45°	$I \xrightarrow{T^* = 0.925} M^+_{b-}\ R^+_{b+}$
60°	$I \xrightarrow{T^* = 0.975} M^+_{b-} R^+_{b-}$
75°	$I \xrightarrow{T^* = 0.925} M^+_{b-}\ R \xrightarrow{T^* = 0.825} M^+_{b-}\ R^+ \xrightarrow{T^* = 0.7} M^+_{b-}\ R^+_{b+}$
90°	$I \xrightarrow{T^* = 0.75} M^+_{b-}\ R^-_{b+}$
180°	$I \xrightarrow{T^* = 0.75} M^+_{b-}\ R_{b+}$

Table 4.1 The phases observed in the Monte Carlo simulation of the m.m.r. model as the temperature is reduced. "I" = isotropic, "M R" symbols as in text.

Flex angle	$T^*_{transition}$	ΔE^*	ΔS_m	ΔS_r	ΔB_m	ΔB_r
0°	.9 ± .025	-.43 ± .10	-.20 ± .15	+.40 ± .30	-.07 ± .04	-.13 ± .07
15°	.775 ± .025	-.50 ± .17	-.29 ± .10	+.57 ± .20	-.06 ± .04	-.11 ± .07
30°	.79 ± .013	-.39 ± .26	+.25 ± .18	-.19 ± .19	———	———
	.74 ± .013	-.22 ± .22	-.02 ± .02	+.89 ± .21	———	———
45°	.925 ± .025	-.74 ± .24	+.23 ± .10	———	-.07 ± .03	+.11 ± .08
60°	.975 ± .025	-1.64 ± .36	+.34 ± .11	+.74 ±.28	-.06 ± .02	-.17 ± .08
75°	.925 ± .025	-.40 ± .50	+.16 ± .16	———	+.02 ±.02	———
	.825 ± .025	-.50 ± .50	+.08 ± .08	+.50 ± .39	+.62 ± .01	———
	.7 ± .025	———	———	———	———	+.17 ± .03
90°	.75 ± 0.25	-.34 ± .34	———	———	———	+.15 ± .05
180°	.75 ± .025	-.30 ± .21	———	———	———	+.12 ±.06

Table 4.2 The changes in the reduced internal energy and the order parameters for the m.m.r. model at transitions occurring as the system was cooled from an isotropic state.

low temperature phase, a phase diagram of the behaviour of the m.m.r. model has been created which shows the variation of behaviour with flex angle. This phase diagram is shown in figure 4.19, where the indicated temperature of the transition from isotropic to the ordered phase is that of the higher temperature transition in each case where more than one transition has been indicated in the above discussion. Hence it is the onset of ordering that is indicated in the diagram rather than the transition to the final low temperature state. The shape of the diagram would be little changed by the choice of one of the lower transition temperatures.

Three distinct regions are identified on the phase diagram. In the 'discotic' region the uniaxial ring order parameter is large and positive, and the mesogen uniaxial order parameter is negative. The ring normals tend to align parallel and the mesogen axes are forced to lie in planes perpendicular to the director of the ring system. There is a single transition from isotropic to discotic which is probably first order. The discotic behaviour is observed for small flex angles of 15° or less.

For flex angles of 90° or greater the low temperature phase is labelled 'calamitic/biaxial'. In this phase the mesogenic units tend to align parallel with a large positive S_m and the ring normals form a biaxial phase. The transition from the isotropic phase is continuous for the mesogens and discontinuous for the ring normals. The changes in the internal energy are continuous or small.

For intermediate flex angles both the mesogen and ring systems exhibit positive uniaxial ordering at low

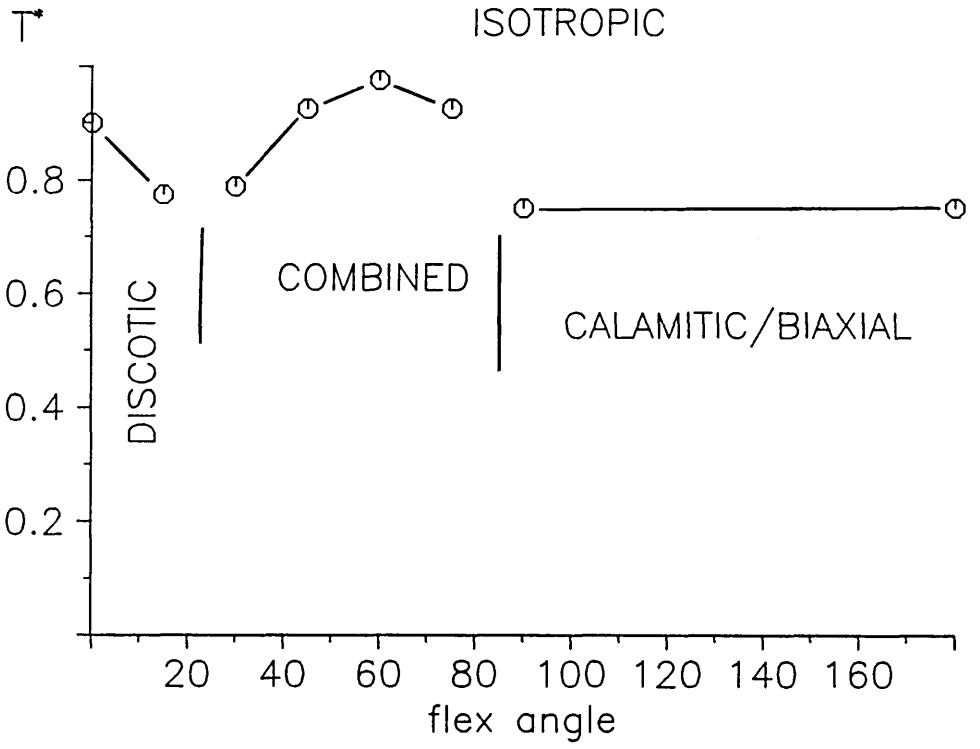

Figure 4.19 Simplified phase diagram of temperature against flex angle for the m.m.r. model.

temperature. This region is labelled as 'combined'. For flex angles of 60° the strength of the ordering is the maximum observed and the transition from the isotropic to the ordered phase is especially distinct and almost certainly first order. As the flex angle is either increased or decreased away from 60° the strength of the ordering is reduced, especially in the case of the rings, the size of the discontinuity in the internal energy at the transition diminishes and the ring systems become biaxial at low temperature.

The end configuration of each temperature stage of each simulation was stored to allow further study of the phases. The interpretation of data obtained from these configurations needs to be considered with caution because the single configuration does not represent the ensemble average state of the system. However, this does not prevent the study of such configurations providing some insight into the behaviour of the systems.

The angles between the ring and mesogen uniaxial directors have been calculated from these end configurations and have shown a definite angular correlation between the directors in the 'discotic' and 'combined' regions of the phase diagram. In these regions it is found that the mesogen and ring directors align parallel to each other to within a few degrees when the rings are positively uniaxially ordered and the mesogens are negatively ordered. When both the rings and the mesogens are positively uniaxially ordered the directors are, to within a few degrees, perpendicular. However, if the flex angle is increased to 90° or beyond then the coupling between the ring and mesogen directors is lost.

Similarly, it is also found in the 'discotic' and

'combined' regions that at least one of the eigenvectors of each of the ordering matrices is aligned along an axis of the containing box. This alignment is a result of the periodic boundary conditions, although the exact mechanism is unknown. The interaction with the periodic boundaries would be expected to be more pronounced for systems of a small number of molecules, in which the size of the molecule is comparable to the size of the box. Indeed, some alignment with the box axes has been observed in a simulation of 15 lone mesogens, where no such alignment was observed in a simulation of 60 mesogens. The alignment with the box axes is observed for the m.m.r. molecules in the cases of moderate to strong coupling between the rings and the mesogens. In these cases the ring structure is a more substantial entity than in the cases of weak coupling and some interaction between the 15 rings and the boundaries may be expected.

A simulation of nematogens in an external field [53] has shown that the alignment of an ordered phase may be forced along a specific direction without incurring a substantial change in the magnitude of the ordering of the phase. Similarly, we suggest here that the aligning nature of the periodic boundaries of the container make only a second order contribution to the formation of the ordered phases observed.

Diagrams of the positions and orientations of the mesogens and rings have been created from the configuration data. Such a diagram is given in figure 4.20a for the rigid ring simulation in the ordered phase. The mesogen and ring axes are plotted in separate squares as indicated and the view is down the 'y' axis, compressed so that all of the molecules appear in the one 'x-z' plane. The asterisk symbols represent the centres

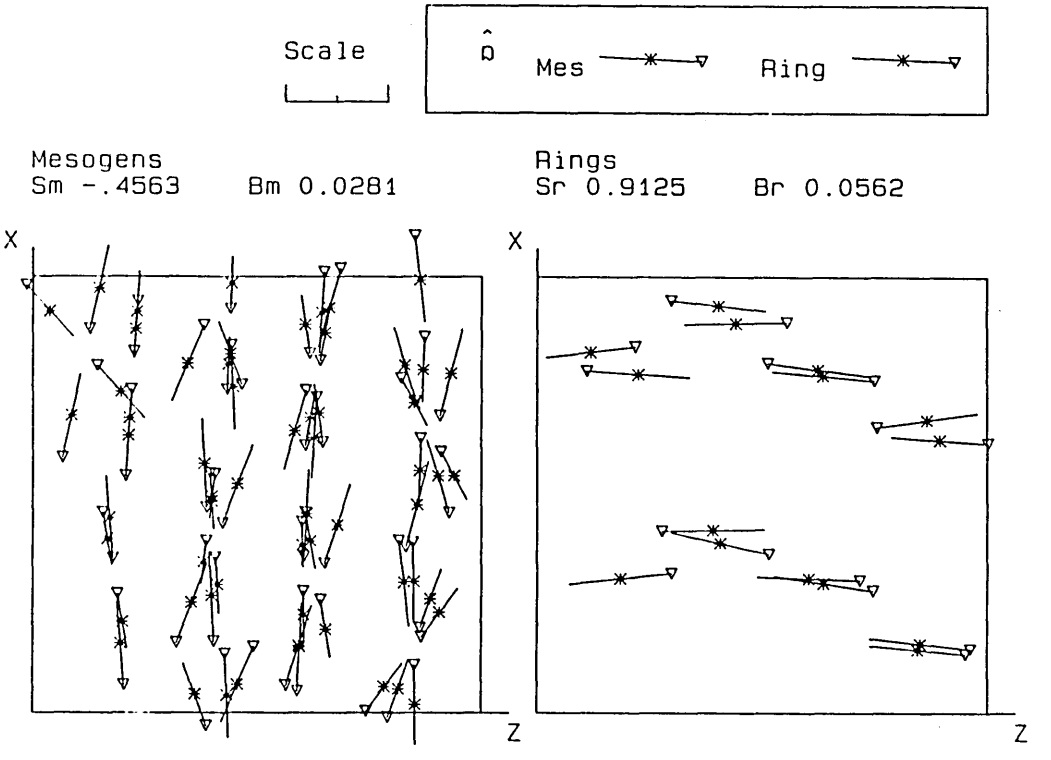

Figure 4.20 The end configuration of the simulation of the m.m.r. model with a flex angle of 0° at a temperature of $T^{*} = 0.90$. Symbols as in text.

a) viewing x-z plane. continued over...

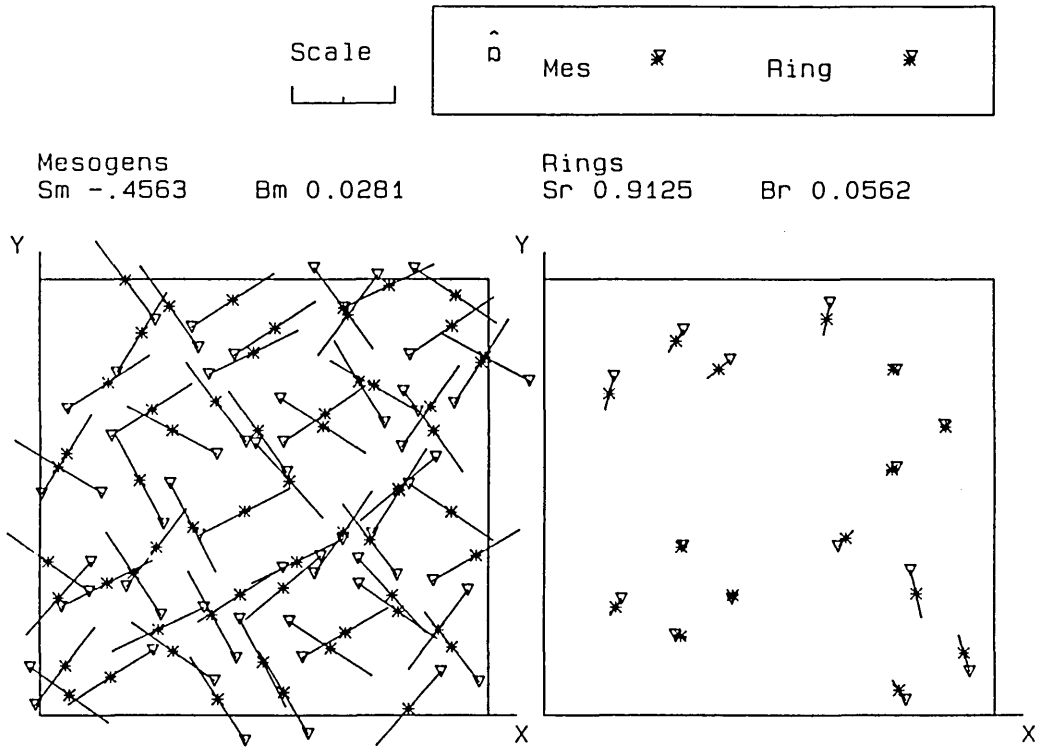

Figure 4.20 b) viewing x-y plane.

of mass of the mesogens and the geometric centres of the rings. The lines represent the long axes of the mesogens and the normals to the rings. The lengths of the lines indicate the components of the molecular axes in the 'x-z' plane. The length of an axis which is parallel to the 'x-z' plane is indicated by the scale, the length of which is also σ in the definition of the mesogen-mesogen interaction potential. The triangles indicate which end of the molecular axis is pointing downwards. The directions of the ring and mesogen directors are indicated in the box labelled '$\hat{\underset{\sim}{n}}$'.

For the case of the rigid rings given in the figure, well defined spatial ordering is observed for both the mesogens and the rings. Figure 4.20b gives a view of the same configuration down the 'z' axis. Some of the rings are stacked in staggered columns and the mesogens are forced to lie in planes perpendicular to the columns of rings with many of the mesogens aligned in pairs. This indicates how the uniaxial ordering of the rings produces a stable state when the only anisotropic energy contribution is that between the attached mesogens. As the temperature is reduced further the pairing of the mesogenic units and the grouping of the rings into columns becomes more complete, as shown in figure 4.21.

The well defined layering of the mesogenic units is typical of a smectic mesophase. However, only a small system of molecules has been studied here and it is uncertain whether the observed structure would persist over long distances in a large system. Also it should be noted that the spatial packing of the molecules may be strongly related to the dimensions of the periodic box [38].

As the flex angle is increased, the definition of

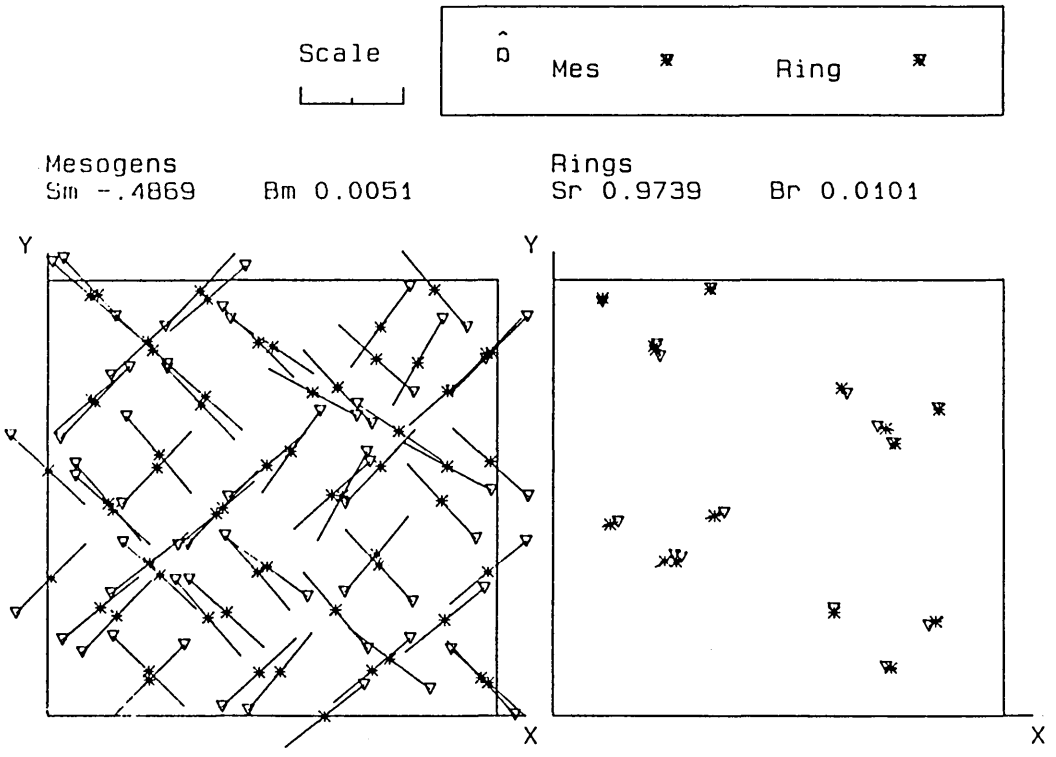

Figure 4.21 The end configuration of the simulation of the m.m.r. model with a flex angle of 0° at a temperature of $T^{*} = 0.85$. Symbols as in text.

the spatial ordering is reduced. Figure 4.22 shows an ordered configuration of the 15° flex angle case. Correlations can be seen between pairs of ring normals, but no columnar stacking is present. There is still some layering of the mesogens, but this is less well defined than for the rigid rings.

As the flex angle is increased further the spatial ordering remains partial with some stacking of the mesogens in layers until a flex angle of 60° is reached. In this case the mesogens stack quite well in layers and exhibit some hexagonal packing as shown in figure 4.23. However, no clear structure is observed in the spatial packing of the rings. The short-range hexagonal packing of the mesogenic units is likely to be an artefact of the spherical space packing properties of the model mesogens, as discussed earlier, and it is unlikely that this type of packing would be observed in a system of genuinely rod-shaped mesogens.

As the flex angle is increased even further the spatial ordering of the mesogens is diminished, although some tendency for packing in layers is retained up to the full flexibility, as can be seen in figure 4.24 for a 180° flex angle. No layering of the mesogens has been observed in the simulation of lone mesogens.

From these configuration plots we conclude that the attachment to rings induces layering of the mesogens for all flex angles. Well defined layering is observed in the extreme case of rigid rings, combined with the stacking of the rings in staggered columns. Some short-range hexagonal packing is observed in the case of a 60° flex angle, but it is not expected that this would be observed if the mesogenic units possessed more realistic rod-like space packing properties. For other

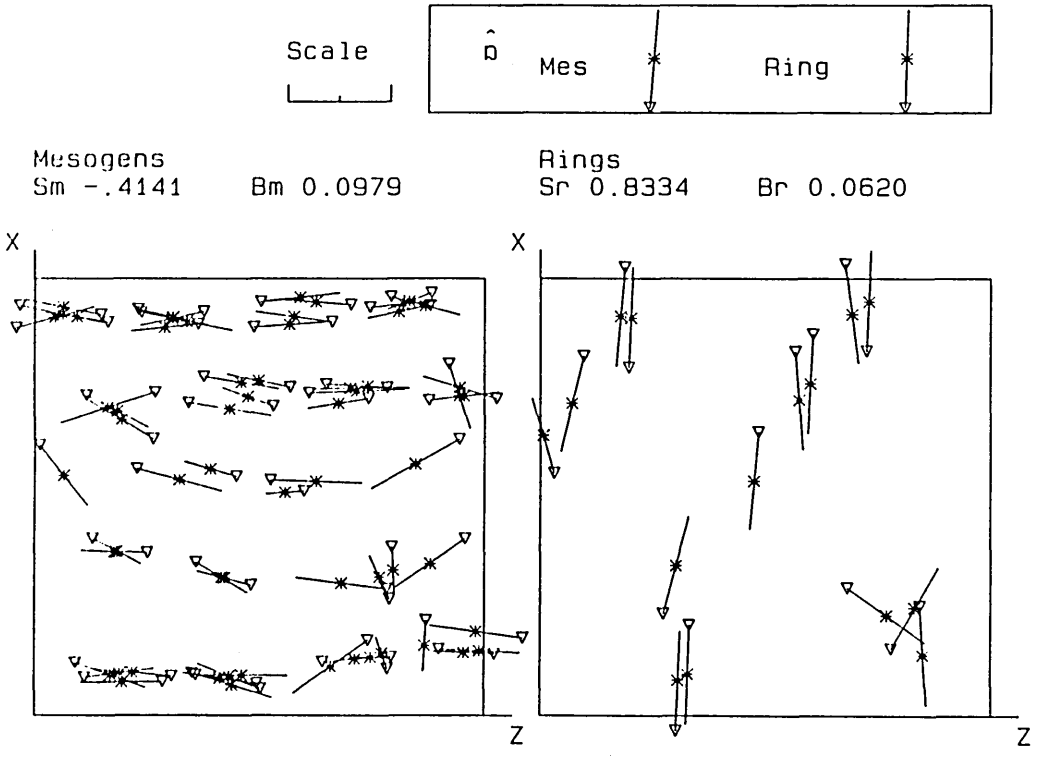

Figure 4.22 The end configuration of the simulation of the m.m.r. model with a flex angle of 15° at a temperature of $T^* = 0.70$.

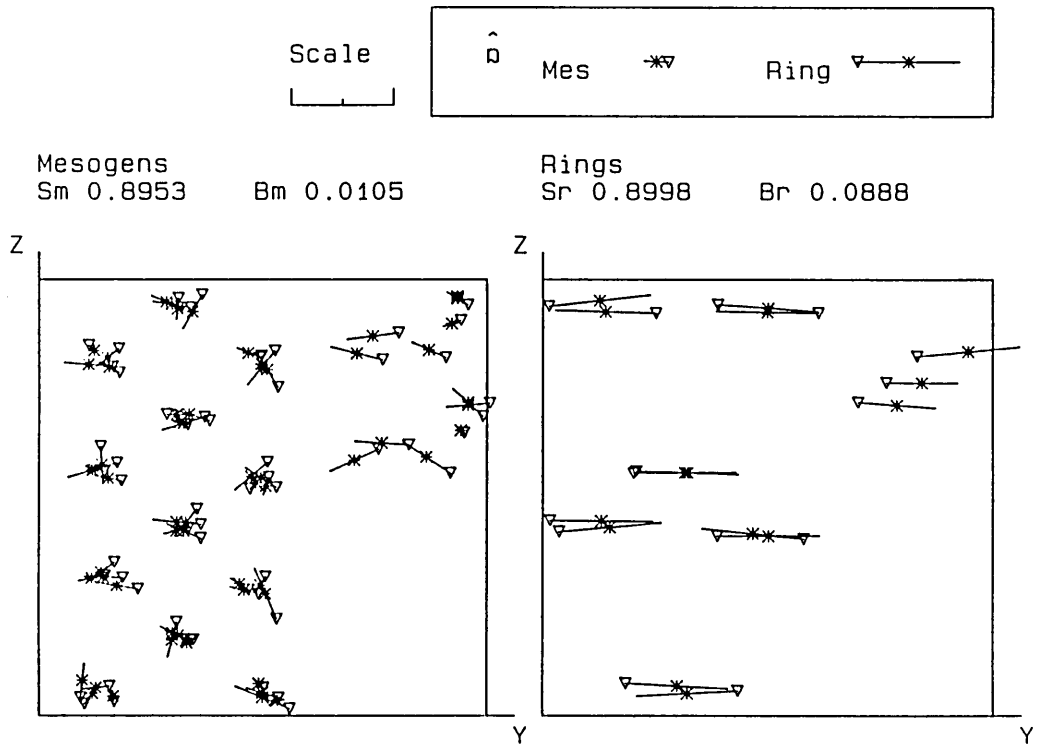

Figure 4.23 The end configuration of the simulation of the m.m.r. model with a flex angle of 60° at a temperature of $T^* = 0.90$.

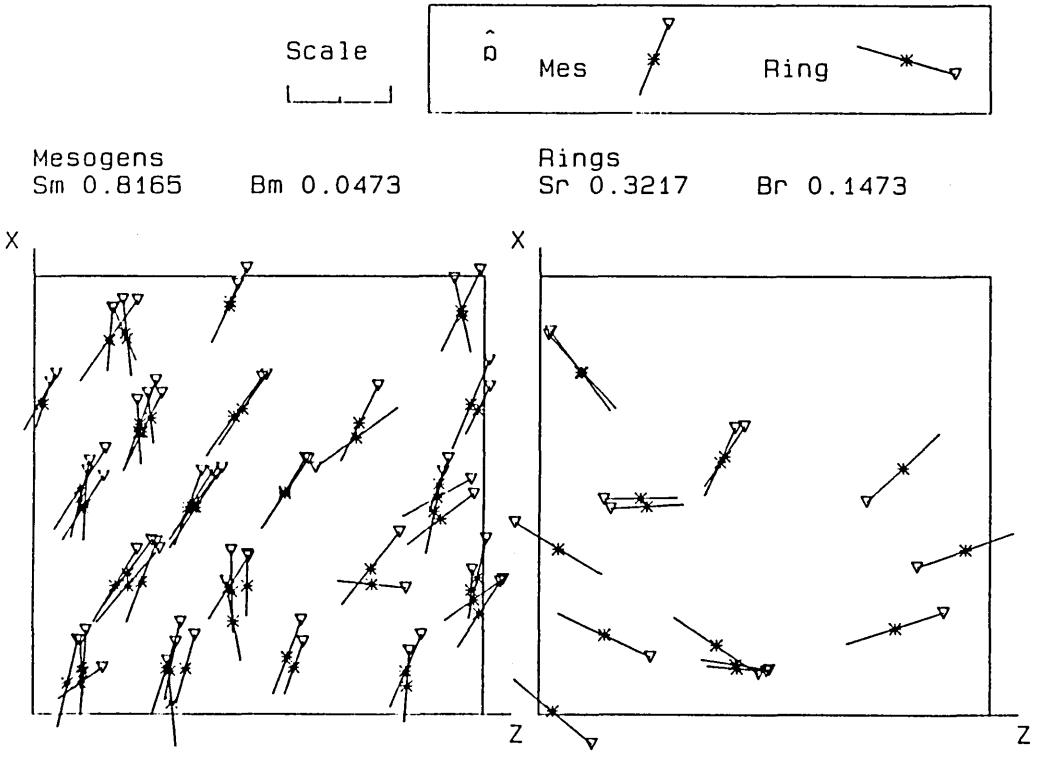

Figure 4.24 The end configuration of the simulation of the m.m.r. model with a flex angle of 180° at a temperature of $T^* = 0.70$.

values of the flex angle the packing of the mesogens is less definite and it is suggested that all of the ordered mesogenic phases are smectic.

CONCLUSIONS

A multi-component model has been used to model the behaviour of cyclic side-chain liquid crystal oligomers. Because of the large amount of computing time required, the simulations have been restricted to systems of 60 mesogens and 15 rings. Consequently, there has been some difficulty in the precise location of some phase transitions and the identification of the phases produced. However, it has been possible to produce a clear phase diagram of the change in behaviour of the system of molecules as the flexibility of the linkage between the mesogens and the rings is increased. A change from ring dominated to mesogen dominated behaviour is observed, with the formation of a phase of combined ring and mesogen order at intermediate flexibilities. This combined phase is particularly stable for a mesogen flexing angle of 60°.

Substantial biaxiallity has been observed in the ordering of the rings at low temperature for the system with large flex angles. Some low temperature biaxiallity has also been observed between the discotic and combined regions on the phase diagram.

Simulations near the boundaries of the three regions identified on the phase diagram exhibited several successive transitions as the temperature was reduced. Owing to the poor statistics provided by the small

system of molecules and the possibility of too rapid cooling below the first transition we cannot be confident of the correct succession of the lower temperature phases or the transition temperatures. However, the good agreement between the 'forward' and 'reverse' transitions for the rigid ring case indicates that the equilibration time and cooling rate were adequate to locate the major transition in the system. Further investigations using larger systems of molecules and a slower cooling rate would be required determine the true polymorphism of the model, if any.

From the configurational data collected at the end of each simulation it has been shown that in the low temperature phases the mesogen and ring director systems are strongly coupled to each other and to the laboratory axes for the simulation of the m.m.r. model with a flex angle below about 90°. It is thought that these correlations do not significantly alter the magnitudes of the order parameters in these phases.

From diagrams of the end configurations it has been observed that the mesogenic rod units tend to stack in layers, typical of smectic phases. The layering is especially well defined for the cases where the flex angle is 0° or 60°. These flex angles correspond to regions of the phase diagram in which the mesophases are particularly stable. For the case of 0° flex angle some stacking of the rings into staggered columns is observed, becoming more distinct as the system is cooled. For these simulations in the NVT ensemble it would be expected that the nature of the spatial packing of the molecules may be influenced by the dimensions of the periodic box. Consequently, the observed spatial packing may not be evident in macroscopic systems.

CHAPTER 5 A MEAN FIELD THEORY

INTRODUCTION

The classic mean field treatment of the nematic phase is that developed by Maier and Saupe [45-47] in the late 1950s. Their work predicted a first order phase change from nematic at low temperatures to isotropic at high temperatures for rod-like molecules. This type of calculation has also been applied to a variety of liquid crystal systems including binary mixtures of rods and plates [85-86] and several polymer liquid crystal systems [28,29,31]. Of particular interest to us is the work of Wang and Warner [31] in which the uniaxial phases of comb-like liquid crystal polymers are explored. Nematic phases were found in which either the polymer backbones or the rod-like side groups or both together exhibited positive ordering.

A mean field model of cyclic side-chain oligomeric liquid crystals has been developed in parallel with the multi-mesogen ring model described in the previous chapter. In the mean field model, the ring backbone and the rod-like mesogenic side-chains are again represented separately. Energetic contributions to the mean field are included for rod-rod interactions, ring-ring interactions and the coupling between a ring and its attached mesogens.

The usual second rank order parameter is used to quantify the ordering of the two structural components.

For the rod-like mesogens the order is given by:

$$S_m = \langle P_2 \rangle_m = \left\langle \frac{1}{2} \left(3 \cos^2\theta_m - 1 \right) \right\rangle \qquad 5.1$$

where '<..>' denotes a thermal average and θ_m is the angle between a mesogen and the unique director of the phase. The order of the rings, $\langle P_2 \rangle_r$, is defined similarly in terms of the angles, θ_r, between the ring normals and the same director. Two possible ordered, uniaxial phases for the oligomers are shown diagrammatically in figure 5.1. In the calamitic nematic (N_c) phase the mesogens tend to align parallel to the director and the ring normals tend to lie in a plane perpendicular to the director, whilst in the discotic nematic (N_d) phase it is the rings that tend to align parallel and the mesogens which are perpendicular to the director.

The phase behaviour of cyclic side-chain liquid crystal oligomers has been explored in the multi-mesogen ring model by using the Metropolis Monte Carlo technique [40]. However, mean field calculations are generally much cheaper in computational terms than Monte Carlo techniques and so the model presented here is used to assess the suitability of the mean field approach to the prediction of the phase behaviour of these types of mesogenic oligomer.

THE MODEL

We consider a system of rigid ring polymers each with n rod-like mesogens attached by flexible spacer units and consider only uniaxial phases. We assume that

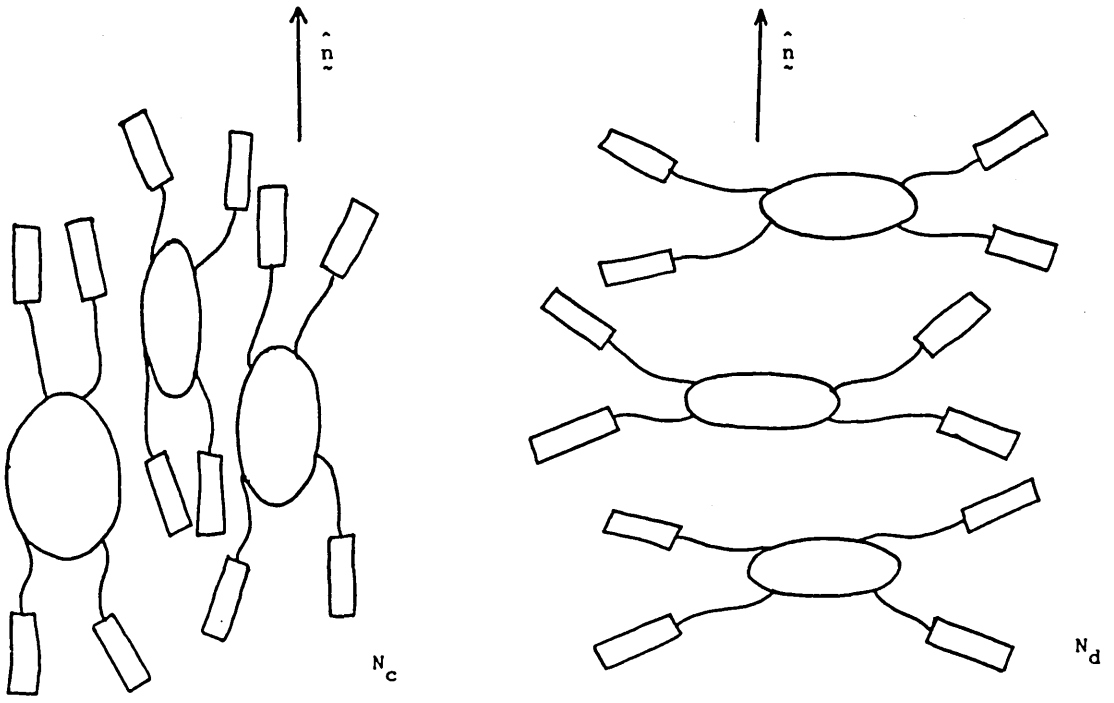

a. b.

Figure 5.1 A diagrammatic representation of a) the calamitic nematic phase (N_c) and b) the discotic nematic phase (N_d) for the cyclic oligomers. ' $\hat{n}$ ' indicates the director of the phase.

each mesogen moves in a mean field potential of the form:

$$V_m(\cos\theta_m) = - V_0 \left(\langle P_2\rangle_m - \lambda_c\langle P_2\rangle_r\right) P_2(\cos\theta_m) \qquad 5.2$$

where θ_m is the angle between the mesogen long axis and the unique director in the system and P_2 is the second order Legendre Polynomial. The first term in this equation is a standard Maier-Saupe term and represents the drive towards parallel ordering which is caused by the steric and long-range forces between the mesogens. The second term represents a coupling between a ring and its attached mesogens which arises from the spacer unit. The strength of the coupling is determined by the positive dimensionless parameter λ_c which is the ratio of the coupling potential to the mesogen-mesogen potential. We assume that the molecules are such that as the coupling strength is increased the molecules will adopt conformations in which the ring normals and the long axes of the rods tend to be mutually perpendicular.

The polymer rings are assumed to experience a mean field potential of the form:

$$V_r(\cos\theta_r) = - V_0\lambda_c\left(\lambda_r\langle P_2\rangle_r - n\langle P_2\rangle_m\right)P_2(\cos\theta_r) \qquad 5.3$$

where θ_r is the angle between the ring normal and the unique director in the system. The first term is a Maier-Saupe potential which will tend to induce parallel ordering of the polymer ring backbones. The mesogenic ordering of small chain cyclic poly(dimethylsiloxane) molecules has not been reported and so the polymer rings are assumed not to have any intrinsic drive towards

parallel order. However, we envisage that if the mesogenic rods attached to the rings are forced to adopt a planar splay conformation perpendicular to the ring normal then the resultant rigid molecules will be approximately disc shaped and will tend to align with their normals parallel owing to local packing effects. We account for this steric interaction by scaling the ring-ring interaction by λ_c. The parameter λ_r is a positive dimensionless constant which determines the strength of the ring-ring interaction. The second term in the ring potential is a ring-mesogen coupling term which is scaled by the number of mesogens, n, attached to each ring.

We are only interested in oligomers with a small number of repeat units and so do not consider the drive towards maximal chain entropy which would be more appropriate for long chain polymers Also the interaction between rods and rings other than via the attachment spacer is not considered, as it is thought that rod-ring interactions are likely to be a second order influence on the formation of ordered phases.

The above potentials define the nature of the molecules with three independent parameters λ_r, λ_c, and n. These together with T^* determine the phase of the material where T^* is a reduced temperature defined by:

$$T^* = \frac{k_B T}{V_0} \qquad 5.4$$

From the two mean field potentials the following

self consistent equations may be written:

$$\langle P_2 \rangle_m = \frac{\int_0^1 P_2(\cos\theta_m)\, \exp(-V_m(\cos\theta_m)/k_BT)\, d(\cos\theta_m)}{\int_0^1 \exp(-V_m(\cos\theta_m)/k_BT)\, d(\cos\theta_m)}$$

and

$$\langle P_2 \rangle_r = \frac{\int_0^1 P_2(\cos\theta_r)\, \exp(-V_r(\cos\theta_r)/k_BT)\, d(\cos\theta_r)}{\int_0^1 \exp(-V_r(\cos\theta_r)/k_BT)\, d(\cos\theta_r)} \qquad 5.5$$

These equations were solved numerically for $\langle P_2 \rangle_m$ and $\langle P_2 \rangle_r$ for selected values of λ_c, λ_r, n and T^*. In the regions of interest three solutions were found at low temperature: a calamitic nematic phase, a discotic nematic phase and an isotropic phase. At these temperatures the equilibrium phase of the system was taken as that with the lowest total free energy, F_{Tot}, whilst at high temperatures the isotropic phase was the only solution.

The entropic contribution to the free energy was obtained from the partition functions, Z_m and Z_r, for the mesogen and ring components:

$$Z_m = \int_0^1 \exp(-V_m(\cos\theta_m)/k_BT)\, d(\cos\theta_m)$$

$$Z_r = \int_0^1 \exp(-V_r(\cos\theta_r)/k_BT)\, d(\cos\theta_r) \qquad 5.6$$

The free energy terms for a mesogen and a ring are then [13]:

$$F_m = - k_B T \ln(Z_m) - \frac{1}{2} \langle V_m \rangle$$

$$F_r = - k_B T \ln(Z_r) - \frac{1}{2} \langle V_r \rangle$$

And the total free energy, F_{Tot}, is

$$F_{Tot} = F_m + \frac{1}{n} F_r \qquad 5.7$$

The results obtained were in agreement with Maier-Saupe in the limit $\lambda_c \rightarrow 0$. Extrapolation of the numerical results to $T^* = 0$ are also in agreement with the expected values, which were calculated exactly without recourse to numerical techniques.

RESULTS

Solutions to the model are presented for those values of n, λ_c and λ_r which might be expected to provide the best comparison with actual liquid crystal oligomers and the m.m.r. model. The mean field model was solved for values of n=4 and n=6, while for the m.m.r. model n=4 was used and oligomers have been synthesised with a range of repeat units from 4 to 7. As already discussed, we would expect the ring-ring interaction to result from steric interactions and to be comparatively small, and so we arbitrarily restrict λ_r to take values between 0 and 2.

The ring-ring interaction is also scaled by λ_c, and

so for non-zero λ_r the model may be expected to correspond to the real oligomers more successfully for low values of λ_c.

Figure 5.2 shows the ring and mesogen order parameters as functions of reduced temperature for $\lambda_r = 0$, $\lambda_c = 1.8$ and $n = 4$. A transition from a strongly ordered calamitic nematic phase ($\langle P_2 \rangle_m = 0.69$) at low temperature to a strongly ordered discotic nematic phase ($\langle P_2 \rangle_r = 0.85$) at high temperature is observed at a reduced temperature of $T^* = 0.403$, with an associated increase in entropy of 2.65 J $K^{-1}mol^{-1}$. A further transition from a weakly ordered discotic nematic phase ($\langle P_2 \rangle_r = 0.07$) to isotropic is observed at $T^* = 0.828$, with an increase in entropy of 0.063 J $K^{-1}mol^{-1}$. Figure 5.3 shows the over all phase behaviour as a function of λ_c for the model with $\lambda_r = 0$. For values of λ_c below a particular value only a single transition from calamitic nematic to isotropic is observed. For $\lambda_c = 0$ the transition from calamitic nematic to isotropic occurs at a reduced temperature of $T^* = 0.220$, in agreement with the Maier-Saupe results. The model exhibits an isotropic phase at high temperature and a calamitic nematic phase at low temperature. If $\lambda_r = 0$ and λ_c is greater than a specific value, a N_d phase exists between the isotropic and N_c phases. This specific value of λ_c corresponds to a 'triple point' at which the three phases co-exist in equilibrium.

The spontaneous order parameters at the phase transitions are given as a function of λ_c in figure 5.4. The spontaneous order in every case is seen to weaken dramatically in the region close to the triple point.

It is especially interesting to note the formation of a discotic nematic phase in the absence of specific

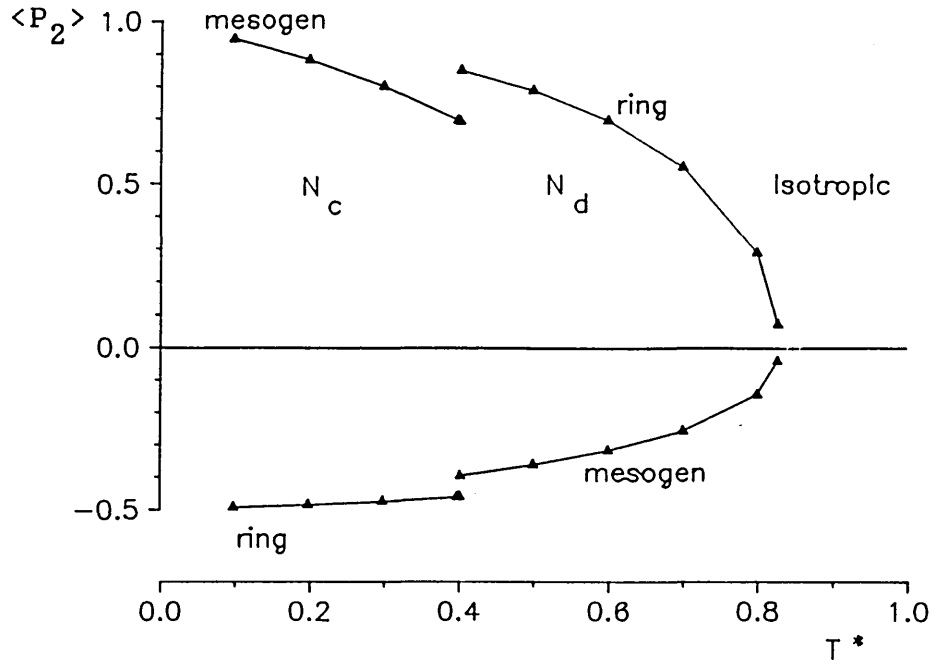

Figure 5.2 The equilibrium values of $\langle P_2 \rangle$ for the rings and the mesogens as a function of reduced temperature for $\lambda_r = 0$, $\lambda_c = 1.8$ and $n = 4$.

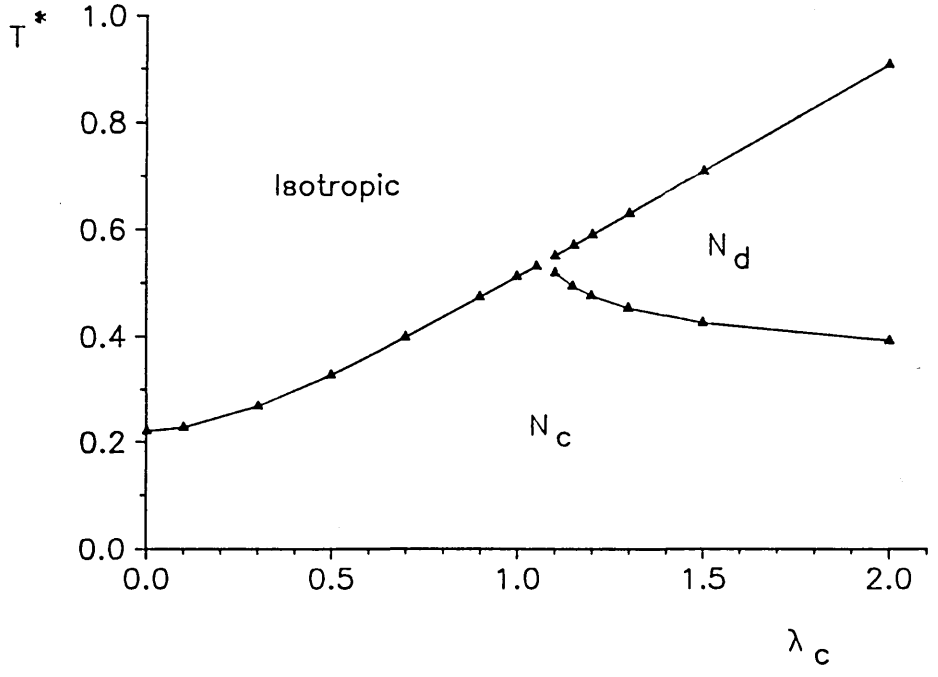

Figure 5.3 The phase diagram for $\lambda_r = 0$, $n = 4$.

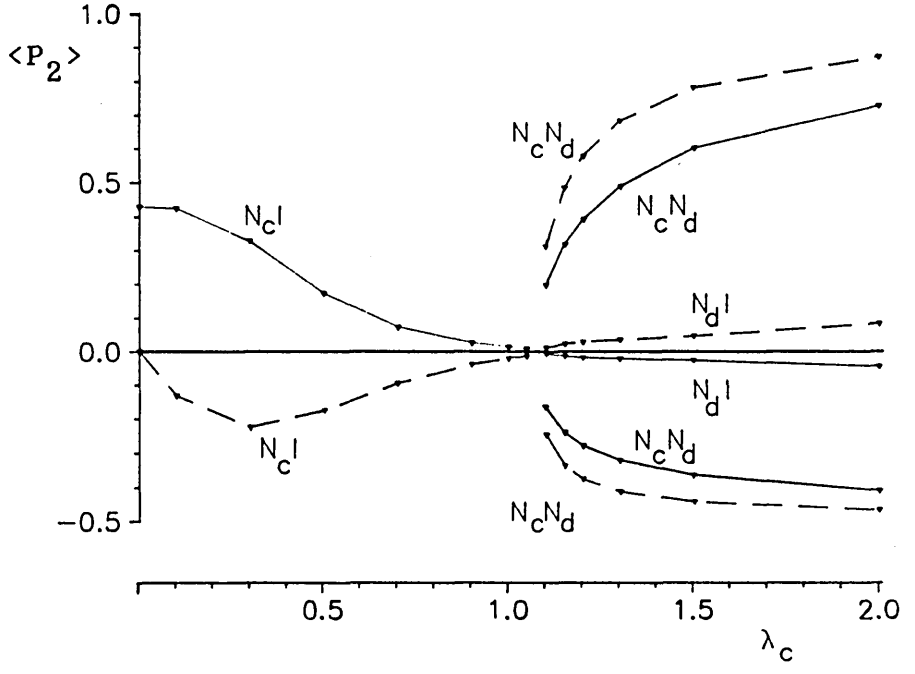

Figure 5.4 The spontaneous order parameters at transitions for $\lambda_r = 0$, $n = 4$. The phase transitions are labelled, for example, N_cI = calamitic nematic to isotropic. The solid line represents mesogen order and the broken line, ring order.

ring-ring interactions. Analysis of the numerical data indicates that the ring based ordering results from the forces between the attached mesogens and the increased entropic contribution to the free energy over the more ordered calamitic nematic phase.

The phases of the model when $\lambda_r = 1$ are shown in figure 5.5. The main effect of introducing a finite ring-ring interaction is to enlarge the discotic region at the expense of the calamitic and isotropic phases. Thus for $\lambda_r = 1$ both the reduced temperature and coupling strength decrease at the triple point.

For non-zero λ_r the calamitic phase is not the only equilibrium solution at $T^* = 0$. For values of the coupling strength greater than $\lambda_c = n/\lambda_r$ the discotic phase is favoured. Hence, for large λ_c only the discotic and isotropic phases are observed, in agreement with the results from the m.m.r. model for rigid molecules.

The values of coupling strength and reduced temperature at the triple point for various λ_r are given in table 5.1. The stronger the ring-ring coupling the more dominant the N_d phase becomes, with associated decrease of λ_c and T^* at the triple point. Also given are the triple point values for n = 6. Again, the discotic phase dominates at the expense of both the isotropic and calamitic phases as the number of mesogens attached to a ring is increased. However in real materials increasing the number of mesogens necessitates an increase in ring size which may give rise to a decrease in ring rigidity. In the model presented no account is taken of such a decrease in ring rigidity.

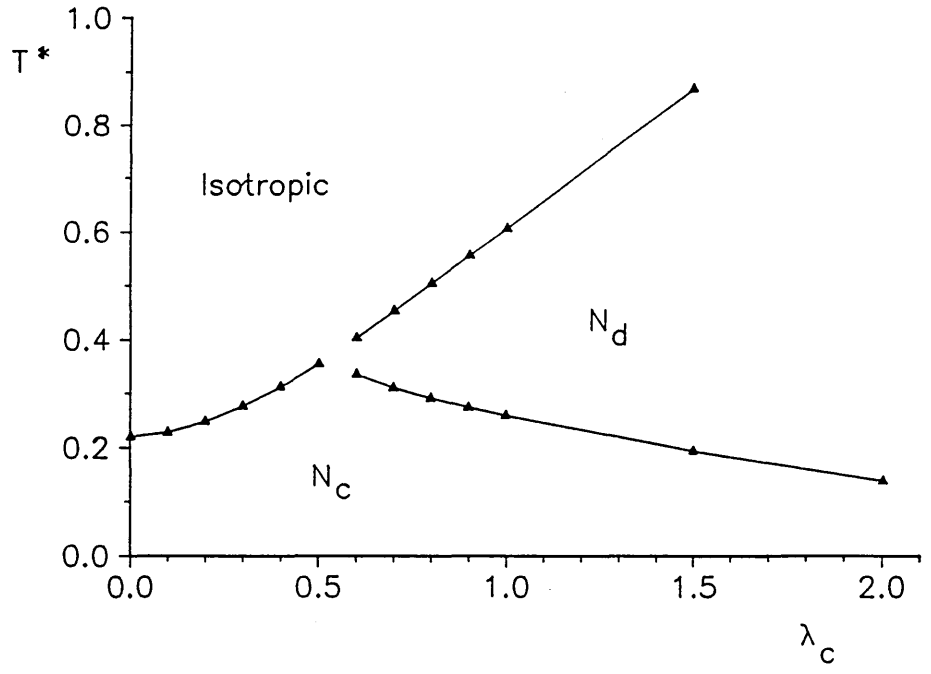

Figure 5.5 The phase diagram for λ_r = 1.0, n = 4.

n	λ_r	T^*_{triple}	$\lambda_{c,triple}$
4	2.0	0.31	0.34
4	1.0	0.37	0.53
4	0.5	0.42	0.69
4	0.0	0.54	1.07
6	0.0	0.44	0.67

Table 5.1 Values of T^* and λ_c at the triple point for a range of n, λ_r.

CONCLUSIONS

The phase behaviour of liquid crystal cyclic oligomers is the result of a variety of influences owing to the composite nature of the molecules, and as such is generally more complicated than the phase behaviour of low molecular weight liquid crystals. We have presented a mean field model which predicts both calamitic and discotic liquid crystal phases for small ring, cyclic oligomers with side-chain mesogens. A discotic nematic phase is shown to result from the long-range interactions of splay clusters of rod-like mesogens in the absence of specific ring-ring interactions.

We have also shown the transition from a calamitic nematic phase to a discotic nematic phase as a result of a change in temperature in the cases where the ring-mesogen coupling energy is substantial. However, it should be noted that the results are restricted to uniaxial phases, precluding the formation of phases in which the mesogen and ring systems possess different directors or biaxial phases of the type observed in the m.m.r. model.

In our model, the specific phase behaviour was shown to be dependent upon the relative strengths of the various component interactions. However, the form of the phase diagram was not greatly affected by a change in the number of repeat units in a ring or the strength of the ring-ring interaction for the range of values investigated. The effect of increasing the ring-ring interaction or increasing the number of rods per ring was in each case to enhance discotic tendencies.

SUMMARY AND CONCLUSIONS

The phase behaviour of cyclic side chain liquid crystals has been related to the physical structure of the molecules by the use of two modelling techniques: the Metropolis Monte Carlo method and the mean field approximation. The models were supported by experimental measurements on several new oligomeric compounds comprising cyclic poly(dimethylsiloxane) backbones with mesogenic side groups attached by alkyl spacer units. The compounds available formed two homologous series, varying only in the number of repeat units in the siloxane ring or only in the length of the alkyl spacer units.

The construction of a molecular graphics model of one of the oligomers, D4C4, has given insight into the relative dimensions of the major structural elements of the molecules and spatial relationships between them. The largest of these structural units are the lath-like mesogenic moieties which, if approximated to the conventional rod shape of a nematogen, would have a length a little greater than three times the diameter. The alkyl spacer unit is comparatively short, measuring a little under half the length of the rod-like mesogen for a four-membered spacer and a little over half the length of the rod for a six-membered spacer. The diameter of the polysiloxane backbone ring is also of the order of one half of the length of the mesogenic rods for the range of ring sizes in the available samples.

The molecular graphic construction of a planar form of the four-membered cyclic poly(dimethylsiloxane) backbone revealed that it should be possible to attach the side chains to the ring by bonds which are radially splay in the plane of the ring backbone. However, it was expected that in the samples provided the side chains would be attached by other bonds also.

Optical microscopy and direct scanning calorimetry measurements on the available samples have shown the formation of mesogenic phases over temperature ranges from about 10°C up to 80° - 90°C. The samples were highly viscous at room temperature but became more fluid as the transition to the isotropic phase was approached. The optical textures of the samples just below the transition to the isotropic phase were indicative of a nematic phase, but further investigation by, for example, X-ray diffraction would be required to confirm the exact mesogenic phase. Two of the samples exhibited a second, possibly crystalline, form when annealed for a period of time at a temperature of about 50°C, and in one of the samples, D4C4, crystallites persisted at temperatures above the clearing point of the bulk of the fluid. Fuller examination of the other samples was not possible, though it is not unlikely that these would also exhibit some polymorphism.

Dielectric relaxations were observed in these materials below the clearing temperature. Relaxations were observed in the materials when the director of the mesophase was parallel to the applied alternating electric field but not when perpendicular. This suggested that the relaxation mechanism was associated with the end to end motion of the rod-like mesogenic units. The extent of the broadening of the relaxations and the size of the Arrhenius energy barriers of the

relaxations were shown to be dependent upon the length of the alkyl spacer unit and the size of the polymeric ring backbone. The size of the energy barrier was significantly lower for sample with a six-membered alkyl spacer than for the four-membered alkyl spacer, demonstrating the decoupling of the mesogenic units from the cyclic backbones by the longer spacers.

The Monte Carlo technique has been used in the study of two separate models of cyclic liquid crystalline oligomers, both in the NVT ensemble. In the soft disc model the complete oligomer molecules were represented individually by an approximately disc-shaped interaction potential derived from the standard Lennard-Jones 12-6 potential by the addition of an r^{-9} term. Simulations were performed in which fifty molecules were allowed two dimensional translational freedom and three dimensional orientational freedom. At low temperature or at high density or both, the molecules were observed to pack in aligned columns in domains, but no uniform order was observed.

A more complicated model, the multi-mesogen ring (m.m.r.) model, was developed to investigate the effects of altering the structural components of the molecules upon the phase behaviour of the macroscopic system. In this model the mesogenic units and the cyclic backbones were represented separately. The mesogenic units were assigned an interaction potential which had been used by other workers in the simulation of rod-like mesogens. The ring-like backbones were represented solely as constraints upon relative motions of the mesogens, and the coupling between a ring and attached mesogen provided by the alkyl spacer unit was represented by a restriction upon the orientations the mesogen may adopt with respect to the ring. This orientational restriction was

implemented by means of an imagined cone within which the mesogen was allowed to orient, the half angle of the cone being referred to as the flex angle.

Simulations of the m.m.r. model were performed on a system of sixty mesogenic units attached four to a ring, with full three dimensional freedom. Transitions from isotropic to an ordered phase were observed as the temperature was reduced, for all values of the flex angle. In the cases of strong coupling between the mesogens and the rings (small flex angle) the transition was distinct and probably first order and the ordered phase was discotic. In the cases of weak coupling (large flex angle) the observed transitions were either continuous or very weakly first order and the ordered phase was a calamitic nematic in which the ordering of the ring normals was significantly biaxial. For intermediate coupling the uniaxial order parameters of both the ring and the mesogen systems were large and positive in the low temperature phase. For some of these simulations with intermediate coupling, several transitions were observed in succession as the temperature was lowered. However, it was shown for the 30° flex angle case that the low temperature phases formed were influenced by the rate of cooling of the system. Therefore, further simulations with lower cooling rates would be required to confirm the true polymorphism of these systems. For the case of intermediate coupling provided by a 60° flex angle, the system showed a single phase transition from the isotropic phase to a phase in which the mesogens and the rings both exhibited particularly strong uniaxial ordering. This transition was accompanied by large discrete changes in the internal energy and the order parameters, and was most probably first order.

The diagrammatic representation of individual configurations from the simulations indicated that the mesogens tended to stack in planes in the ordered phases for all of the values of the flex angle. This spatial packing was particularly distinct for flex angles of 0° and 60°. In the case of 0° flex angle, the ring units were observed to stack in staggered columns, but this packing was lost as the flex angle was increased.

A model of cyclic side-chain mesogenic oligomers was also solved by means of a mean field approach. The mean field potentials included terms for mesogen-mesogen interactions, ring-ring interactions and the coupling between rings and attached mesogens. There were three independent variables in the model: the number of mesogens attached to each ring, a measure of the relative strength of the mesogen-ring coupling and a measure of the relative strength of the ring-ring interaction. Uniaxial solutions to the mean field equations were sought for values of these parameters which were thought appropriate for comparison with the actual mesogenic oligomers and the molecules in the m.m.r. model.

In cases where the ring-mesogen coupling was low a first order transition from a calamitic nematic phase to isotropic was observed as the temperature was raised, whereas for cases where the coupling was strong discotic phases were observed at low temperature, even in the absence of a specific ring-ring interaction. For intermediate values of the coupling the low temperature phase was calamitic, with a transition to discotic as the temperature was raised and a further transition to isotropic. An increase in the number of mesogens attached to a ring or in the strength of the ring-ring interaction in each case caused an enhancement in the discotic region of the phase diagram.

Quantitative comparisons between the results of the m.m.r. model and the mean field model are difficult owing to differences in the definitions of the reduced temperature and the coupling strength between the rings and attached mesogens. At the extremes of the phase diagram the two models exhibit similar behaviour. Where the ring-mesogen coupling is strong, for both models a discotic phase is formed at low temperature, with a single transition to the isotropic phase as the temperature is raised. The transition is first order in the mean field model and there is evidence that this may also be the case in the m.m.r. model. However, the pretransitional ordering observed in the m.m.r. model is excluded by the mean field approach in which localised ordering has no meaning.

For cases where the ring-mesogen coupling is weak, both models exhibit calamitic phases at low temperature. A definite first order transition to the isotropic phase is observed in the mean field model, whereas the nature of the transition in m.m.r. model was less clear. However, it is known that the changes in the configurational properties of the mesogenic system at the transition predicted by the Maier-Saupe mean field model are too large and, hence, it is thought that the mean field approach may enhance the first-order nature of the transitions in our model. The biaxiallity observed in the m.m.r. model is precluded in the mean field model by the restriction to uniaxial solutions.

Further agreement between the models is noted, in that the temperature of the transition is higher for the case of strong coupling than it is for weak coupling. Therefore, with a few reservations, the mean field approach correctly predicts the phase behaviour of the

model molecules at the extremes of ring-mesogen coupling. However, the mean field approach is less suited to the intermediate region of the phase diagram. The m.m.r. model predicted the formation of a combined phase in which the mesogens and the rings were both strongly, uniaxially ordered. This phase was not identified in the mean field model, which, instead, predicted the formation of a calamitic phase at low temperature and a discotic phase at higher temperature, below the clearing point. The failure of the mean field model to predict the combined phase results from the restriction to uniaxial solutions. In the combined phase in the m.m.r. model, the mesogen and ring directors are perpendicular, a conformation excluded in the mean field model in which the ring and mesogen directors are forced to be coincident. The construction of a more complicated mean field model in which biaxial phases are permitted would be required if the true behaviour of the molecules with intermediate ring-mesogen coupling are to be observed.

The measurements on the real materials are limited but do not disagree with the predictions of the models. Some of the materials have exhibited more than one ordered phase below the clearing temperature, although the exact nature of these phases has not been established. Both the m.m.r. model and the mean field model predict some polymorphism for intermediate strength coupling between the mesogens and the rings. The formation of crystallites below the clearing temperature, as observed for some of the oligomers, was predicted in the m.m.r. model for certain strengths of coupling, for example a 60° flex angle.

From the optical texture of the oligomers it is suggested that the phase exhibited just below the clearing temperature is likely to be nematic, with no

confirmed observation of a discotic phase. The synthesis of molecules in which the mesogens are attached to the backbones by radially splay bonds is required for a fair comparison with the results of the models. The dielectric measurements support the notion that the coupling strength may be adjusted by a change in the length of the alkyl spacer units, a concept fundamental to both the m.m.r. model and the mean field model. Furthermore, the molecular graphics construction model has indicated that the synthesis of a molecule in which the mesogenic units are in a planar splay conformation should be possible; such a molecule corresponding to cases of strong ring-mesogen coupling in the m.m.r. model and the mean field model.

The oligomeric samples were quite viscous at room temperatures and it is likely that this viscosity would slow down, or possibly inhibit, the formation of some of the low temperature phases predicted by the models. The true anisometry of the rod-like mesogenic units is not reflected in any of the models and so it is expected that the ability of the molecules to rotate into the equilibrium phase is enhanced in the models.

The mean field and Monte Carlo models presented have predicted a shift from discotic to nematic phases as the flexibility of the ring-mesogen attachment is varied for a homologous series of cyclic side-chain mesogenic oligomers. Some of the predictions of the models and some of the assumptions made in the models have been supported by the physical measurements on a limited range of sample oligomers. However, further and different measurements would be required before a reliable phase diagram can be constructed for the real materials.

FUTURE WORK

Although further and different measurements, such as by X-ray diffraction, would provide useful information about the structure of the mesophases formed by the available oligomers, the systematic synthesis of new materials of this general type is required in order to explore more fully the relationships between the molecular structure and macroscopic physical behaviour of cyclic side-chain liquid crystal oligomers. In particular, the synthesis of molecules in which the side chains are attached to the backbones only by planar splay bonds would allow us to be confident that an approximately disc-shaped molecule would result from the use of short, rigid spacer groups. It is suggested that a four-membered poly(dimethylsiloxane) ring would provide four suitable points of attachment, and the use of a small ring size should provide a fairly rigid structure for the centre of the disc. These molecules should be synthesised with a variety of spacer lengths so that the effects of different coupling strengths between the rings and the mesogens can be observed.

These new materials should, ideally, be constructed with a different choice of mesogenic unit. The interpretation of the results of the dielectric measurements on the available samples was hampered by the large angle between the axis of the dipole moment and the long-axes of the mesogenic units. If the mesogenic moieties had possessed a strong dipole moment approximately parallel to the long axis of the moieties then the order parameter for the mesogenic units could have been estimated from the dielectric measurements in a straight-forward manner. Such a dipole may be provided,

for example, by the exchange of a cyano-group for the methyl- group at the far end of the mesogenic moiety.

The physical analysis of the proposed materials should be more likely to reveal interesting phase behaviour as a function of the variation in the structural components of the molecules than would be observed in the currently available materials, the molecular shape of which is expected to be neither regular nor consistent.

The mean field theory of the cyclic mesogenic oligomers would be greatly improved by the extension to allow for biaxial solutions. Such an extension would permit the formation of combined phases in which the mesogenic units and the rings are both strongly, uniaxially ordered, as were observed in the m.m.r. model for cases of intermediate strength coupling between the mesogenic units and the rings.

There is scope for further study with the m.m.r. Monte Carlo model. Runs with slower cooling rates and larger numbers of molecules are required in order to reduce the uncertainties in the results due to statistical fluctuations, the influence of the periodic boundaries and the possible formation of meta-stable states. However, as has been observed, this model is relatively expensive in terms of computing time and a full investigation of the phase diagram for a large system of molecules would not be envisaged until computing speed in general has improved by a factor of 10 or so. One possible solution may be to transfer the model to a dedicated micro-computer with parallel processing capabilities.

Until adequate computing power is available for a

fuller study, a small region of the phase diagram may be chosen for closer scrutiny with a larger system of molecules. For example, the polymorphism of the cross-over region between the 'discotic' and the 'combined' regions could be explored. Variations in the adjustable parameters of the model, other than the mesogen-ring coupling strength, may be explored. In particular, changes in the size of the ring backbone or the number of mesogens attached to each ring could be directly related to a homologous series of physical oligomers.

Some saving in computing time may possibly be achieved by the use of a simpler mesogen-mesogen interaction potential, such as a hard-core potential. Such a model may mimic the space packing of the mesogens better than the current m.m.r. model, although the temperature dependence of the phases would be lost.

It is proposed that the major thrust of any future work in this area should be in the synthesis and analysis of new cyclic liquid crystalline oligomer materials, the molecular structures of which are regular and known, in anticipation of advances in computer technology which would allow for a more thorough investigation with the m.m.r. or similar model in parallel with the physical measurements.

REFERENCES

1. H. Kelker, Mol. Cryst. Liq. Cryst., 2, 1 (1973).

2. E.A. Poe, "Narrative of Arthur Gordon Pym", (Ed.Doubleday, 1966) ch. 18, p. 706.

3. F. Reinitzer, Montash Chem., 9, 421 (1888).

4. O. Lehmann, Z. Krist., 18, 464 (1890).

5. "Proceedings of the International Conference on Liquid Crystal Polymers", Bordeaux, France, July 1987. Published in two volumes as Mol. Cryst. Liq. Cryst., 153, (1987), and Mol. Cryst. Liq. Cryst., 155, (1988).

6. S. Chandrasekhar, "Liquid Crystals" (Cambridge University Press, 1977), ch. 1.

7. W.H. de Jeu, "Physical Properties of Liquid Crystalline Materials" (Gordon and Breach, 1980), ch. 1.

8. S. Chandrasekhar, Phil. Trans. R. Soc. Lond., A, 309, 93 (1983).

9. H. Sackmann, D. Demus, Mol. Cryst. Liq. Cryst., 21,239 (1973).

10. G. Friedel, Ann. Physique, 18, 273 (1922).

11. E.I. Kats, Usp. Fiz. Nauk., 142, 99 (1984).

12. G.W. Gray, "Molecular Structure and the Properties of Liquid Crystals" (Plenum Press, 1974), ch. 3.

13. E.B. Priestley, P.J. Wojtowicz, P. Sheng, "Introduction to Liquid Crystals" (Plenum Press, 1974), ch. 3 and ch. 4..

14. R.Alben, J.R. McColl, C.S.Smith, Solid State Comm., 11, 1081 (1972).

15. W.H. de Jeu, W.P. Claassen, J. Phys. Chem., 68(1), 102 (1978).

16. W.H. de Jeu, P. Bordewijk, J. Phys. Chem., 68(1), 109 (1978).

17. E.P. Raynes, "Chemistry and Physics of Thermotropic Liquid Crystals", in "Electro-optic and Photo-refractive Materials", ed. P. Gunter. Proceedings of the International School on Material Technology, Erice, Italy, 1986.

18. K. Herrmann, Z. Krist., 92, 49 (1935).

19. S. Chandrasekhar, B.K. Sadishiva, K.A. Suresh, Pramana, 9(5), 471 (1977).

20. C.R. Safinya, K.S. Liang, W.A. Varady, N.A. Clark, G. Anderson, Phys. Rev. Lett., 53(12), 1172 (1984).

21. C. Destrade, M.C. Mondon-Bernaud, N.H. Tinh, Mol.Cryst. Liq. Cryst.,49(lett.), 169 (1979).

22. M. Engel, B. Hisgen, R. Keller, W. Kreuder, B. Reck, H. Ringsdorf, H. Schmidt, P. Tschirner, Pure & App. Chem., 57(7), 1009 (1985).

23. V.P. Shibaev, N.A. Plate, Pure & App. Chem., 57(11), 1589 (1985).

24. N.A. Plate, Ya.S. Friedzon, V.P. Shibaev, Pure & App. Chem., 57(11), 1715 (1985).

25. G.S. Attard, G. Williams, Chemistry in Britain, Oct 1986, pp. 919-924.

26. H. Ringsdorf. Oral presentation at the International Conference on Liquid Crystal Polymers, July, 1987, Bordeaux, France.

27. E.J. Roche, S.R. Allen, C.R. Fincher, C. Paulson, Mol. Cryst. Liq. Cryst., 153, 547 (1987).

28. X.J. Wang, M. Warner, J. Phys. A, 19, 2215 (1986).

29. M. Warner, J.M.F. Gunn, A.B. Baumgrtner, J.Phys. A, 18, 3007 (1985).

30. W. Renz, M. Warner, Phys. Rev. Lett., 56(12), 1268 (1986).

31. X.J. Wang, M. Warner, J. Phys. A, 20, 713 (1987).

32. J. Pinsl, C. Bruchle, F.H. Kreuzer, J. Mol. Electronics, 3, 9 (1987).

33. T.M. Leslie, R.N. Demartino, E. Won Choe, G. Khanarian, D. Haas, G. Nelson, J.B. Stamatoff, D.E. Stuetz, C. Teng, H. Yoon, Mol. Cryst. Liq. Cryst., 153, 451 (1987).

34. Private communication, S. Cockett, D. Simmonds, K. Dodgson, Sheffield City Polytechnic.

35. Consortium fur Elekrochemische Industrie GMBH.

36. G.R. Luckhurst, in "The Molecular Physics of Liquid Crystals", ed. G.R. Luckhurst, G.W. Gray (Academic Press,1979), ch. 4.

37. J.M. Hammersley, D.C. Handscomb, "Monte Carlo Methods" (Methuen, 1964).

38. K. Binder, in "Monte Carlo Methods in Statistical Physics", ed. K. Binder (Springer-Verlag, 1979), Ch. 1.

39. K. Binder, in "Applications of the Monte Carlo Method in Statistical Physics", ed. K. Binder (Springer-Verlag, 1984), ch. 1.

40. N. Metropolis, A.W. Rosenbluth, M.N. Rosenbluth, A.H. Teller, E. Teller, J. Chem. Phys., 21(6), 1087 (1953).

41. C. Zannoni, in "The Molecular Physics of Liquid Crystals", ed. G.R. Luckhurst, G.W. Gray (Academic Press, 1979), ch. 9.

42. H.F. King, J. Chem. Phys., 57(5), 1837 (1972).

43. G. Lasher, Phys. Rev. A, 5, 1350 (1972).

44. P.A. Lebwohl, G. Lasher, Phys. Rev. A, 6(1), 429 (1972).

45. W. Maier, A. Saupe, Z. Naturforsch., 13a, 564 (1958).

46. W. Maier, A. Saupe, Z. Naturforsch., 14a, 882 (1959).

47. W. Maier, A. Saupe, Z. Naturforsch., 15a, 287 (1960).

48. H.J.F. Jansen, G. Vertogen, J.G.J. Ypma, Mol.Cryst. Liq. Cryst., 38, 87 (1977).

49. G.R. Luckhurst, P. Simpson, Molec. Phys., 47(2), 251 (1982).

50. G.R. Luckhurst, S. Romano, P. Simpson, Chem. Phys., 73, 337 (1982).

51. G.R. Luckhurst, S. Romano, Molec. Phys., 40(1), 129 (1980).

52. R. Hashim, G.R. Luckhurst, S. Romano, Molec. Phys., 53(6), 1535 (1984).

53. G.R. Luckhurst, P. Simpson, C. Zannoni, Chem. Phys. Lett., 78(3), 429 (1981).

54. R.L. Humphries, G.R. Luckhurst, Proc. R. Soc. Lond.,A, 382, 307 (1982).

55. G.R. Luckhurst, P. Simpson, C. Zannoni, Liquid Crystals, 2(3), 313 (1987).

56. J.Y. Denham, R.L. Humphries, G.R. Luckhurst, Mol. Cryst. Liq. Cryst., 41(letters), 67 (1977).

57. J.Y. Denham, G.R. Luckhurst, C. Zannoni, J.W. Lewis, Mol. Cryst. Liq. Cryst, 60, 185 (1980).

58. R.L. Humphries, G.R. Luckhurst, S. Romano, Molec. Phys., 42(5), 1205 (1981).

59. G.J. Fuller, G.R. Luckhurst, C. Zannoni, Chem. Phys., 92, 105 (1985).

60. R. Hashim, G.R. Luckhurst, S. Romano, Molec. Phys., 56(6), 1217 (1985).

61. R. Hashim, G.R. Luckhurst, S. Romano, 2(1), 133 (1986).

62. S. Romano, Europhys. Lett., 2(6), 431 (1986).

63. S. Romano, Il Nuovo Cimento, 100B(4), 447 (1987).

64. S. Romano, Liquid Crystals, 3(3), 323 (1988).

65. D. Brindle, C.M. Care, accepted for publication in Molecular Simulation. Publication Pending.

66. J. Viellard-Baron, J. Chem. Phys., 56(10), 4729 (1972).

67. J. Viellard-Baron, Molec. Phys., 28(3), 809 (1974).

68. R.L. Coldwell, T.P. Henry, C-W Woo, Phys. Rev. A,10(3), 897 (1974).

69. I.Nezbeda, T. Boublik, O. Trnka, Czech. J. Phys. B, 25, 119 (1975).

70. T. Boublik, I. Nezbeda, O. Trnka, Czech. J. Phys. B, 26,1081 (1976).

71. D. Frenkel, R. Eppenga, Phys. Rev. Lett., 49(15), 1089 (1982).

72. D. Frenkel, B.M. Mulder, 55(5), 1171 (1985).

73. D. Frenkel, Computer Phys. Comm., 44, 243 (1987).

74. D. Frenkel, Molec. Phys., 60(1), 1 (1987).

75. M.C. Duro, J.A. Martin-Pereda, Mol. Cryst. Liq. Cryst., 155, 495 (1988).

76. G.A. Few, M. Rigby, Chem. Phys. Lett., 20(5), 433 (1973).

77. A.J. Stone, in "The Molecular Physics of Liquid Crystals", ed. G.R. Luckhurst, G.W. Gray (Academic Press,1979), ch. 2.

78. G.R. Luckhurst, S. Romano, Proc. R. Soc. Lond., A, 373, 111 (1980).

79. D.R.R. Everitt, C.M. Care, R. M. Wood, Mol. Cryst. Liq. Cryst., 153, 55 (1987).

80. D.R.R. Everitt, C.M. Care, accepted for publication in Molecular Simulation. Publication pending.

81. J. Kushik, B.J. Berne, J. Chem. Phys., 64(4),1362 (1976).

82. T.D. Schultz, in "Liquid Crystals 3, part I", ed. G.H. Brown, M.M. Labes (Gordon and Breach, 1972), p. 263.

83. S. Chandrasekhar, N.V. Mahusudana, Acta Cryst., A, 27, 303 (1971).

84. R.L. Humphries, P.G.James, G.R. Luckhurst, J. Chem. Soc., Faraday Trans. II, 68,1031 (1972).

85. P. Palffy-Muhoray, J.R. de Bruyn, D.A. Dunmur, J. Chem. Phys., 82(11),5294 (1985).

86. S.R. Sharma, P. Palffy-Muhoray, B. Bergerson, D.A. Dunmur, Phys. Rev. A, 32(6), 3752 (1985).

87. D.R.R. Everitt, C.M. Care, R.M. Wood, accepted for publication in Mol.Cryst. Liq. Cryst. Publication pending.

88. H. Finkelmann, G. Rehage, Makromol. Chem., Rapid Comm., 1, 31 (1980).

89. H. Finkelmann, G. Rehage, Makromol. Chem., Rapid Comm., 1, 733 (1980).

90. M.J. Forster, "Molgraph - A Molecular Graphics Program for the Atari ST" (The ST Club, Nottingham, 1990).

91. "Nuffield Advanced Science Book of Data", ed. H. Ellis (Longman, 1984), Ch. 4.

92. G.W. Gray, "Molecular Structure and the Properties of Liquid Crystals" (Plenum Press, 1974), Ch. 8.

93. G.W. Gray, in "Advances in Liquid Crystals, Volume 2" (Academic Press, 1976), Ch. 1.

94. H.Kelker, R. Hatz, "Handbook of Liquid Crystals" (Verlag Chemie, 1980), Ch. 2.

95. C.J.C. Edwards, D. Rigby, R.F.T. Stepto, K. Dodgson, J.A. Semlyn, Polymer, 24, 391 (1983).

96. C.J.C. Edwards, D. Rigby, R.F.T. Stepto, J.A. Semlyn, Polymer, 24, 395 (1983).

97. F-J. Bormuth, W. Haase, R. Zentel, Mol. Cryst. Liq. Cryst., 148, 1 (1987).

98. J.C. Anderson, "Dielectrics" (Chapman and Hall, 1964), Ch. 6.

99. V.V. Daniel, "Dielectric Relaxation" (Academic Press, 1967), Ch. 2 [99a], Ch. 7 [99b].

100. I. Oto, K. Ito, J. Phys. C, 15, 4417 (1982).

101. C. Zannoni, in "The Molecular Physics of Liquid Crystals", ed. G.R. Luckhurst, G.W. Gray (Academic Press,1979), ch. 3.

102. M.P. Allen. Publication pending.

103. Private communication, D.A. Dunmur, University of Sheffield.

104. D.P. Landau, in "Monte Carlo Methods in Statistical Physics", ed. K. Binder (Springer-Verlag, 1979), ch. 3.